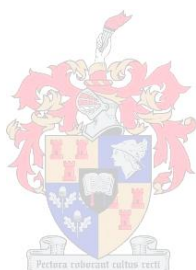


**Synthesis and evaluation of inhibitors targeting
Coenzyme A biosynthesis and metabolism in
*Staphylococcus aureus***

Renier van der Westhuyzen

Dissertation presented for
the degree of

**Doctor of Philosophy
(Chemistry)**



at

Stellenbosch University

Supervisor: Prof. Erick Strauss

Department of Biochemistry, University of Stellenbosch

December 2010

Declaration

By submitting this dissertation electronically, I declare that the entirety of the work contained therein is my own, original work, that I am the owner of the copyright thereof (unless to the extent explicitly otherwise stated) and that I have not previously in its entirety or in part submitted it for obtaining any qualification.

18 November 2010

.....
Signature

.....
Date

Summary

The human pathogen *Staphylococcus aureus* is a major cause of hospital-, and more recently, community-acquired infections. The rate at which this organism is acquiring resistance to antibiotics is increasing while the development of new antibiotics is slowing down. There is therefore a desperate need for new antistaphylococcal agents, and in particular ones with novel mechanisms of action that can be used to circumvent established resistance pathways. Unlike humans, *S. aureus* employs the essential cofactor coenzyme A (CoA) as its major low molecular weight thiol. Together, CoA and the enzyme CoA disulfide reductase (CoADR) are responsible for maintaining the internal redox homeostasis in this organism, and disruption of this balance (or reduction of CoA levels) may therefore be potential mechanisms by which new antistaphylococcal agents may act. In this study we set out to achieve this by direct inhibition of CoADR, and by inhibition of one or more of the CoA biosynthetic enzymes.

For the inhibition of CoADR CoA analogues containing Michael acceptors were designed and prepared by employing a chemo-enzymatic approach. This strategy involved the chemical synthesis of pantothenamides containing α,β -unsaturated ester, ketone and sulfone moieties as Michael acceptors, followed by their biotransformation into the corresponding CoA analogues by three CoA biosynthetic enzymes. The compounds prepared in this manner all inhibited CoADR potently. A full kinetic evaluation of the inhibition by these compounds suggested that these compounds act by alkylation of the single active site cysteine of CoADR in an irreversible fashion.

In this study we also set out to determine the mechanism of action of the antistaphylococcal compound CJ-15,801, which is structurally similar to pantothenic acid, the biosynthetic precursor of CoA. Due to this similarity we proposed that the antibiotic properties of CJ-15,801 are based on the inhibition of enzymes involved in CoA biosynthesis and metabolism. Our investigations confirmed that the second enzyme of the CoA pathway, phosphopantothenoylcysteine synthetase (PPCS), acts as the main target of CJ-15,801. These studies were followed by an investigation into alternative synthetic methodologies for the preparation of CJ-15,801 and its analogues. As a result an established Pd-catalyzed coupling reaction was modified and applied in the third known total synthesis of CJ-15,801, as well as of several of its analogues. This protocol has several advantages over its predecessors, most importantly its suitability for preparing these compounds on large (up to one gram) scale.

Opsomming

Die menslike patogeen *Staphylococcus aureus* is 'n wesenlike oorsaak van hospitaal- en meer onlangs gemeenskap-verworwe infeksies. Terwyl die tempo waarteen hierdie organisme weerstandbiedig teenoor antibiotika raak toeneem, neem die ontwikkeling van nuwe antibiotiese middels af. Dit is dus van kardinale belang dat nuwe antistafilokokale middels ontwikkel word, en meer spesifiek antibiotika met 'n nuwe meganisme van aksie wat gebruik kan word om huidige weerstandbiedende padweë te ontwyk. In teenstelling met mense, gebruik *S. aureus* die essensiele kofaktor koënsiem A (KoA) as sy vernaamste lae molekulere gewig tiol. Die ensiem KoA disulfied reduktase (KoADR) en KoA is saam verantwoordelik om die interne redoks homeostase in hierdie organisme te handhaaf, en ontwrigting van die balans (of vermindering van KoA vlakke) kan dus potensieel 'n meganisme van aksie wees waardeur nuwe antistafilokokale middels kan optree. In hierdie studie het ons gepoog om dit te bewerkstellig deur KoADR direk te inhibeer, asook deur inhibisie van een of meer van die KoA biosintetiese ensieme.

Vir die inhibisie van KoADR is KoA-analoë wat Michael-akseptor groepe bevat ontwerp en berei deur van 'n chemo-ensiematiese benadering gebruik te maak. Met hierdie strategie is pantoteenamiede gesintetiseer wat α,β -onversadigde ester, ketoon en vinielsulfoon funksionaliteite as Michael-akseptore bevat, gevolg deur biotransformasie na die ooreenstemmende KoA-analoë met behulp van drie CoA biosintetiese ensieme. Die verbindings gesintetiseer met hierdie metode het almal KoADR potent geïnhibeer. 'n Omvattende kinetiese evaluasie het voorgestel dat al hierdie verbindings funksioneer deur alkielering van die enkele aktiewe setel sisteïen van KoADR op 'n onomkeerbare wyse.

In die studie het ons ook gepoog om die meganisme van aksie van die antistafilokokale verbinding CJ-15,801 te bepaal. Hierdie verbinding is struktureel soortgelyk aan pantoteensuur, die biosintetiese voorganger van KoA. As gevolg van hierdie ooreenkomste het ons voorgestel dat die antibiotiese aktiwiteit van CJ-15,801 die gevolg is van die inhibisie van een of meer van die ensieme wat verantwoordelik is vir KoA biosintese en metabolisme. Ons ondersoek het bevestig dat die tweede ensiem in die KoA biosintetiese padweg, naamlik fosfopantotenoïelsisteïensintetase, die hoofteiken van CJ-15,801 is. Hierdie studie is gevolg deur die ondersoek van alternatiewe metodologieë vir die sintese van CJ-15,801 en analoë daarvan. 'n Gevestigde Pd-gekataliseerde koppelings reaksie was gevolglik gemodifiseer en toegepas om slegs die derde totale sintese van CJ-15,801 te bewerkstelling, asook die sintese van verskeie analoë daarvan. Hierdie protokol hou verskeie voordele in vergelyking met sy voorgangers, waarvan die mees belangrikste die bereiding van hierdie verbindings op groot (tot een gram) skaal is.

The financial assistance of the National Research Foundation (NRF) towards this research is hereby acknowledged. Opinions expressed and conclusions arrived at, are those of the author and are not necessarily to be attributed to the NRF.

Acknowledgements

For me the decision to do a PhD was always the next logical step after an MSc. However, I soon realized that doing a PhD was a great sacrifice and that I would have to pour all my energy into it. Unfortunately, a PhD is not something that one can complete without the help of others and therefore I would like to thank those people I am indebted to.

Firstly, I would like to thank God for giving me the strength to complete this degree.

Without the constant support and guidance from my fearless supervisor Prof Erick Strauss, the work presented in this dissertation would not have been possible. I can still remember when you started talking about publishing in JACS, at the time I thought it was impossible. I truly owe a lot to you and would like to firstly thank you for giving me the opportunity of working in your lab. Secondly, I want to congratulate you on the accomplishment of establishing what I think is a world class lab. The lab is a place where I found I could develop myself into a good scientist.

Then I would like to thank all the Strauss lab members for always being willing to help and all the chats. I have become friends with all of you and wish you all the best for the future. We have become a big lab with many personalities and still there is a place for everyone. Thank you very much: Marianne, Jandre, Dirk, Ilse, Lizbie, Albert, Collins, Cristiano and Rene. Simon Herbert and Dewald Kleinhans along with their supervisor Dr Gareth Arnott has also contributed significantly to my research. Dirk thank you very much for preparing supper during the writing up of this thesis.

Lastly, I want to thank all my friends and family that has supported me throughout the last 3 years. You would never know how much it helped having you in my life. I'm not going to name everyone, since most of you will never read this thesis, but even though you have no idea what I've been doing the last 3 years you have contributed a lot to my research and emotional well being. I would especially like to thank my parents for their never-ending support and encouragement to pursue my dreams. Hopefully, I can repay your confidence in me.

Additional Acknowledgements

- The University of Stellenbosch for the opportunity to study at this institution.
- Financial assistance from the National Research Foundation (NRF) and Prof. Erick Strauss.
- Dr Marietjie Stander of the MS-unit of the Central Analytical Facility of the University of Stellenbosch.
- Dr D.J. Brand and Ms Elsa Malherbe of the NMR-unit of the Central Analytical Facility of the University of Stellenbosch.
- L.A. Brand for cloning of the *SaCoADR* and *EcPPCS* expression vectors and efforts towards the cloning of the *SaCoaBC* expression vector.
- Prof. Erick Strauss for his unabated support and – more importantly – his patience.

Table of Contents

<i>Declaration.....</i>	<i>ii</i>
<i>Summary.....</i>	<i>iii</i>
<i>Opsomming.....</i>	<i>iv</i>
<i>Acknowledgements.....</i>	<i>vi</i>
<i>Additional Acknowledgements.....</i>	<i>vii</i>
<i>Table of Contents.....</i>	<i>viii</i>
<i>List of abbreviations.....</i>	<i>xiv</i>

Chapter 1

Introduction

1.1 The need for new antibiotics	1
1.2 Treatment of Staphylococcal infections	2
1.2.1 Current treatments	2
1.2.2 New targets/drugs for antistaphylococcal agents	3
1.2.2.1 CoADR and redox state	3
1.2.2.2 CoA biosynthetic enzymes as drug targets in bacteria	3
1.2.2.3 The Antibiotic CJ-15,801	5
1.3 Previous work on identified targets	5
1.3.1 CoADR	5
1.3.2 CoA biosynthesis and utilization as target in antibacterial development	6
1.3.2.1 PanK and the CoA salvage pathway	6
1.3.2.2 PPCS/PPCDC	9
1.3.2.3 PPAT and DPCK	9
1.3.2.4 CoA-utilizing enzymes and the <i>holo</i> -acyl carrier protein as down-stream targets	10
1.3.3 CJ-15,801	12

1.4 Objectives of this study	12
1.4.1 Objective 1: Development of Michael acceptor-containing CoA analogues as inhibitors of CoADR.....	13
1.4.2 Objective 2: Mechanism of action of antibiotic CJ-15,801	14
1.4.3 Objective 3: Synthesis of antibiotic CJ-15,801 and its analogues	14
1.5 References.....	16

Chapter 2

Design, synthesis and evaluation of inhibitors of CoADR

2.1 JACS Communication.....	Error! Bookmark not defined.
Supporting Information.....	23
<i>Materials and Methods</i>.....	23
<i>Synthesis of pantothenamides</i>.....	23
<i>Overexpression and purification of CoA biosynthetic enzymes</i>.....	27
<i>Biotransformation of pantothenamides into CoA analogues</i>.....	27
<i>Cloning, expression and purification of SaCoADR</i>.....	30
<i>Synthesis of the CoADR substrate</i>	30
<i>CoADR activity and inhibition assay procedures</i>	31
<i>Staphylococcus aureus growth assays</i>.....	38
<i>References</i>.....	39
2.2 Synthesis of inhibitors of SaCoADR.....	40
2.2.1 Inhibitor design	40
2.2.2 Synthesis of epoxide-containing pantothenamides	41
2.2.2.1 Synthesis of protected epoxides 9a-c as a model system	42
2.2.2.2 Epoxidation of protected pantothenamides	43
2.2.2.3 Characterization of epoxide 11c.....	44
2.2.2.4 Attempted deprotection of epoxide 11c.....	47
2.3 Conclusion.....	47
2.4 Experimental Section.....	48

2.4.1	Ethyl 3-(2-(<i>tert</i> -butoxycarbonylamino)ethyl)oxirane-2-carboxylate (9a).....	48
2.4.2	<i>tert</i> -Butyl 3-(2-(<i>tert</i> -butoxycarbonylamino)ethyl)oxirane-2-carboxylate (9b).....	48
2.4.3	<i>tert</i> -Butyl 2-(3-benzoyloxiran-2-yl)ethylcarbamate (9c)	49
2.4.4	General procedure for PMB protection of pantothenamides (10a-c).....	49
2.4.5	(<i>E</i>)-Ethyl 5-(3-((4 <i>R</i>)-2-(4-methoxyphenyl)-5,5-dimethyl-1,3-dioxane-4-carboxamido)propanamido) pent-2-enoate (10a)	49
2.4.6	(<i>E</i>)- <i>tert</i> -Butyl 5-(3-((4 <i>R</i>)-2-(4-methoxyphenyl)-5,5-dimethyl-1,3-dioxane-4-carboxamido)propanamido) pent-2-enoate (10b)	50
2.4.7	(4 <i>R</i>)-2-(4-methoxyphenyl)-5,5-dimethyl-N-(3-oxo-3-((<i>E</i>)-5-oxo-5-phenylpent-3-enylamino) propyl)-1,3-dioxane-4-carboxamide (10c)	50
2.4.8	(4 <i>R</i>)-N-(3-(2-(3-benzoyloxiran-2-yl)ethylamino)-3-oxopropyl)-2-(4-methoxyphenyl)-5,5-dimethyl-1,3-dioxane-4-carboxamide (11c)	51
2.5	References.....	52

Chapter 3

Determination of the mechanism of action of CJ-15,801

3.1	Discovery of CJ-15,801 as an antistaphylococcal agent	53
3.2	Potential targets for the antibiotic action of CJ	54
3.2.1	Competitive inhibition of PanK	54
3.2.2	Inhibition of PPCS.....	55
3.2.3	CoADR as target.....	58
3.3	Results: CJ acts as a substrate, not an inhibitor, of PanK.....	60
3.4	Results: PPCS is the main target inhibited by CJ	61
3.4.1	<i>In situ</i> generation of P-CJ	61
3.4.2	PPCS inhibition assay.....	62
3.4.3	PPCS is inhibited by P-CJ, but not by its ester.....	62
3.4.4	Determining the IC ₅₀ of <i>Ec</i> PPCS inhibition by P-CJ	62
3.4.5	Determining the reversibility of inhibition of PPCS by P-CJ.....	63
3.4.6	Progress curve analysis of the inhibition of <i>Ec</i> PPCS by CJ	65

3.5	Discussion: Mechanism of <i>EcPPCS</i> inhibition by CJ	67
3.6	Results: Cloning, expression and purification of <i>SaCoaBC</i>	68
3.7	Results: The <i>PPCS</i> activity of <i>SaCoaBC</i> is also inhibited by P-CJ.....	68
3.8	Conclusion.....	69
3.9	Experimental.....	69
3.9.1	Materials and methods.....	69
3.9.2	HPLC analysis of the conversion reaction by <i>SaPanK</i> under assay conditions.	70
3.9.3	Preliminary tests for inhibition of <i>EcPPCS</i> by CJ compounds:	71
3.9.4	Determination of IC_{50}	72
3.9.5	Test for irreversibility.....	72
3.9.6	Test for irreversibility using gel filtration	72
3.9.7	Progress curve analysis.....	72
3.9.8	Cloning, overexpression and purification of <i>SaCoaBC</i>	73
3.9.9	<i>PPCS</i> inhibition assays with <i>SaCoaBC</i>	73
3.10	References.....	74

Chapter 4

Synthesis of CJ-15,801 and its analogues

4.1	Introduction	75
4.2	Overview of published syntheses of CJ-15,801 and its precursors	75
4.2.1	<i>Methodology 1</i> : Cu-catalyzed synthesis of <i>N</i> -acyl vinylogous carbamates and ureas via amidation of β -iodoacrylates and β -iodoacrylamides	76
4.2.2	<i>Methodology 2</i> : Synthesis of <i>N</i> -acyl vinylogous carbamates and ureas via oxidation of amides with Dess-Martin periodinane	77
4.2.3	<i>Methodology 3</i> : Pd-catalyzed synthesis of <i>Z</i> -enamides via oxidative amidation of conjugated olefins.....	78
4.2.4	<i>Methodology 4</i> : Synthesis of enamides via Wittig-olefination of imides	79
4.2.5	Evaluation of the suitability of <i>Methodologies 1-4</i> for the synthesis of CJ-15,801	79

4.3	Proposed novel methodology: Pd-catalyzed synthesis of <i>N</i>-acyl vinylogous carbamates and ureas via amidation of β-bromoacrylates and β-bromoacrylamides.....	80
4.4	Results: Applying <i>Methodology 5</i> on a model system	81
4.5	Results: Applying <i>Methodology 5</i> in the synthesis of di-protected CJ-15,801	81
4.6	Results: A new total synthesis of CJ-15,801	82
4.7	Results: Heat-induced isomerization of enamides	84
4.8	Results: Synthesis of CJ analogues using newly established methodology	84
4.8.1	Synthesis of (<i>E</i>)- β -bromoacrylic ester and (<i>E</i>)- β -bromoacrylamide substrates	84
4.8.2	Coupling of amide 4.2 and β -bromoacrylates and β -bromoacrylamides	85
4.8.3	Acetonide deprotection of prepared <i>N</i> -acyl vinylogous carbamates and ureas	89
4.9	<i>S. aureus</i> growth inhibition by synthesized enamides.....	89
4.10	Preliminary <i>M. smegmatis</i> growth inhibition studies by enamides	90
4.11	Chemo-enzymatic synthesis of P-CJ	91
4.12	Conclusion.....	92
4.13	Experimental.....	93
4.13.1	Materials and methods.....	93
4.13.2	Synthesis of 2,4-Dihydroxy-3,3-dimethyl-butylamide	93
4.13.3	Synthesis of 2,2,5,5-Tetramethyl-[1,3]dioxane-4-carboxylic acid amide (4.2)	93
4.13.4	Synthesis of (<i>E</i>)- β -bromoacrylic acid (4.11)	94
4.13.5	General procedure for the synthesis of β -bromoacrylates:	94
4.13.6	(<i>E</i>)-Benzyl 3-Bromoacrylate (4.17).....	95
4.13.7	General procedure for the synthesis of β -bromoacrylamides	95
4.13.8	General procedure for Pd-catalyzed couplings	96
4.13.9	General procedure for the deprotection of the acetonide group	99
4.13.10	Synthesis of CJ-15,801	103
4.13.11	Growth inhibition of <i>S. aureus</i> by CJ ester and amide analogues	103
4.13.12	Growth inhibition of <i>M. smegmatis</i> by CJ ester and amide analogues.....	103
4.13.13	Biosynthesis of P-3.2 and P-4.5.....	104

4.14	References.....	105
-------------	------------------------	------------

Chapter 5

Conclusion and future work

5.1	Summary of results achieved.....	106
5.1.1	Objective 1: Michael acceptor-containing CoA analogues as inhibitors of CoADR .	106
5.1.2	Objective 2: Determination of the mechanism of action of CJ-15,801	107
5.1.3	Objective 3: Synthesis of CJ-15,801 and its analogues.....	107
5.2	Follow up work on the inhibition of CoADR	107
5.2.1	Inhibition by CoA analogues with electrophile removed	107
5.2.2	Synthesis of compounds with improved inhibition	108
5.2.3	Inhibition of <i>S. aureus</i> growth under oxidative stress conditions	108
5.3	Future studies on mechanism of action of CJ-15,801	109
5.3.1	Inhibition of PPCS by P-CJ	109
5.3.2	Pd-catalyzed synthesis of CJ-15,801 and its analogues	109
5.4	Final remarks.....	109
5.5	References.....	111

Abbreviations

aq.	Aqueous
ADP	Adenosine 5'-diphosphate
AllylOH	Allyl alcohol
Asp	Aspartate
Asn	Asparagine
ATP	Adenosine 5'-triphosphate
Boc	<i>tert</i> -butyl carbonate
BuLi	<i>n</i> -butyl lithium
Cbz	Carbobenzoxo
CA-MRSA	Community associated MRSA
CJ	CJ-15,801
CoA	Coenzyme A
CoAS ₂	CoA disulfide
CoADR	CoA disulfide reductase
CMP	Cytidine 5'-monophosphate
CTAB	Cetyltrimethylammonium bromide
CTP	Cytidine 5'-triphosphate
CSA	10-Camphorsulfonic acid
Cys	Cysteine
DCM	Dichloromethane
DIC	<i>N,N</i> -diisopropylcarbodiimide
DMAP	<i>N,N</i> -dimethyl aminopyridine
DMF	<i>N,N</i> -Dimethylformamide
DMP	Dess-Martin periodinane
DMSO	Dimethyl sulfoxide
DPCK/CoaE	Dephospho-CoA kinase
DTNB	5,5-Dithiobis-(2-nitrobenzoic acid)
DTT	Dithiothreitol
<i>E. coli</i>	<i>Escherichia coli</i> (also <i>Ec</i>)
EDC	1-(3-Dimethylaminopropyl)-3-ethylcarbodiimide
Eq	equivilants
ESI-MS	Electrospray Ionization Mass Spectroscopy
EtOH	Ethanol

EtOAc	Ethyl acetate
FDA	Food and drug administration
GR	Glutathione reductase
His	Histidine
HOBt	<i>N</i> -Hydroxybenzotriazole
HPLC	High Performance Liquid Chromatography
IC ₅₀	Concentration required for 50% inhibition
IDSA	Infectious Disease Society of America
IMAC	Immobilized Metal Affinity Chromatography
IPM	Isopropenyl methy ether
IPTG	Isopropyl β-D-1-thiogalactopyranoside
k_{cat}	Turnover number
K_i^{app}	Apparent dissociation constant of enzyme inhibitor complex
K_i	Dissociation constant of enzyme inhibitor complex
K_i	Concentration of inactivator at rate equal to 1/2 k_{inact}
k_{inact}	Maximum rate of inactivation
k_{obs}	Rate of inactivation
K_M	Michaelis constant
LB	Luria Bertani
LC-MS	Liquid Chromatography Mass Spectroscopy
MeCN	Acetonitrile
MeOH	Methanol
MIC	Minimum inhibitory concentration
MRSA	Methicillin resistant <i>Staphylococcus aureus</i>
<i>M. tuberculosis</i>	<i>Mycobacterium tuberculosis</i>
NADH	Nicotinamide adenine dinucleotide (reduced)
NADPH	Nicotinamide adenine dinucleotide phosphate (reduced)
NEM	<i>N</i> -ethyl morpholine
NMR	Nuclear Magnetic Resonance Spectroscopy
OD	Optical density
PanCOOH	Pantothenic acid
PanK/CoaA	Pantothenate kinase
PCC	Pyridinium chlorochromate
P-CJ	Phosphorylated CJ-15,801
PEP	Phosphoenolpyruvate
PhCl	Chlorobenzene

PhF	Fluorobenzene
PhH	Benzene
PhMe	Toluene
PMB	<i>p</i> -Methoxybenzylidene
P-PanCOOH	Phosphopantothenic acid
PPAT/CoaD	Phosphopantetheine adenylyltransferase
PPCS/CoaB	Phosphopantetheinecysteine synthetase
PPCDC/CoaC	Phosphopantetheinecysteine decarboxylase
PPI	Inorganic pyrophosphate
PNDOR	Pyridine nucleotide disulfide oxidoreductase
<i>p</i> -TsOH	<i>p</i> -Toluenesulfonic acid
ROS	Reactive oxygen species
rt	Room temperature
<i>S. aureus</i>	<i>Staphylococcus aureus</i> (also <i>Sa</i>)
SDS PAGE	Sodium dodecyl sulphate polyacrylamide gel electrophoresis
SPE	Solid phase extraction
TBHP	Tertiary butylhydroperoxide
TEM DP	Tetraethyl methylenediphosphonate
TFA	Trifluoroacetic acid
THF	Tetrahydrofuran
TR	Trypanothione reductase
TLC	Thin Layer Chromatography
TRIS	Tris(hydroxymethyl)aminomethane
Tyr	Tyrosine
v_s	Steady state rate
VRSA	Vancomycin-resistant <i>S. aureus</i>

Chapter 1

Introduction

1.1 The need for new antibiotics

One of the major achievements of the previous century was progress made towards controlling infectious diseases. This was achieved via the introduction of better sanitation practices, vaccinations and the discovery of antibiotics. After the introduction of antibiotics for the treatment of bacterial infections in the 1940s, it was assumed that these infections would be controllable by these compounds.¹ Unfortunately, widespread misuse of antibiotics and the ability of bacteria to adapt to their surroundings caused these organisms to become resistant to these so-called “wonder drugs”.

A recent report by the Infectious Disease Society of America (IDSA) identified among others methicillin-resistant *Staphylococcus aureus* (MRSA) and the declining investments in antimicrobial development as significant threats to human health.² Furthermore, the startling contrast between new classes of antibiotics introduced in the period 1940-1962 (during which eight classes were introduced) and the period 1962-2000 (when none were introduced) is an additional cause for concern. This so-called “innovation gap” is due a variety reasons. One of these may be the fact that antibacterial research is not regarded to be worthy of pursuit by some drug companies – especially in comparison to the development of other pharmaceuticals that is used in the treatment of certain “lifestyle” diseases. Investments in such drug development efforts, and those that are used in the treatment of heart disease and diabetes - all of which have treatment periods that are much longer than the short span of antibacterial treatment which only last weeks – are considered to be much more lucrative.^{2, 3} Antibacterial drug development is also not easy: many of the known antibacterials are natural products, and the drug discovery processes cannot be directed by following rules of thumb such as Lipinski’s “Rule of five”.⁴ As a result of this reduced investment in the research and development of new antibacterial agents, the number of these compounds approved by the FDA has also steadily declined to such an extent that none was approved in 2008. At the same time, the prevalence of resistance in disease-causing bacteria has steadily been increasing.⁵ In order to avert an impending health crisis new antibiotics are therefore desperately needed.

Two strategies for discovering new antibacterial compounds are currently employed. The first relies on synthetic tailoring of known antibiotic scaffolds in order to circumvent resistance pathways and/or to improve such a drug’s properties.⁶ The second strategy seeks new targets which have

not been exploited previously, and which could lead to new classes of antibiotics. Comparing these two strategies, it is clear that the discovery of new scaffolds acting on the well-defined targets of known antibiotics is more likely to lead to new antibiotics in the short term. However, a drawback of this strategy is that resistance to such compounds could rapidly be acquired by modification of the resistance mechanisms that have already developed against these targets. Ideally, these two strategies should therefore be pursued in combination and in a complementary fashion.

1.2 Treatment of Staphylococcal infections

Staphylococcus aureus is a Gram-positive bacterium that is a major cause of nosocomial infections, and is therefore also the bacterial pathogen most frequently isolated from patients with hospital-acquired infections.⁷ *S. aureus* was the first organism that was identified to show resistance against penicillin in the 1950s, a mere decade after it was first used clinically. After the introduction of methicillin - a β -lactam antibiotic which is resistant to the penicillinase enzyme produced by most penicillin-resistant bacteria - in the 1960s, *S. aureus* also acquired resistance to this antibiotic within two years.⁷ These methicillin-resistant strains of *S. aureus* (referred to as MRSA, although the abbreviation is also used to indicate multi-drug resistant *S. aureus*) are only treatable by vancomycin. Since MRSA account for nearly 50% of all hospital-acquired *S. aureus* infections it is therefore not surprising that vancomycin-resistant strains of *S. aureus* (VRSA) have also been identified.

Although not all infections by *S. aureus* are invasive, it is now the leading cause of death by infectious agents in the USA and has surpassed HIV/AIDS.⁸ Deaths due to *S. aureus* infections have almost doubled during the period of 2001 to 2005 in the UK. In addition, a recent study conducted in the emergency departments of US hospitals showed that in 59% of patients with skin and soft tissue infections, MRSA was the most prevalent causative organism.⁹ MRSA has also recently emerged in healthy individuals outside of health care facilities, and this is referred to as community-associated MRSA (CA-MRSA). This was revealed by a study which showed that 13% of ~9000 observed cases of MRSA was in fact CA-MRSA.¹⁰ These observations show that alternative antibiotics for the treatment of *S. aureus* infections are desperately needed.

1.2.1 Current treatments

Only three new classes of antibacterial agents were approved for treatment of bacterial infections since 1962. These are the oxazolidinones (linezolid) in 2000, the lipopeptides (daptomycin) in 2003 and the mutilins (retapamulin) in 2009.^{3,6} The successful introduction of these new antibiotic classes is a great cause for optimism, however they all target the same cellular processes that

serve as the point of action of the established antibiotic agents. These include four processes: protein synthesis, nucleic acid synthesis, cell-wall synthesis or folate biosynthesis.⁴ Consequently the discovery of these new antibiotic classes does not expand the scope of antibiotic targets that can be clinically exploited.

In regards to *S. aureus* infections, vancomycin (which was discovered in the 1950s) currently still remains the last line of treatment.¹¹ In light of this fact, and considering the rise of also VRSA, we therefore set out in this study to identify new targets for the development of antistaphylococcal agents which have novel and as yet unexploited mechanisms of action.

1.2.2 New targets/drugs for antistaphylococcal agents

1.2.2.1 CoADR and redox state

In most organisms redox homeostasis is maintained by a low molecular weight thiol/disulfide reductase enzyme system. When the redox homeostasis of a pathogen is disturbed by the reactive oxygen species (ROS) produced by the defense mechanisms of the host's immune system, these low molecular weight thiols are sacrificially oxidized and form disulfides in the process. The redox balance is maintained by restoration of the reduced thiol by reduction of the disulfides by specific disulfide reductase enzymes which form part of the family of pyridine nucleotide disulfide oxidoreductases (PNDORs).

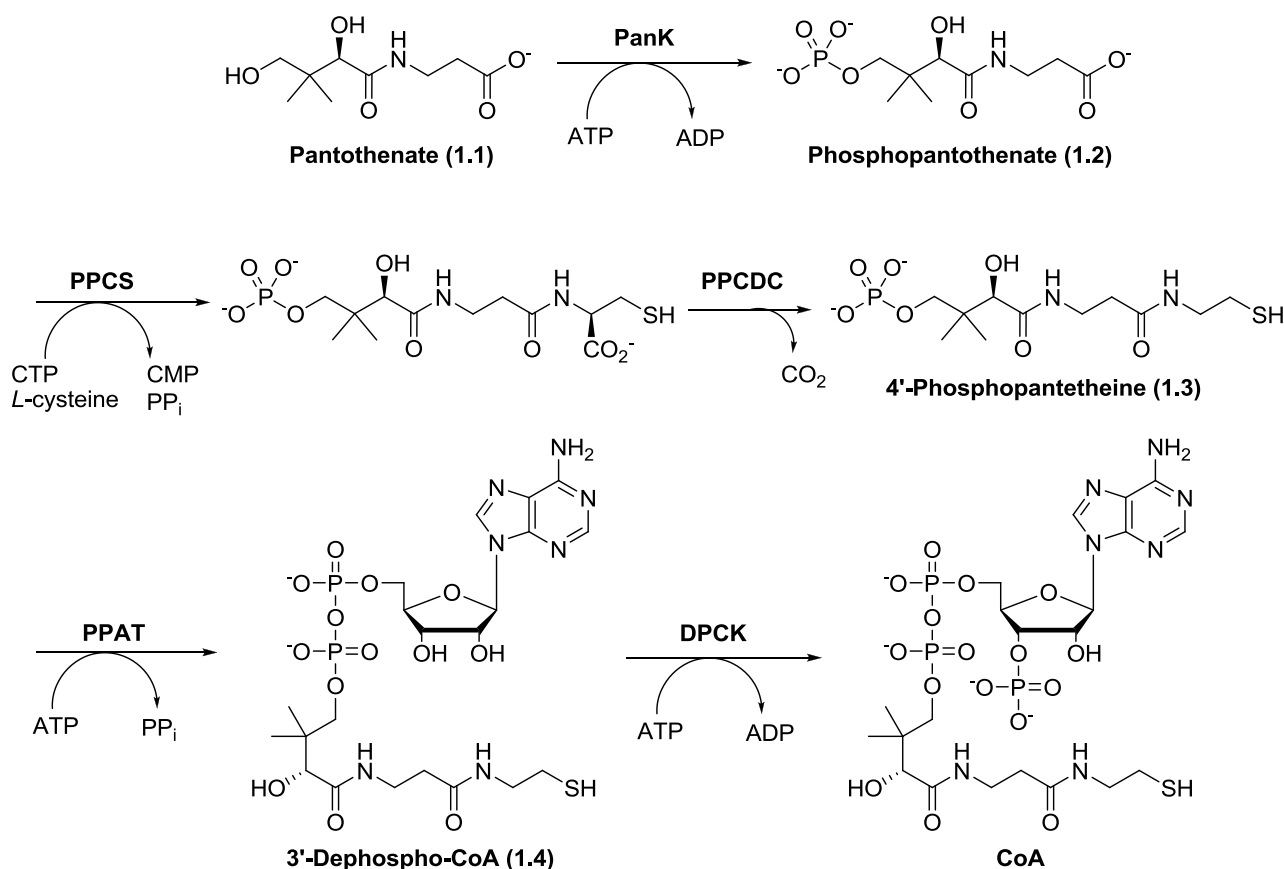
In most organisms (including humans, *E. coli* and the malaria parasite *Plasmodium falciparum*) glutathione and glutathione reductase (GR) constitute the main low molecular weight thiol/disulfide reductase system.¹² However, many pathogens use their own unique disulfides to achieve the same result. For example, in *Trypanosoma* species (the causative agents of diseases such as sleeping sickness and Chagas' disease) a glutathione-derivative called trypanothione is the major low molecular thiol, and is maintained in a reduced state by the enzyme trypanothione reductase (TR). Interestingly, redox homeostasis in *S. aureus* and some species of *Bacillus* is maintained by high concentrations of the essential central metabolite coenzyme A (CoA) and the enzyme CoA disulfide reductase (CoADR).¹³ This suggests that the production of CoA (i.e. CoA biosynthesis) and the maintenance of redox balance (the CoADR enzyme) could be potential drug targets in *S. aureus*.

1.2.2.2 CoA biosynthetic enzymes as drug targets in bacteria

CoA is an important co-factor in many enzymatic reactions and is the major acyl carrier in biological systems. Consistent with these important roles associated with CoA it has been shown

that all of the enzymes involved in its biosynthesis are essential in *E. coli*.¹⁴ Since CoA functions as the major low molecular weight thiol in *S. aureus*, its biosynthesis is also fundamentally important to this organism for other reasons. While some of the CoA biosynthetic enzymes have been targeted in drug discovery efforts, most remain unexploited with no known inhibitors.

CoA is biosynthesized in five steps from pantothenate (vitamin B₅) in bacteria. In the first step the ATP-dependent phosphorylation of the 4-hydroxy group of pantothenate is catalyzed by pantothenate kinase (PanK; CoaA) (Scheme 1.1). In the second step, catalyzed by phosphopantothenoylcysteine synthetase (PPCS; CoaB), the carboxylate of phosphopantothenate is activated by cytidylylation, followed by nucleophilic attack by the amine of cysteine on the CMP-activated carboxylate to form phosphopantothenoylcysteine. This is followed by decarboxylation of the carboxylate of the introduced cysteine moiety by the enzyme phosphopantothenoylcysteine decarboxylase (PPCDC; CoaC). The product of this reaction, 4'-phosphopantetheine (1.3), is adenylated in the next step by phosphopantothenoyl adenyltransferase (PPAT; CoaD) to form dephospho-CoA. In the fifth and last step, ATP-dependent phosphorylation of dephospho-CoA is performed by dephospho-CoA kinase (DPCK; CoaE).



Scheme 1.1. Summary of the biosynthetic pathway of CoA.

1.2.2.3 The Antibiotic CJ-15,801

In 2001 Sugie *et al.* isolated a pantothenic acid analogue (referred to as CJ-15,801) from the fungus *Seimatosporium* sp which potently inhibited the growth of various strains of MRSA (Figure 1.1).¹⁵ Since the structures of pantothenic acid and CJ-15,801 are so similar, it is more than likely that this compound exerts its antibacterial effect through the inhibition of one or more of the CoA biosynthetic enzymes, or of a CoA-utilizing enzyme. The elucidation of its mechanism of action could therefore lead to the identification of a new CoA-based target for antistaphylococcal agents.

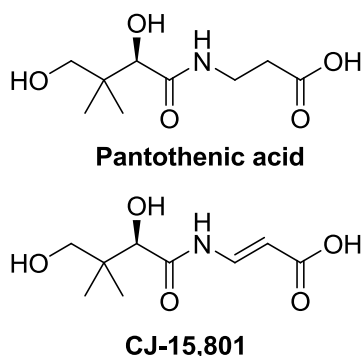


Figure 1.1. Comparison of pantothenic acid and the reported antibiotic CJ-15,801.

1.3 Previous work on identified targets

In this section, a discussion of the current status of the drug development efforts regarding the targets highlighted above will be presented.

1.3.1 CoADR

To date only a few studies on *S. aureus* CoADR (SaCoADR) have been published. These are all concerned with the identification, production, kinetic and structural characterization of the enzyme. Kinetic studies on CoADR have revealed that, unlike glutathione and trypanothione reductase enzymes, CoADR utilizes only a single active site cysteine for the reduction of its substrate instead of the usual two used by other disulfide reductases. The crystal structure of SaCoADR has been solved and shows CoA bound to the enzyme by means of a mixed disulfide bond between the active site cysteine of the enzyme and the thiol of CoA.¹⁶ The majority of the non-covalent interactions between CoADR and CoA involves the latter's phosphopantetheine moiety, with its adenine and ribose moieties being less important for CoA recognition. Analysis of the crystal structure also revealed an active site tyrosine in close proximity to the disulfide bond, which the authors propose participated in acid-base catalysis during the reduction of CoA disulfide.

CoADR homologues are also found in a small group of other organisms of which the human pathogen *Borrelia burgdorferi*, the causative agent of Lyme disease, and *Bacillus anthracis* (*BaCoADR*), a category A biodefense pathogen, are the most important.¹⁷ The crystal structure as well as a full kinetic characterization of *BaCoADR* have recently been published.^{18,19}

The idea of pursuing disulfide reductase enzymes as targets for drug development is not new, and both GR and TR have been targeted by numerous drug discovery efforts.^{12,20,21} While these observations suggest that CoADR might also be a viable target for antibacterial drug development, no inhibition studies of CoADR have been published to date.

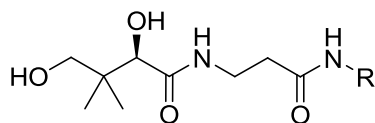
1.3.2 CoA biosynthesis and utilization as target in antibacterial development

The CoA biosynthetic enzymes that are involved in the salvage of CoA (i.e. PanK, PPAT and DPCK) from various bacteria, including *S. aureus*, have been identified and overexpressed.²² A short discussion on each of these enzymes, with a focus on the status of the drug developments that target them, follows below.

1.3.2.1 PanK and the CoA salvage pathway

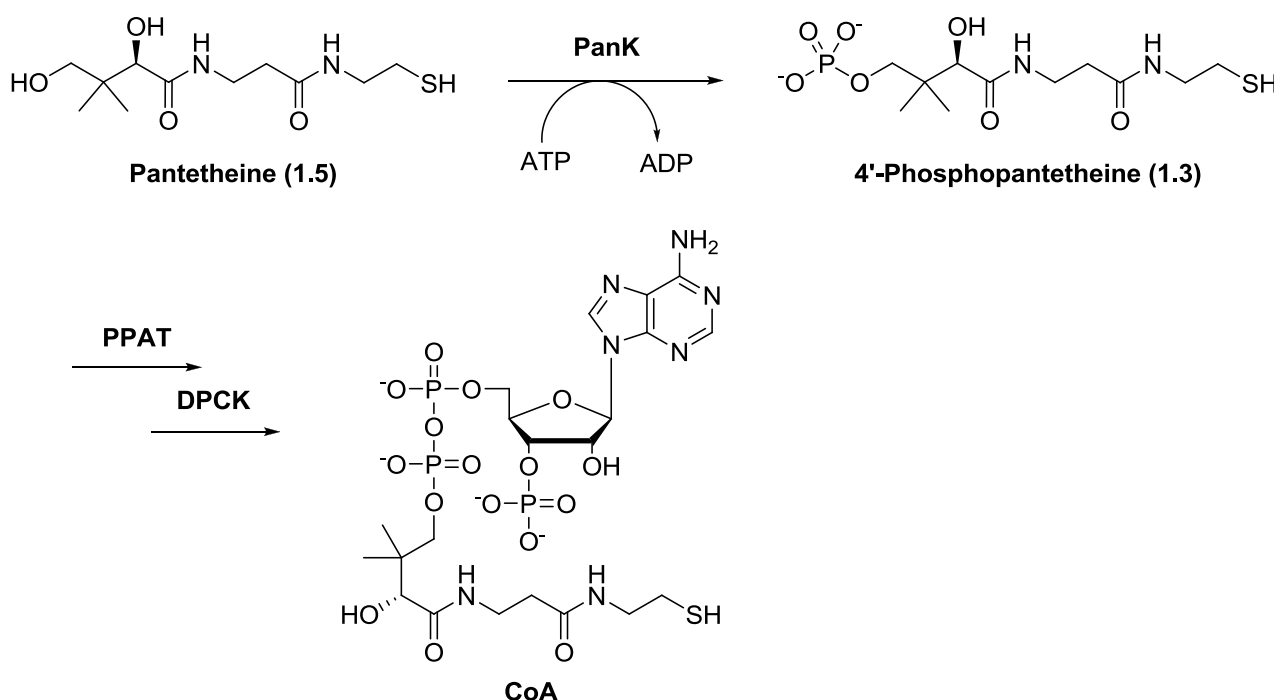
PanK catalyses the ATP dependant phosphorylation of the 4'-hydroxyl group of pantothenate and is the first committed step of CoA biosynthesis. It has been studied extensively and has been proposed to be the gatekeeper of this pathway. It has also been established that bacterial PanK enzymes are able to phosphorylate a group of compounds known as the pantothenamides. As their name suggests, pantothenamides are *N*-substituted amides of pantothenate and are typified by the compounds presented in Table 1.1. Many of these compounds have been shown to be potent inhibitors of *S. aureus* growth in studies conducted in our laboratory (M de Villiers & E Strauss unpublished results) as well as in those of others.²³ The relaxed substrate specificity of particularly *S. aureus* PanK (*SaPanK*) and the availability of a crystal structure of this enzyme have made it an attractive drug target.

Table 1.1. Most potent inhibitors of staphylococcal growth with accompanying minimal inhibitory concentration (MIC) as determined in our laboratory (M de Villiers & E Strauss unpublished results).



R =	MIC (μM)	R =	MIC (μM)
	50		50
	25		25
	5		25
	1.25		50
	1.25		50

The ability of PanK to phosphorylate a variety of pantothenamides (i.e. its relaxed substrate specificity) stems from the CoA salvage pathway (Scheme 1.2), in which this enzyme also phosphorylates pantetheine to produce phosphopantetheine directly, without the involvement of the PPCS and PPCDC enzymes. Under circumstance in which the CoA salvage pathway is in operation, inhibitors of PPCS and PPCDC would therefore not necessarily block CoA biosynthesis. However, since pantothenate is much more readily available than pantetheine this is unlikely to be of a huge concern in most cases.



Scheme 1.2. The CoA salvage pathway is enabled by the ability of PanK to phosphorylate pantetheine which is then transformed to CoA by PPAT and DPCK.

The antibacterial properties of pantothenamides are thought to be caused by one of two possible mechanisms of action. First, they may inhibit PanK's pantothenate kinase activity directly or by acting as alternate substrates of the enzyme that occupy it in this manner. If they act as PanK substrates, a second mechanism of action is also possible in which these amides are subsequently transformed by the PPAT and DPCK enzymes into CoA analogues which can then act as inhibitors of CoA-dependent and -utilizing enzymes. To distinguish between these two possibilities the causes of the pantothenamide-induced growth inhibition of *E. coli* and *S. aureus* have been studied extensively in recent years.²³ These studies have shown that in *E. coli*, pantothenamides mainly act as substrates of PanK, and do not directly inhibit the enzyme's ability to perform a phosphoryl transfer reaction. Therefore, in *E. coli* pantothenamides that are substrates of PanK will be converted to the corresponding potentially inhibitory CoA analogues. In contrast, preliminary studies conducted in our group have shown that in the case of *S. aureus* some pantothenamides may act as direct inhibitors of PanK, while others are also converted to CoA analogues that exert their effect down-stream. How the distinction between these mechanisms of action is made is the focus of on-going studies.

1.3.2.2 PPCS/PPCDC

In bacteria, PPCS and PPCDC are expressed as a single enzyme that is capable of performing both these functions. This bifunctional protein performs both the second and third step of CoA biosynthesis to produce 4-phosphopanthoine **1.3** from phosphopantothenate **1.4**. However, most studies reported on either of these activities were performed on a monofunctional *E. coli* enzyme obtained by cloning and expression of desired domain of either PPCS or PPCDC. While PPCDC has not been investigated in any drug discovery efforts to date (a mechanism-based inhibitor has been described²⁴), the first report of PPCS inhibitors that act on the enzymes found in Enterobacteria was recently published (Figure 1.2).²⁵ These compounds are substrate mimics of the phosphopantothenoyl cytidylate reaction intermediate that were created by replacing the phospho-anhydride group with a stable phosphodiester or sulfamate functionality. These compounds prevented amide formation by nucleophilic attack and were found to be potent tight-binding inhibitors that were also selective for bacterial PPCS enzymes compared to their human counterpart. Unfortunately, the polar nature of these compounds prevents them from crossing the bacterial cell membrane, and they therefore do not show bacterial growth inhibition.

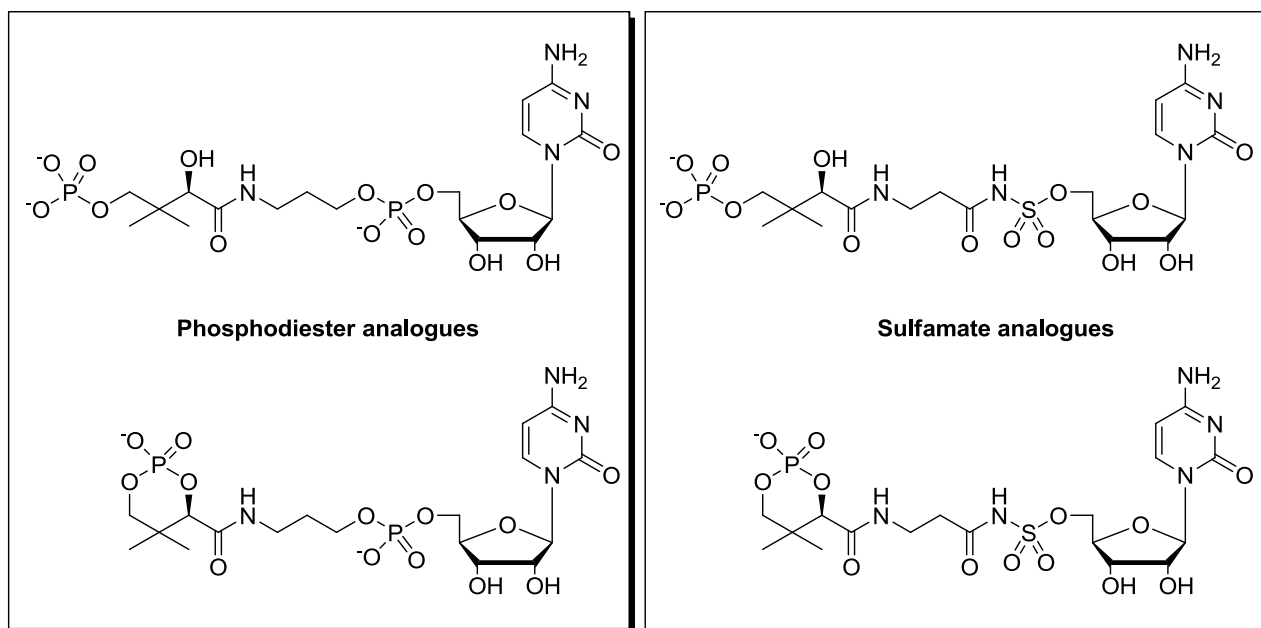


Figure 1.2. Reported selective inhibitors of bacterial PPCS. These inhibitors were designed to mimic the reaction intermediate.

1.3.2.3 PPAT and DPCK

Similarly to PanK, bacterial PPAT and DPCK enzymes also show relaxed substrate specificity. Furthermore, *E. coli* PPAT (*EcPPAT*) and human PPAT enzymes are completely different proteins

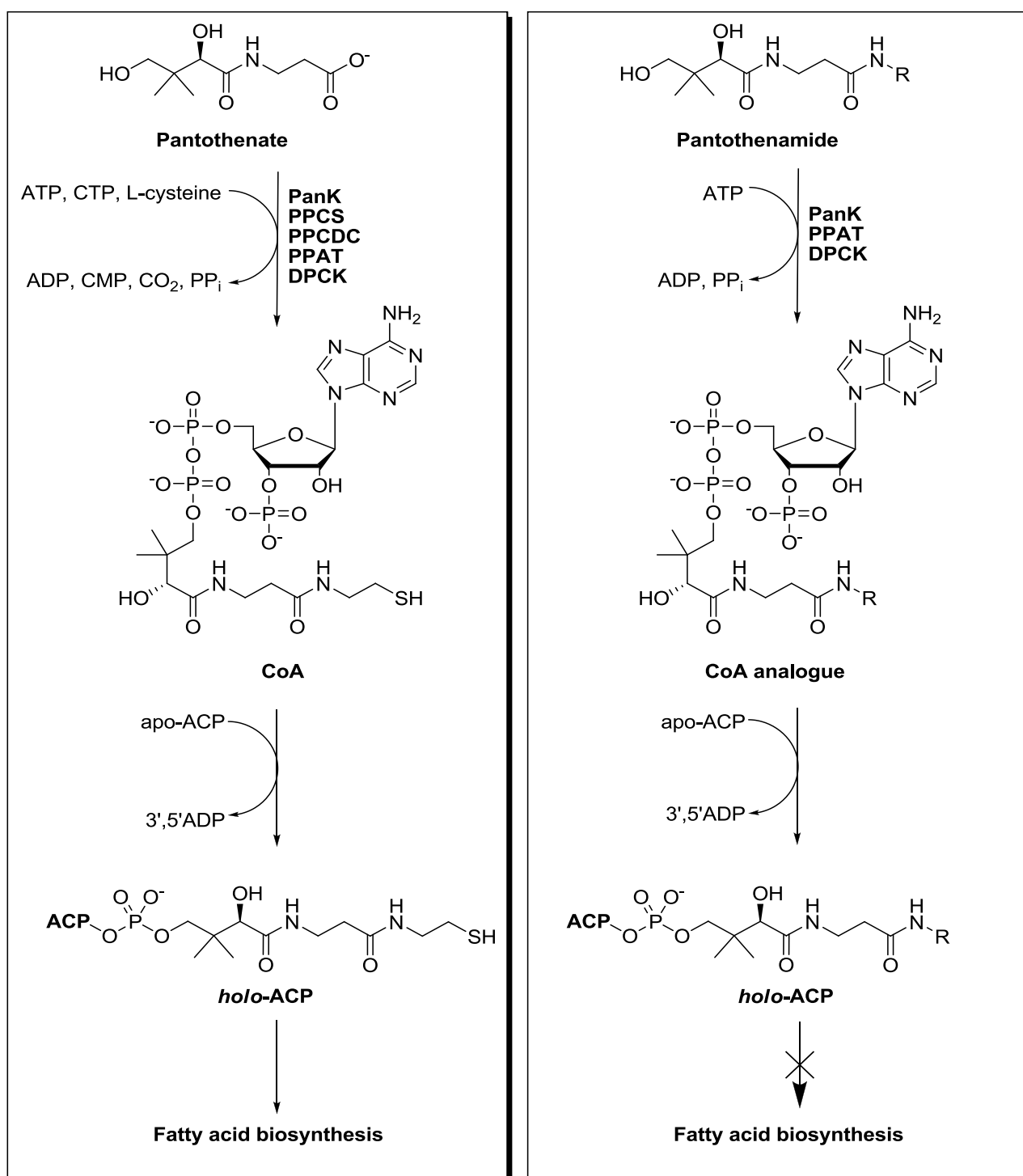
with little sequence homology.²⁶ In a recent study of bacterial CoA biosynthetic enzymes PPAT emerged as the most attractive candidate for development of broad spectrum antibacterials due to the conserved nature of its encoding gene among a wide diversity of bacteria.¹⁴ It is therefore not surprising that a number of potent *Ec*PPAT inhibitors have been described, although many of these have only been reported in the patent literature.²⁷ The classes of compound that have been tested included drug-like scaffolds such as bispiperidines, [(heterocyclyl)methylene]-substituted benzoic acids and nicotinic acids, aromatic sulfonamides, dipeptides, and tetrahydro- β -carboline derivatives. Of these, the dipeptide Fmoc-Glu-D-His-NHCH₂CH(CH₃)₂ was the most potent and selective inhibitor with an IC₅₀ of 6 nM against the *Ec*PPAT, while porcine PPAT was not inhibited. Unfortunately, these compounds showed no bacterial growth inhibition.

In contrast, no inhibitors of DPCK enzymes have been identified to date. While *E. coli* DPCK (*Ec*DPCK) and its human counterpart show similar sequence homology, *Ec*DPCK has a remarkably low affinity for its substrate with K_M close to the mM range. This characteristic may potentially be exploited in the design of selective *Ec*DPCK inhibitors. Moreover, the *E. coli* PPAT and DPCK enzymes have been fully characterized kinetically and several crystal structures have been solved for both enzyme activities.

1.3.2.4 CoA-utilizing enzymes and the *holo*-acyl carrier protein as down-stream targets

It is well-documented that once pantothenamides are taken up by *S. aureus* they are converted to CoA analogues inside the cell by the CoA salvage pathway enzymes PanK, PPAT and DPCK.²² CoA analogues formed in this manner can potentially inhibit two sets of down-stream targets. The first set involves the CoA-utilizing and -dependent enzymes that may be competitively inhibited by these analogues of their natural substrate. The second set of affected enzymes depends on the acyl carrier protein (ACP). The *holo*-ACP derives its 4'-phosphopanthetheine arm directly from CoA, and therefore the presence of CoA analogues in the cell can similarly lead to the transfer of their phosphopantothenamide moieties to *apo*-ACP (Scheme 1.3).²⁸ Since these moieties do not contain a thiol that can be esterified to the various fatty acids of which ACP is a carrier, the inactive ACP that accumulates in the cell as a result leads to the disruption of fatty acid biosynthesis. It is this latter effect that has been proposed to be the main cause of the antibiotic effect of pantothenamides in most bacteria, rather than interference with CoA biosynthesis as was initially thought.

The success with these approaches inspired us to design pantothenamides which could inhibit CoADR after being converted to a CoA analogue *in vivo*.



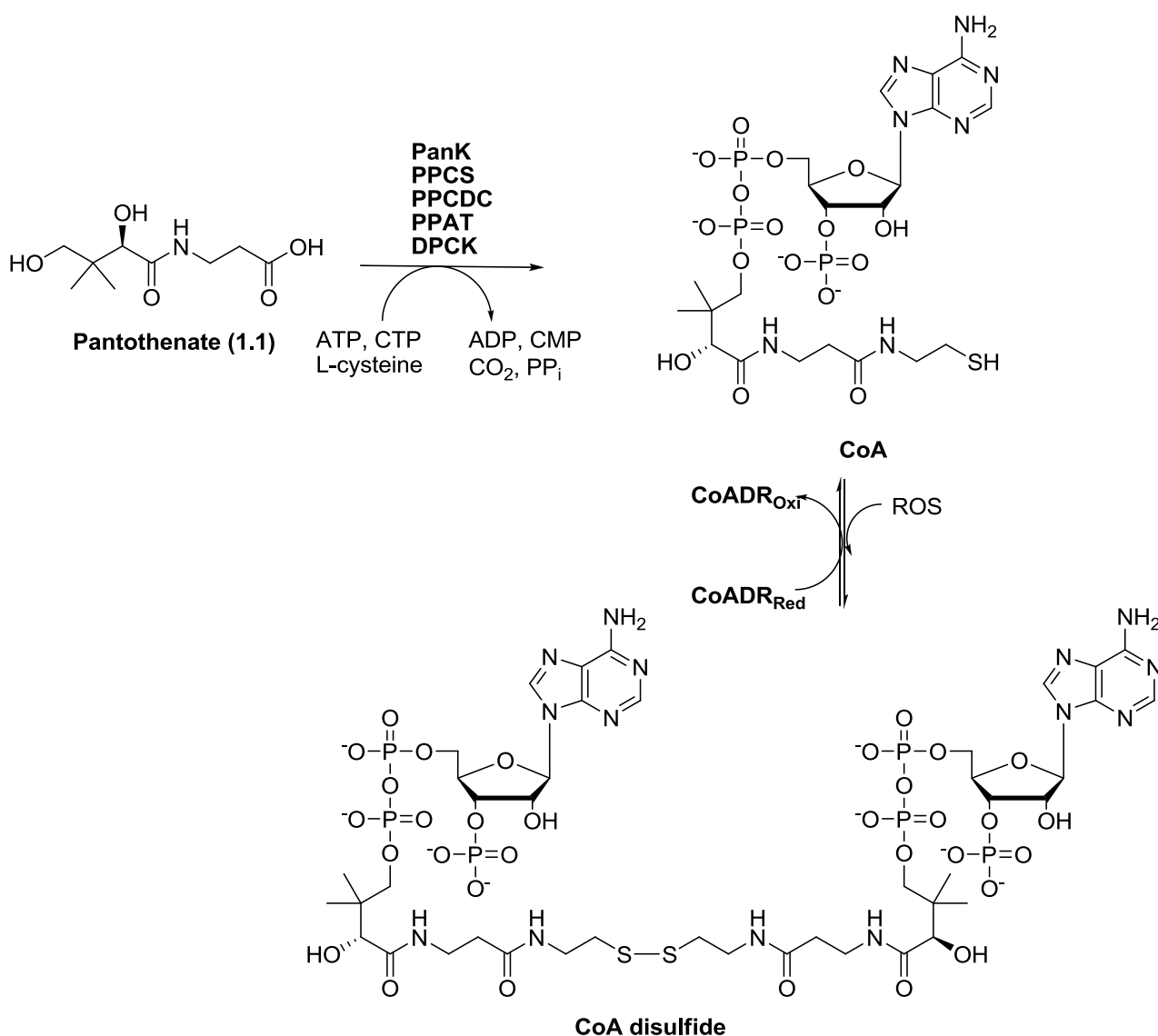
Scheme 1.3. Metabolism of pantothenate and pantothenamides in *E. coli* and *S. aureus*. Left panel: the phosphopantetheine moiety of CoA is transferred to apo-ACP to form holo-ACP for fatty acid biosynthesis. Right panel: when pantothenamides are transformed to CoA analogues by PanK, PPAT and DPCK they are also transferred to apo-ACP, thereby inactivating ACP and blocking fatty acid biosynthesis.

1.3.3 CJ-15,801

Since the antistaphylococcal properties of CJ-5,801 was first reported, only a few studies in this regard have been published, most of which are concerned with the synthesis of this interesting compound.²⁹ To date only one study on the mechanism of action of CJ-15,801 has been published.³⁰ This study was conducted on *Plasmodium falciparum* (the causative agent of malaria) and showed that it disrupts pantothenate metabolism in this organism. Furthermore, it also showed that CJ-15,801 had no effect on the growth of mammalian cells. These findings suggest that further investigations on the antibacterial properties of this natural product are warranted.

1.4 Objectives of this study

In this study we were interested in exploiting the unique CoA-based metabolism of the human pathogen *S. aureus*, which solely relies on this compound and the associated CoADR enzyme to maintain its intracellular redox balance, as potential targets for drug development (Scheme 1.4). We set out to achieve this by following two approaches: first, by inhibition of the CoADR enzyme directly to interfere with the organism's ability to counter oxidative damage, and second, by inhibition of the CoA biosynthetic enzymes to reduce the amount of available CoA. Keeping these approaches in mind the objectives of this study are three-fold as discussed below.

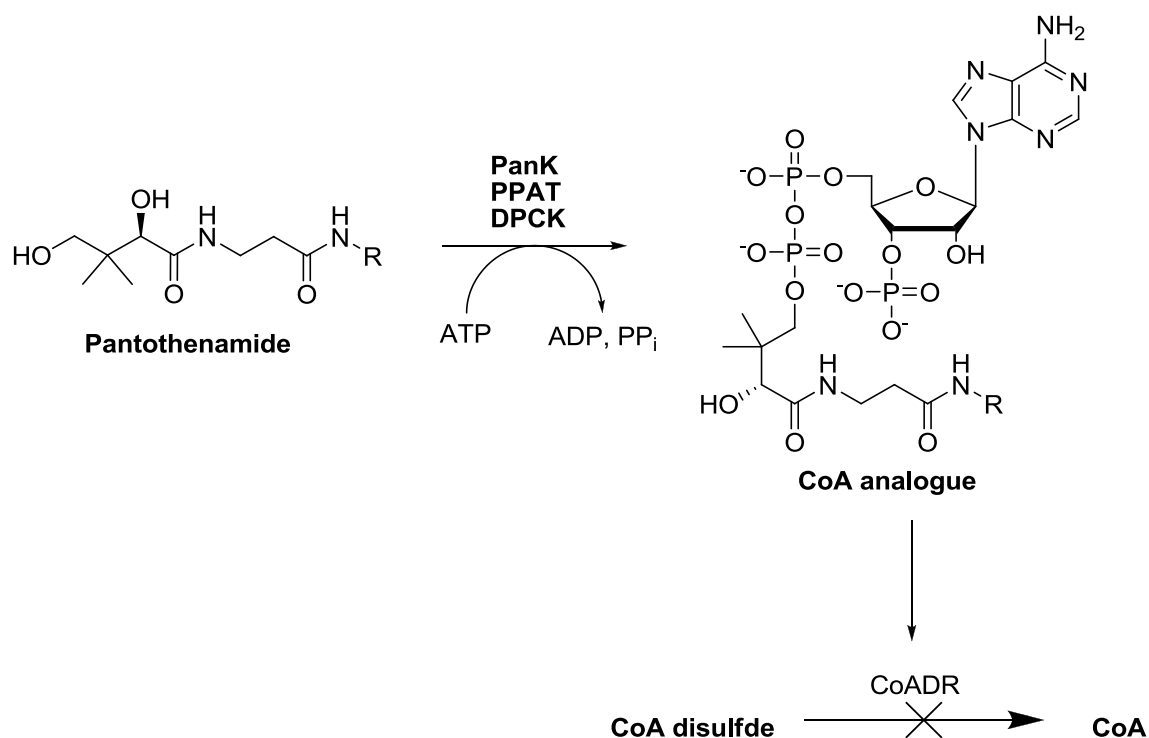


Scheme 1.4. Summary of CoA metabolism in *S. aureus*. After being biosynthesized from pantothenate, CoA can react with ROS to form CoA disulfide which is then reduced by the enzyme CoADR.

1.4.1 Objective 1: Development of Michael acceptor-containing CoA analogues as inhibitors of CoADR

The first objective is targeted at the discovery of specific CoADR-directed inhibitors. Since CoADR has a unique mechanism that depends on a single active site cysteine for catalysis, we proposed to achieve this by employing an inhibition strategy similar to the approach that has been used successfully in the irreversible inhibition of cysteine proteases. We therefore set out to synthesize Michael acceptor-containing CoA analogues which could inhibit CoADR by alkylation of the active site cysteine. This target-based strategy involved the synthesis of Michael acceptor-containing pantothenamides, followed by biotransformation of these pantothenamides to the corresponding

CoA analogues. A full kinetic characterization was subsequently performed on analogues which showed inhibition of CoADR. Finally, we also determined if the parent pantothenamides of identified CoA analogue inhibitors also inhibits *S. aureus* growth (Scheme 1.5). This was done to explore the potential of using this strategy in the development of novel antistaphylococcal agents. The work pertaining to this objective is described in Chapter 2.



Scheme 1.5. After entering the cell pantothenamides are converted to CoA analogues which could inhibit SaCoADR.

1.4.2 Objective 2: Mechanism of action of antibiotic CJ-15,801

The second objective is to elucidate the mechanism of action of the natural product CJ-15,801. Demonstration of a mechanism of action that results in the reduction of the available CoA concentration would confirm this as a viable strategy for the development of antistaphylococcal agents. The studies and results aimed at achieving this goal is given in Chapter 3.

1.4.3 Objective 3: Synthesis of antibiotic CJ-15,801 and its analogues

The last objective of this study was to find a new, scalable synthesis of the antibiotic CJ-15,801 that can also be modified for the production of CJ-15,801-based analogues. Although methodologies for the preparation of this compound have been published, they all suffer from one or other drawback. We seek to introduce a methodology that would facilitate the production of CJ-

15,801 and its analogues, using a more convenient methodology and on a larger scale. Our efforts and successes towards employing such an alternative method are described in Chapter 4.

1.5 References

1. Davies, J.; Davies, D., Origins and evolution of antibiotic resistance. *Microbiol. Mol. Biol. Rev.* **74** (3), 417-33.
2. Talbot, G. H.; Bradley, J.; Edwards, J. E., Jr.; Gilbert, D.; Scheld, M.; Bartlett, J. G., Bad bugs need drugs: an update on the development pipeline from the Antimicrobial Availability Task Force of the Infectious Diseases Society of America. *Clin. Infect. Dis.* **2006**, *42* (5), 657-68.
3. Lock, R. L.; Harry, E. J., Cell-division inhibitors: new insights for future antibiotics. *Nat. Rev. Drug. Discov.* **2008**, *7* (4), 324-38.
4. Walsh, C., Where will new antibiotics come from? *Nat. Rev. Microbiol.* **2003**, *1* (1), 65-70.
5. Liu, C. I.; Liu, G. Y.; Song, Y.; Yin, F.; Hensler, M. E.; Jeng, W. Y.; Nizet, V.; Wang, A. H.; Oldfield, E., A cholesterol biosynthesis inhibitor blocks *Staphylococcus aureus* virulence. *Science* **2008**, *319* (5868), 1391-1394.
6. Fischbach, M. A.; Walsh, C. T., Antibiotics for Emerging Pathogens. *Science* **2009**, *325* (5944), 1089-1093.
7. de Lencastre, H.; Oliveira, D.; Tomasz, A., Antibiotic resistant *Staphylococcus aureus*: a paradigm of adaptive power. *Curr. Opin. Microbiol.* **2007**, *10* (5), 428-435.
8. DeLeo, F. R.; Chambers, H. F., Reemergence of antibiotic-resistant *Staphylococcus aureus* in the genomics era. *J. Clin. Invest.* **2009**, *119* (9), 2464-74.
9. Moran, G. J.; Krishnadasan, A.; Gorwitz, R. J.; Fosheim, G. E.; McDougal, L. K.; Carey, R. B.; Talan, D. A., Methicillin-resistant *S. aureus* infections among patients in the emergency department. *N. Engl. J. Med.* **2006**, *355* (7), 666-674.
10. Klevens, R. M.; Morrison, M. A.; Nadle, J.; Petit, S.; Gershman, K.; Ray, S.; Harrison, L. H.; Lynfield, R.; Dumyati, G.; Townes, J. M.; Craig, A. S.; Zell, E. R.; Fosheim, G. E.; McDougal, L. K.; Carey, R. B.; Fridkin, S. K., Invasive methicillin-resistant *Staphylococcus aureus* infections in the united states. *J. Am. Med. Assoc.* **2007**, *298* (15), 1763-1771.
11. Weigel, L. M.; Clewell, D. B.; Gill, S. R.; Clark, N. C.; McDougal, L. K.; Flannagan, S. E.; Kolonay, J. F.; Shetty, J.; Killgore, G. E.; Tenover, F. C., Genetic analysis of a high-level vancomycin-resistant isolate of *Staphylococcus aureus*. *Science* **2003**, *302* (5650), 1569-1571.
12. Bauer, H.; Fritz-Wolf, K.; Winzer, A.; Kuehner, S.; Little, S.; Yardley, V.; Vezin, H.; Palfey, B.; Schirmer, R. H.; Davioud-Charvet, E., A Fluoro Analogue of the Menadione Derivative 6-[2'-(3'-Methyl)-1',4'-naphthoquinolyl]hexanoic Acid Is a Suicide Substrate of Glutathione Reductase. Crystal Structure of the Alkylated Human Enzyme. *J. Am. Chem. Soc.* **2006**, *128* (33), 10784-10794.
13. delCardayre, S. B.; Stock, K. P.; Newton, G. L.; Fahey, R. C.; Davies, J. E., Coenzyme A disulfide reductase, the primary low molecular weight disulfide reductase from *Staphylococcus aureus*. Purification and characterization of the native enzyme. *J. Biol. Chem.* **1998**, *273* (10), 5744-5751.
14. Gerdes, S. Y.; Scholle, M. D.; D'Souza, M.; Bernal, A.; Baev, M. V.; Farrell, M.; Kurnasov, O. V.; Daugherty, M. D.; Mseeh, F.; Polanuyer, B. M.; Campbell, J. W.; Anantha, S.; Shatalin, K. Y.; Chowdhury, S. A. K.; Fonstein, M. Y.; Osterman, A. L., From genetic footprinting to antimicrobial drug targets: examples in cofactor biosynthetic pathways. *J. Bacteriol.* **2002**, *184* (16), 4555-4572.

15. Sugie, Y.; Dekker, K. A.; Hirai, H.; Ichiba, T.; Ishiguro, M.; Shiomi, Y.; Sugiura, A.; Brennan, L.; Duignan, J.; Huang, L. H.; Sutcliffe, J.; Kojima, Y., CJ-15,801, a novel antibiotic from a fungus, *Seimatosporium* sp. *J. Antibiot.* **2001**, *54* (12), 1060-1065.
16. Mallett, T. C.; Wallen, J. R.; Karplus, P. A.; Sakai, H.; Tsukihara, T.; Claiborne, A., Structure of Coenzyme A-Disulfide Reductase from *Staphylococcus aureus* at 1.54 Å Resolution. *Biochemistry* **2006**, *45* (38), 11278-11289.
17. Boylan, J. A.; Hummel, C. S.; Benoit, S.; Garcia-Lara, J.; Treglown-Downey, J.; Crane, E. J., III; Gherardini, F. C., *Borrelia burgdorferi* bb0728 encodes a coenzyme A disulphide reductase whose function suggests a role in intracellular redox and the oxidative stress response. *Mol. Microbiol.* **2006**, *59* (2), 475-486.
18. Wallen, J. R.; Paige, C.; Mallett, T. C.; Karplus, P. A.; Claiborne, A., Pyridine Nucleotide Complexes with *Bacillus anthracis* Coenzyme A-Disulfide Reductase: A Structural Analysis of Dual NAD(P)H Specificity. *Biochemistry* **2008**, *47* (18), 5182-5193.
19. Wallen, J. R.; Mallett, T. C.; Boles, W.; Parsonage, D.; Furdui, C. M.; Karplus, P. A.; Claiborne, A., Crystal structure and catalytic properties of *Bacillus anthracis* CoADR-RHD: Implications for flavin-linked sulfur trafficking. *Biochemistry* **2009**, *48* (40), 9650-9667.
20. Friebohn, W.; Jannack, B.; Wenzel, N.; Furrer, J.; Oeser, T.; Sanchez, C. P.; Lanzer, M.; Yardley, V.; Becker, K.; Davioud-Charvet, E., Antimalarial Dual Drugs Based on Potent Inhibitors of Glutathione Reductase from *Plasmodium falciparum*. *J. Med. Chem.* **2008**, *51* (5), 1260-1277.
21. Krauth-Siegel, R. L.; Bauer, H.; Schirmer, R. H., Dithiol proteins as guardians of the intracellular redox milieu in parasites: Old and new drug targets in trypanosomes and malaria-causing plasmodia. *Angew. Chem., Int. Ed.* **2005**, *44* (5), 690-715.
22. Leonardi, R.; Chohnan, S.; Zhang, Y.-M.; Virga, K. G.; Lee, R. E.; Rock, C. O.; Jackowski, S., A pantothenate kinase from *Staphylococcus aureus* refractory to feedback regulation by coenzyme A. *J. Biol. Chem.* **2005**, *280* (5), 3314-3322.
23. Virga, K. G.; Zhang, Y.-M.; Leonardi, R.; Ivey, R. A.; Hevener, K.; Park, H.-W.; Jackowski, S.; Rock, C. O.; Lee, R. E., Structure-activity relationships and enzyme inhibition of pantothenamide-type pantothenate kinase inhibitors. *Bioorg. Med. Chem.* **2006**, *14* (4), 1007-1020.
24. Strauss, E.; Zhai, H.; Brand, L. A.; McLafferty, F. W.; Begley, T. P., Mechanistic Studies on Phosphopantothenoylcysteine Decarboxylase: Trapping of an Enethiolate Intermediate with a Mechanism-Based Inactivating Agent. *Biochemistry* **2004**, *43* (49), 15520-15533.
25. Patrone, J. D.; Yao, J.; Scott, N. E.; Dotson, G. D., Selective Inhibitors of Bacterial Phosphopantothenoylcysteine Synthetase. *J. Am. Chem. Soc.* **2009**, *131* (45), 16340-16341.
26. Daugherty, M.; Polanuyer, B.; Farrell, M.; Scholle, M.; Lykidis, A.; De, C.-L. V.; Osterman, A., Complete reconstitution of the human coenzyme A biosynthetic pathway via comparative genomics. *J. Biol. Chem.* **2002**, *277* (24), 21431-21439.
27. Zhao, L.; Allanson, N. M.; Thomson, S. P.; Maclean, J. K. F.; Barker, J. J.; Primrose, W. U.; Tyler, P. D.; Lewendon, A., Inhibitors of phosphopantetheine adenylyltransferase. *Eur. J. Med. Chem.* **2003**, *38* (4), 345-349.
28. Mercer, A. C.; Meier, J. L.; Hur, G. H.; Smith, A. R.; Burkart, M. D., Antibiotic evaluation and *in vivo* analysis of alkynyl Coenzyme A antimetabolites in *Escherichia coli*. *Bioorg. Med. Chem. Lett.* **2008**, *18* (22), 5991-5994.

29. Han, C.; Shen, R.; Su, S.; Porco, J. A., Jr., Copper-Mediated Synthesis of *N*-Acyl Vinylogous Carbamic Acids and Derivatives: Synthesis of the Antibiotic CJ-15,801. *Org. Lett.* **2004**, 6 (1), 27-30.
30. Saliba, K. J.; Kirk, K., CJ-15,801, a fungal natural product, inhibits the intraerythrocytic stage of *Plasmodium falciparum in vitro* via an effect on pantothenic acid utilization. *J. Molbioparra.* **2005**, 141 (1), 129-131.

Chapter 2

Design, synthesis and evaluation of inhibitors of CoADR

2.1 JACS Communication

Parts of results of the studies described in this chapter have been published in the *Journal of the American Chemical Society* as a communication. The actual publication is reprinted¹ on the next page, followed by the accompanying supplementary information. The unpublished parts of the studies are presented thereafter.

¹ Reproduced with permission from “Van der Westhuyzen, R. and Strauss, E. (2010) *J. Am. Chem. Soc.* Articles ASAP. DOI: 10.1021/ja106204m”. Copyright [2010] American Chemical Society.
<http://pubs.acs.org/doi/abs/10.1021/ja106204m>

Michael Acceptor-Containing Coenzyme A Analogues As Inhibitors of the Atypical Coenzyme A Disulfide Reductase from *Staphylococcus aureus*

Renier van der Westhuyzen and Erick Strauss*

Department of Biochemistry, Stellenbosch University, Private bag X1, Matieland 7602, South Africa

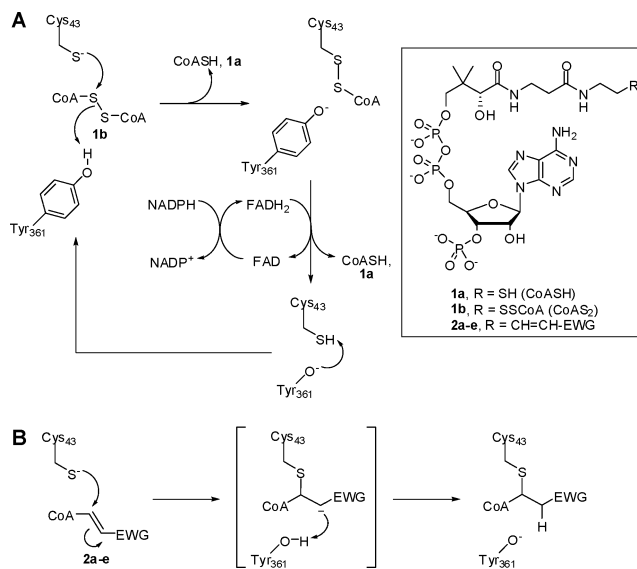
Received July 13, 2010; E-mail: estrauss@sun.ac.za

Abstract: Coenzyme A (CoA) analogues containing α,β -unsaturated ester, ketone, and sulfone moieties were prepared by chemo-enzymatic synthesis as inhibitors of coenzyme A disulfide reductase (CoADR), a proven and as yet unexploited drug target in *Staphylococcus aureus*. Among these Michael acceptor-containing CoA analogues, which were designed to target CoADR's single essential active site cysteine for conjugate addition, a phenyl vinyl sulfone-containing analogue showed the most potent inhibition with a competitive K_i of ~ 40 nM, and time-dependent inactivation with a second-order rate of inactivation constant of $\sim 40\,000\text{ s}^{-1}\cdot\text{M}^{-1}$. Our results suggest that electrophilic substrate analogues should be considered as potential inhibitors of other medicinally relevant disulfide reductase enzymes.

Staphylococcus aureus, the causative agent of most nosocomial and many other opportunistic infections in humans, is rapidly becoming resistant to the current arsenal of available antibacterial agents, and the development of new antistaphylococcal treatments is therefore urgently needed. Interestingly, *S. aureus* offers a target for drug development that remains unexploited as yet, based on the unique thiol/disulfide redox system it uses to counteract environmental stress and to protect itself against the reactive oxygen species produced by the host's immune system. While most organisms (including humans) use glutathione and a flavin-dependent glutathione reductase (GR) enzyme to uphold their intracellular redox balance, *S. aureus* and some other Gram-positive bacteria such as *Bacillus anthracis* achieve the same result by maintaining high concentrations of the essential thiol-containing metabolite coenzyme A (CoA, **1a**) in its reduced form by means of a CoA disulfide reductase (CoADR) enzyme.¹ This distinction and the fact that various studies have highlighted the importance of CoADR in the growth, survival, and virulence of *S. aureus*² make this enzyme an attractive drug target.

Most pyridine nucleotide-disulfide oxidoreductases (PNDORs) such as GR and trypanothione reductase (TR), an enzyme unique to *Trypanosoma* spp. parasites that has also been extensively targeted by various drug development efforts, share a reaction mechanism that is based on two active site cysteine residues joined in a redox active disulfide linkage when the enzyme is in its resting state. Catalysis is initiated by reduction of this disulfide by the reduced FAD cofactor, followed by a thiol/disulfide interchange reaction between the active site cysteines and the disulfide substrate which results in formation of the reduced thiol products and the active site disulfide. However, CoADR is a mechanistically unique PNDOR as it utilizes only a single active site cysteine (Cys₄₃ in *S. aureus* CoADR), which reacts directly with its substrate (CoAS₂, **1b**) to form a mixed enzyme–substrate disulfide. In contrast to other PNDORs, the enzyme maintains this mixed disulfide in its resting state, and catalysis is also initiated by its

Scheme 1. (A) CoADR Reaction Mechanism;^a (B) Proposed Mechanism of Inhibition of CoADR by Michael Acceptor-Containing CoA Analogues **2a–e**

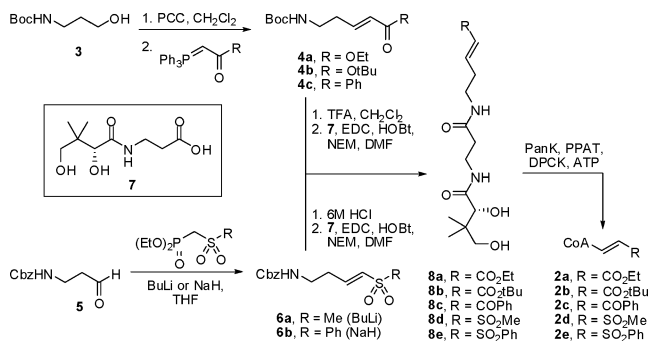


^a CoA disulfide **1b** reacts with Cys₄₃ to release CoASH **1a** while forming a mixed enzyme–substrate disulfide, which is subsequently reduced by FADH₂. Tyr₃₆₁ has been proposed to act as a catalytic acid/base as shown.³

reaction with FADH₂ (Scheme 1A).^{3,4} Based on these mechanistic differences we envisaged the development of new CoADR-selective inhibitors by targeting its essential cysteine with Michael acceptor-containing substrate analogues, a strategy that has been employed with great success in the discovery of cysteine protease inhibitors (Scheme 1B).⁵

Accordingly we set out to synthesize CoA analogues **2a–e** that contain α,β -unsaturated ester, ketone, or vinyl sulfone moieties, as these routinely occur in potent cysteine protease inhibitors (Scheme 2). We used CoA as the recognition motif since the crystal structure of CoADR highlighted the importance of its constituent groups for substrate recognition, and also because the resting state of the enzyme has a CoA molecule bound to Cys₄₃.³ Moreover, the Michael acceptor was positioned in such a manner that its electrophilic center correlated with the disulfide bond in the substrate **1b**. The warheads were obtained by preparing the protected amines **4a–c** and **6a–b** by utilizing either Wittig or Horner–Wadsworth–Emmons olefination reactions that gave the *E*-alkenes in all cases. These amines were subsequently deprotected and coupled to pantothenic acid **7** using standard procedures to give the pantothenamides **8a–e**. Finally, the CoA biosynthetic enzymes PanK, PPAT, and DPCK were used to transform **8a–e** to the corresponding CoA analogues **2a–e** using established protocols.⁶

In this manner four of the five CoA analogues were obtained in purified form; unfortunately the α,β -unsaturated ketone-containing

Scheme 2. Synthesis of the Michael Acceptor-Containing Pantothenamides **8a–e** and CoA Analogues **2a–e**

Table 1. Kinetic Parameters for the Inhibition of CoADR by CoA Analogues

CoA analogue	K_i^a (μM)	k_{inact}/K_i^b ($\text{s}^{-1} \cdot \text{M}^{-1}$)
2a	0.66 ± 0.12	219.1 ± 45.5
2b	5.16 ± 0.96	nd ^c
2d	0.30 ± 0.05	500.2 ± 89.8
2e	0.04 ± 0.01	$39\,690 \pm 10\,980$

^a For competitive inhibition. ^b Second-order rate of inactivation constants. ^c nd, Not determined.

analogue **2c**, although it was successfully prepared by biotransformation of **8c**, decomposed upon purification. The pantothenamides **8a–e** and the analogues **2a–e** were subsequently assayed for inhibition of CoADR using a concentration of 200 μM (**2c** was tested in crude form). While all five CoA analogues showed inhibition of CoADR activity, none of the pantothenamides had any effect, highlighting the essential requirement of CoA's adenosine and phosphate moieties for recognition and binding.

Although the CoA analogues **2a–e** were designed to act as selective, irreversible inhibitors of CoADR by modification of its active site cysteine, it is also possible that the observed inhibition can occur by nonspecific reaction of the Michael acceptor moieties with other enzyme-derived nucleophiles. To demonstrate that these analogues bind specifically in the active site of CoADR, the analogues **2a**, **2b**, **2d**, and **2e** were therefore evaluated for their ability to compete with CoAS₂ in the CoADR reaction. This was done by determining the initial rates of the reaction (i.e., without preincubation) in the presence of increasing substrate concentrations and various set concentrations of the inhibitor.⁷ The resulting rate profiles and corresponding double reciprocal plots (Figures S7–S10) indicated that the inhibition is indeed competitive in all cases. Moreover, with one exception the determined K_i values (Table 1) are all submicromolar, indicating that these CoA analogues are excellent substrate mimics. In fact, the K_i value of ~ 40 nM exhibited by the most potent inhibitor, the phenyl sulfone **2e**, is nearly 50-fold lower than the $K_m(\text{CoAS}_2)$ of ~ 2.0 μM . Based on this limited set of compounds, a structure–activity relationship analysis for binding of these analogues in the CoADR active site suggests that sulfone-based analogues are better suited than their carboxylic acid ester counterparts and that small substituents (e.g., OEt, Me) are preferred over sterically bulky ones (OtBu). In light of this analysis the excellent inhibition seen for the phenyl sulfone **2e** is therefore surprising, although it is possible that this analogue is uniquely able to form π -stacking interactions with the side chain of aromatic residues located nearby, such as Tyr₃₆₁.³ Nonetheless, these results show that the CoADR active site can accommodate a variety of substituents on the Michael acceptor and suggest that their scope and diversity may be expanded in future studies.

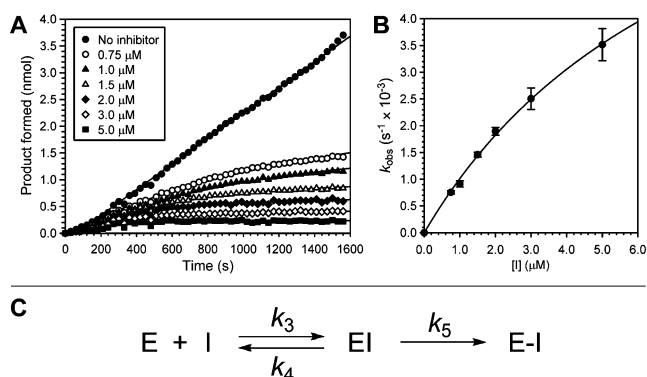


Figure 1. Inhibition of CoADR by CoA analogue **2e**. (A) Reaction progress in the presence of increasing inhibitor concentrations, showing time-dependent inactivation of CoADR. (B) Plot of the observed rate of inactivation constants (k_{obs}) versus the concentration of **2e**, from which the second-order rate of inactivation constant was determined. (C) Scheme showing the two-step mechanism of irreversible inactivation of CoADR that is in operation in the case of **2e**. Results for inhibition by analogues **2a** and **2d** are shown in Figures S11 and S12 respectively.

The finding that the CoA analogues **2a**, **2b**, **2d**, and **2e** bind in the active site of CoADR suggests that their Michael acceptor moieties should be ideally positioned to inactivate the enzyme by conjugate addition as envisaged (Scheme 1B). To determine whether the formed enzyme–inhibitor complexes result in the irreversible inhibition, time-dependence analyses were performed on the most potent inhibitors (i.e., **2a**, **2d**, and **2e**) by using the progress curve method (Figures 1A, S11A, and S12A).⁸ Gratifyingly, the progress curves of all three analogues showed time-dependent irreversible inactivation of CoADR, with the observed rate of inactivation (k_{obs}) also increasing with increasing inhibitor concentration (Figure 1B). In addition, the hyperbolic shape of this plot confirms that a two-step inactivation mechanism (Figure 1C) is at play in the case of **2e**. This provides further explanation for the competitive inhibition that is observed in the previous experiment, as the determined K_i values would refer to the dissociation constant ($K_i = k_4/k_3$) of the enzyme–inhibitor (EI) encounter complex formed in the reversible first step. The second-order rate of inactivation constants (Table 1) determined from these plots of k_{obs} vs [I] showed that, while analogues **2a** and **2d** exhibited modest rates of inactivation, the phenyl sulfone **2e** is a much more potent inhibitor with a rate constant of $\sim 40\,000$ $\text{s}^{-1} \cdot \text{M}^{-1}$. This relative order of inhibition activity is in agreement with the results of a previous study of the relative rates of the conjugate addition of 2'-(phenethyl)thiol to various Michael acceptors, which found the reactivity of a phenyl vinyl sulfone to be higher than that of the corresponding α,β -unsaturated methyl ester.⁹

To further confirm the irreversibility of inhibition, a CoADR sample was incubated in the presence of analogue **2e**, followed by gel filtration to remove all unbound small molecules. As expected, the inhibitor-treated enzyme showed no activity in comparison to a negative control sample treated in the same manner. Interestingly, the inhibitor-treated, gel-filtered enzyme did show a very slow return of activity after ~ 10 min of incubation (Figure S14). This suggests that the enzyme–inhibitor linkage can be broken over time, most probably by an elimination reaction that regenerates Cys₄₃ and the inhibitor. However, in light of the progress curve data the rate of regeneration is seemingly negligible relative to that of inactivation.

In spite of the good CoADR inhibition shown by CoA analogues such as **2e**, these highly polar compounds cannot be used as *in vivo* growth inhibitors since they are not able to cross the bacterial cell membrane. However, previous studies have shown

that pantothenamides similar to the CoA analogue precursors **8a–e** are able to enter bacterial cells, where they are converted to the corresponding CoA analogues.¹⁰ Pantothenamides **8a–e** were therefore tested as inhibitors of *S. aureus* growth in a nutrient-rich medium (1% tryptone). Only the ester-containing **8a** and **8b** showed inhibition at concentrations below 200 μM , with observed minimum inhibitory concentration (MIC) values of 55 and 52 μM respectively. The disappointing lack of inhibition seen for pantothenamides **8c–e** may be due to a reduced cell permeability or to an inability of the native *S. aureus* CoA biosynthetic enzymes to convert them to the corresponding CoA analogues.^{6,11} These factors clearly will have to be considered in the future development of inhibitors that target CoADR in the manner described here.

In conclusion, this report of Michael acceptor-containing CoA analogues is the first, to our knowledge, that describes CoADR inhibitors of any kind. While the potent inhibition reported here may be ascribed to the unique mechanism of CoADR, we believe that this study has demonstrated that Michael acceptor-based substrate analogues may present a new avenue for the development of inhibitors of other medicinally relevant PNDORs.

Acknowledgment. R.v.d.W. was supported by a scholarship from the National Research Foundation (NRF). This work was funded by a grant from the Medical Research Council (MRC) to E.S.

Supporting Information Available: Detailed descriptions of all synthetic, assay, and data analysis procedures, Figures S1–S14, Tables S1–S3, and additional discussion of the inhibition analyses. This material is available free of charge via the Internet at <http://pubs.acs.org>.

References

- (1) (a) delCardayre, S. B.; Stock, K. P.; Newton, G. L.; Fahey, R. C.; Davies, J. E. *J. Biol. Chem.* **1998**, *273*, 5744–5751. (b) delCardayre, S. B.; Davies, J. E. *J. Biol. Chem.* **1998**, *273*, 5752–5757. (c) Wallen, J. R.; Paige, C.; Mallett, T. C.; Karplus, P. A.; Claiborne, A. *Biochemistry* **2008**, *47*, 5182–5193. (d) Wallen, J. R.; Mallett, T. C.; Boles, W.; Parsonage, D.; Furdul, C. M.; Karplus, P. A.; Claiborne, A. *Biochemistry* **2009**, *48*, 9650–9667.
- (2) (a) Coulter, S. N.; Schwan, W. R.; Ng, E. Y. W.; Langhorne, M. H.; Ritchie, H. D.; Westbrook-Wadman, S.; Hufnagle, W. O.; Folger, K. R.; Bayer, A. S.; Stover, C. K. *Mol. Microbiol.* **1998**, *30*, 393–404. (b) Schneider, W. P.; Ho, S. K.; Christine, J.; Yao, M.; Marra, A.; Hromockyj, A. E. *Infect. Immunol.* **2002**, *70*, 1326–1333.
- (3) Mallett, T. C.; Wallen, J. R.; Karplus, P. A.; Sakai, H.; Tsukihara, T.; Claiborne, A. *Biochemistry* **2006**, *45*, 11278–11289.
- (4) Luba, J.; Charrier, V.; Claiborne, A. *Biochemistry* **1999**, *38*, 2725–2737.
- (5) (a) Powers, J. C.; Asgian, J. L.; Ekici, Ö. D.; James, K. E. *Chem. Rev.* **2002**, *102*, 4639–4750. (b) Hernandez, A. A.; Roush, W. R. *Curr. Opin. Chem. Biol.* **2002**, *6*, 459–465.
- (6) Strauss, E.; de Villiers, M.; Rootman, I. *ChemCatChem* **2010**, *2*, 929–937.
- (7) The experimental conditions were specifically chosen to determine whether an initial, reversible enzyme–inhibitor (EI) encounter complex forms, regardless of whether enzyme inactivation follows upon formation of this complex or not. In the case of a two-step mechanism of inactivation, the first step entails formation of the EI complex, and the observed K_i value should be equal to its dissociation constant. See ref 8 for more detailed discussions.
- (8) (a) Bieth, J. G. *Methods Enzymol.* **1995**, *248*, 59–84. (b) Copeland, R. A. *Evaluation of Enzyme Inhibitors in Drug Discovery*; John Wiley & Sons, Inc.: Hoboken, NJ, 2005. (c) Silverman, R. B. *Methods Enzymol.* **1995**, *249*, 240–283.
- (9) Reddick, J. J.; Cheng, J.; Roush, W. R. *Org. Lett.* **2003**, *5*, 1967–1970.
- (10) (a) Clarke, K. M.; Mercer, A. C.; La Clair, J. J.; Burkart, M. D. *J. Am. Chem. Soc.* **2005**, *127*, 11234–11235. (b) Meier, J. L.; Mercer, A. C.; Rivera, H., Jr.; Burkart, M. D. *J. Am. Chem. Soc.* **2006**, *128*, 12174–12184.
- (11) For **8c** we found that purified *S. aureus* PanK was not able to perform the first step in the biotransformation reaction used to prepare **2c**. See Supporting Information for details.

JA106204M

Supporting Information

Materials and Methods

All chemicals were purchased from Sigma-Aldrich Company and were used without further purification unless otherwise noted. Pyruvate Kinase was from Roche and Inorganic Pyrophosphatase was from Sigma. Strata C18-E (55 μ m, 70Å) solid phase extraction (SPE) cartridges (1000 mg/6 mL) were from Phenomenex. Micro Bio-Spin columns and Bio-gel P6 gel filtration media was obtained from Bio-Rad. Tetrahydrofuran (THF) was distilled under nitrogen from sodium wire using benzophenone as an indicator. Dichloromethane (DCM) was distilled under nitrogen from calcium hydride. *N,N*-Dimethylformamide (DMF) was dried and purified by shaking up over potassium hydroxide followed by distillation under reduced pressure and a nitrogen atmosphere, and was stored over 3 Å molecular sieves. All column chromatography was performed using Merck silica gel 60 (particle size 0.040-0.063 mm) using combinations of hexane, ethyl acetate, dichloromethane and methanol as eluants. Thin layer chromatography (TLC) was carried out on aluminium-backed Merck silica gel 60 F254 plates. Visualization was performed with a UV lamp followed by spraying with a cerium ammonium molybdate or ninhydrin solution, followed by heating. All ^1H and ^{13}C nuclear magnetic resonance spectra were obtained using 300 MHz Varian VNMRs (75 MHz for ^{13}C), 400 MHz Varian Unity Inova (100 MHz for ^{13}C) or 600 MHz Varian Unity Inova (125 MHz for ^{13}C) instruments at the Central Analytical Facility (CAF) of the University of Stellenbosch. Chemical shifts (δ) were recorded using the residual solvent peak or an external reference. All chemical shifts are reported in ppm and all spectra were obtained at 25 °C. Proton spectral data are reported as follows: chemical shift, multiplicity (ovlp = overlapping, s = singlet, d = doublet, t = triplet, q = quartet, p = pentet, m = multiplet, br = broad), coupling constant in Hz, and integration. All high resolution mass spectra were performed on a Waters API Q-TOF Ultima spectrometer at the Mass Spectrometry unit of CAF using positive-ion mode ESI-MS. HPLC analysis was performed on an Agilent 1100 instrument using either a Luna 5 μ C18 column (250 x 4.6 mm) (HPLC method A) from Phenomenex or a Supelcosil LC-18-T 3 μ C18 column (150 x 4.6 mm) (HPLC method B) from Supelco. HPLC method A: The column was equilibrated in 95% solution A (10 mM NH_4OAc , pH 6.0) and 5% solution B (acetonitrile), followed by elution with 95% A (0–5 minutes, isocratic), a linear gradient increasing solution B to 20% (5–6 minutes), a linear gradient increasing solution B to 40% (6–10 minutes), an isocratic elution at 40% B (10–15 minutes), a linear gradient increasing solution B to 60% (15–16 minutes), and finally by an isocratic elution at 60% B (16–20 minutes). A flow rate of 1 mL.min $^{-1}$ was maintained throughout. HPLC method B: The column was equilibrated in 95% solution A (100 mM potassium phosphate, pH 6.5) and 5% solution B (methanol), followed by elution with 95% A (0–3 minutes, isocratic), a linear gradient increasing solution B to 30% (5–7 minutes) and by an isocratic elution at 30% B (7–20 minutes). A flow rate of 1 mL.min $^{-1}$ was maintained throughout.

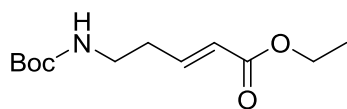
Synthesis of pantothenamides

General procedure for synthesis of Boc-protected α,β -unsaturated esters and ketone (4a–4c)

To a two neck-round bottom flask under a nitrogen atmosphere pyridinium chlorochromate (PCC) (1.85 g, 8.66 mmol), celite (1.9 g) and DCM (15 mL) were added. To this suspension was added alcohol **3** (5.8 mmol, 1.0 g) dissolved in DCM (2 mL). After stirring for 4h at room temperature the appropriate phosphorane (9.71 mmol, 1.70 eq) was added and the reaction stirred for a further 24 h. The reaction mixture

was subsequently vacuum-filtered through a short plug of silica gel, which was washed with EtOAc (100 mL). The combined eluates were concentrated *in vacuo*, and the crude product was purified by flash chromatography.

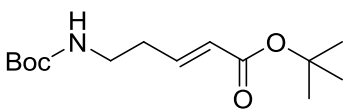
(E)-Ethyl 5-(tert-butoxycarbonylamino)pent-2-enoate (4a)



The reaction was performed according to the general procedure using ethyl (triphenylphosphoranyliden)acetate, and was purified using flash chromatography (Hexane/EtOAc 2:1) to afford **4a** (0.591 g, 42%) as a clear oil. The ^1H NMR spectrum agreed with the previously reported spectrum¹.

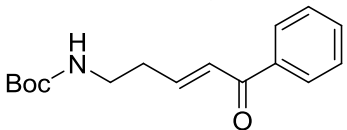
^1H NMR (CDCl_3 , 400 MHz): δ = 1.28 (t, J = 7.0 Hz, 3H), 1.43 (s, 9H), 2.39 (q, J = 6.5 Hz, 2H), 3.26 (q, J = 6.4 Hz, 2H), 4.18 (q, J = 7.0 Hz, 2H), 4.58 (br s, 1H), 5.87 (dt, J = 15.6, 1.60 Hz, 1H), 6.85–6.92 (dt, J = 15.6, 7.0 Hz, 1H).

(E)-tert-Butyl 5-(tert-butoxycarbonylamino)pent-2-enoate (4b)



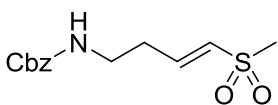
The reaction was performed according to the general procedure using *tert*-butyl (triphenylphosphoranyliden)acetate, and was purified using flash chromatography (Hexane/EtOAc 2:1) to afford **4b** (0.652 g, 43%) as a clear oil. ^1H NMR (CDCl_3 , 400MHz): δ = 1.43 (s, 9H), 1.47 (s, 9H), 2.36 (q, J = 6.6 Hz, 2H), 3.25 (q, J = 6.3 Hz, 2H), 4.58 (br s, 1H), 5.80 (dt, J = 15.6, 1.7 Hz, 1H), 6.89 (dt, J = 15.6, 6.9 Hz, 1H); ^{13}C NMR (CDCl_3 , 150 MHz): δ = 28.1, 28.3, 32.6, 39.0, 79.4, 80.3, 125.1, 144.0, 155.7, 165.6; HRMS–ESI: m/z $[\text{M}+1]^+$ calcd. for $\text{C}_{14}\text{H}_{26}\text{NO}_4$: 272.1862; found: 272.1858.

(E)-5-(tert-Butoxycarbonylamino)-1-phenylpent-2-ene-1-one (4c)



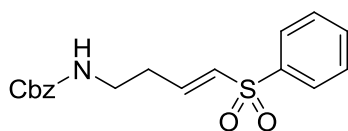
The reaction was performed according to the general procedure using (triphenylphosphoranyliden)acetophenone, and was purified using flash chromatography (Hexane/EtOAc 3:1) to afford **4c** (0.550 g, 35%) as a yellow oil. ^1H NMR (CDCl_3 , 400 MHz): δ = 1.43 (s, 9H), 2.63 (q, J = 6.3 Hz, 2H), 3.34 (q, J = 6.3 Hz, 2H), 4.65 (br s, 1H), 6.93–7.03 (m, 2H), 7.45–7.49 (m, 2H), 7.54–7.58 (m, 1H), 7.92–7.94 (m, 2H); ^{13}C NMR (CDCl_3 , 150 MHz): δ = 28.4, 33.3, 39.1, 79.5, 127.7, 128.5, 128.6, 132.8, 137.6, 145.6, 155.8, 190.43; HRMS–ESI: m/z $[\text{M}+1]^+$ calcd. for $\text{C}_{16}\text{H}_{21}\text{NO}_3$: 276.1600; found: 276.1582.

(E)-Benzyl 4-(methylsulfonyl)but-3-enylcarbamate (6a)

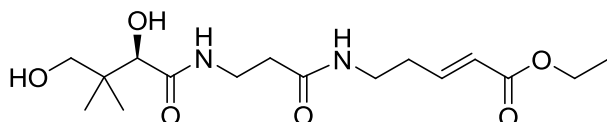


To a solution of diethyl (methylsulfonylmethyl)phosphonate (0.555 g, 2.41 mmol) (prepared by oxidation of diethyl (methylthiomethyl)phosphonate using a published method²) in anhydrous THF (30 mL) at -78°C was added *n*-BuLi (1.61 mL of a 1.50 M solution in hexane, 2.41 mmol). After 5 min **5** (0.500 g, 2.41 mmol) dissolved in THF (10 mL) in another flask was added dropwise at -78°C using an oven dried syringe.

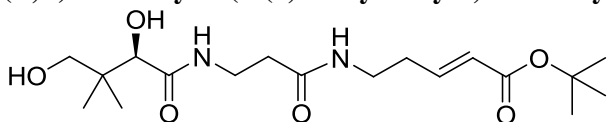
The reaction was allowed to proceed at room temperature overnight. The reaction was quenched by adding water (10 mL), and was transferred to a separatory funnel. EtOAc (120 mL) was added, and the organic layer was washed with NaHCO_3 (2×20 mL), 1 M HCl (2×20 mL) and brine (1×20 mL). The organic layer was dried over Na_2SO_4 , filtered and concentrated *in vacuo* to give the crude product which was purified using flash chromatography (3:1 EtOAc/Hexane) to give the vinylsulfone **6a** as a colorless oil (0.592 g, 87%). ^1H NMR (CDCl_3 , 300 MHz): δ = 2.50 (q, J = 6.2 Hz, 2H), 2.88 (s, 3H), 3.36 (q, J = 6.5 Hz, 2H), 4.98 (br s, 1H), 5.09 (s, 2H), 6.44 (d, J = 15.2 Hz, 1H), 6.88 (dt, J = 14.9, 7.0 Hz, 1H), 7.31–7.39 (m, 5H); ^{13}C NMR (CDCl_3 , 75.5 MHz): δ = 31.9, 39.0, 42.6, 66.9, 128.1, 128.2, 128.6, 131.5, 136.2, 144.6, 156.2; HRMS–ESI: m/z $[\text{M}+1]^+$ calcd. for $\text{C}_{13}\text{H}_{18}\text{NO}_4\text{S}$: 284.0957; found: 284.0960.

(E)-Benzyl 4-(phenylsulfonyl)but-3-enylcarbamate (6b)

To a solution of diethyl (phenylsulfonylmethyl)phosphonate (173 mg, 0.59 mmol) (prepared by oxidation of diethyl (phenylthiomethyl)phosphonate using a published method²) dissolved in anhydrous THF (2.8 mL) at -10 °C was added NaH (25 mg of a 60% dispersion in mineral oil, 0.63 mmol). The mixture was stirred for 10 min before **5** (103 mg, 0.50 mmol) dissolved in THF (2.8 mL) in another flask at -10 °C was added using an oven dried syringe. After warming to room temperature the reaction was stirred for 1 h, after which EtOAc was added (10 mL). This mixture was transferred to a separatory funnel and washed with brine (1×10mL). The organic layer was dried over Na₂SO₄, filtered and concentrated *in vacuo*. The crude product was purified using flash chromatography (2:1 Hexane/EtOAc) to give vinylsulfone **6b** as a colorless oil (119 mg, 70 %). ¹H NMR (CDCl₃, 400 MHz): δ = 2.45 (q, J = 6.1 Hz, 2H), 3.32 (q, J = 6.3 Hz, 2H), 4.88 (br s, 1H), 5.02 (s, 2H), 6.38 (d, J = 15.3 Hz, 1H), 6.92 (dt, J = 15.1, 7.1 Hz, 1H), 7.28–7.36 (m, 5H), 7.49–7.53 (m, 2H), 7.58–7.61 (m, 1H), 7.85–7.90 (m, 2H); ¹³C NMR (CDCl₃, 150 MHz): δ = 31.9, 39.0, 66.7, 127.5, 128.0, 128.1, 128.5, 129.2, 132.3, 133.3, 136.2, 140.2, 143.1, 156.2.

(R,E)-Ethyl 5-(3-(2,4-dihydroxy-3,3-dimethylbutanamido)propanamido)pent-2-enoate (8a)

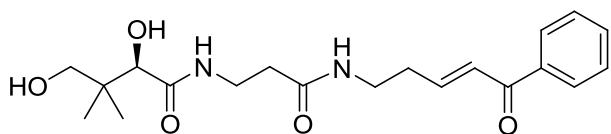
The Boc-protected ester **4a** (0.588 g, 2.42 mmol) was dissolved in a solution of DCM/trifluoroacetic acid (TFA) (1:1) (15 mL) and stirred for 1h at 0 °C. The solvent was removed *in vacuo* to give the TFA salt of (*E*)-ethyl 5-aminopent-2-enoate (0.621 g, 100%) as a brown oil. ¹H NMR (DMSO-*D*₆, 400MHz): δ = 1.22 (t, J = 7.2 Hz, 3H), 2.49 (m, 2H), 2.98 (dt, J = 7.0, 13.1 Hz, 2H), 4.25 (q, J = 7.0 Hz, 2H), 5.95 and 5.99 (d, J = 15.7 Hz, 1H), 6.83–6.90 (dt, J = 6.8, 15.7 Hz, 1H), 7.91 (br s, 3H); ¹³C NMR (DMSO-*D*₆, 400MHz): δ = 14.1, 29.4, 37.2, 59.8, 123.2, 144.2, 165.2. A portion of this residue (0.295 g, 1.15 mmol) was taken up in DMF (4 mL) and added to a flask containing sodium pantothenate **7** (0.299 g, 1.24 mmol), 1-Hydroxybenzotriazole (HOBt) (0.184 g, 1.36 mmol) and *N*-ethyl morpholine (161 μL, 1.26 mmol) dissolved in DMF (10 mL). After cooling to 0 °C *N*-(3-Dimethylaminopropyl)-*N*-ethylcarbodiimide (EDC) (0.262 g, 1.36 mmol) was added and the mixture stirred for 1h at 0 °C, after which it was warmed to room temperature and stirred overnight. The mixture was concentrated *in vacuo*, and the residue was applied to a short silica gel column, eluting with DCM/methanol (9:1). The crude product was purified by flash chromatography (DCM/methanol 19:1 to 9:1) to give **8a** (0.166 g, 41%) as a colorless viscous oil. ¹H NMR (D₂O, 400 MHz): δ = 0.88 (s, 3H), 0.91 (s, 3H), 1.28 (t, J = 7.2 Hz, 3H), 2.42–2.50 (m, 4H), 3.31–3.56 (m, 6H), 3.98 (s, 1H), 4.21 (q, J = 7.1 Hz, 2H), 5.95 (d, J = 15.8 Hz, 1H), 6.90 (dt, J = 15.8, 7.0 Hz, 1H); ¹³C NMR (D₂O, 125 MHz): δ = 14.0, 19.7, 21.1, 32.0, 35.9, 36.1, 38.4, 39.2, 62.2, 69.0, 76.4, 123.0, 148.0, 169.4, 174.5, 175.5; HRMS-ESI: *m/z* [M+1]⁺ calcd. for C₁₆H₂₈N₂O₆: 345.2026; found: 345.2014.

(R,E)-tert-Butyl 5-(3-(2,4-dihydroxy-3,3-dimethylbutanamido)propanamido)pent-2-enoate (8b)

To Boc-protected ester **4b** (0.273 g, 1.0 mmol) in EtOAc (3.75 mL) was added 4 M HCl in anhydrous dioxane (1.25 mL). The reaction mixture was stirred for 4 h at room temperature. Removal of the solvent *in vacuo* afforded the HCl salt of (*E*)-tert-butyl 5-aminopent-2-enoate (0.140 g, 90 %) as a white powder which was used without purification in the next step. The above residue was taken up in DMF (2 mL) and added to a flask containing calcium pantothenate **7** (0.179 g, 0.74 mmol), HOBt (0.109 g, 0.81 mmol) and *N*-ethyl morpholine (94 μL, 0.74 mmol) dissolved in DMF (5 mL). After cooling to 0 °C, EDC (0.155 g, 0.81 mmol) was added and the mixture was stirred for 1h at 0 °C, after which it was warmed to room temperature and stirred overnight. The mixture was concentrated *in vacuo* and the residue was applied to a short silica gel column, eluting with DCM/methanol (9:1). The crude product was purified by flash chromatography

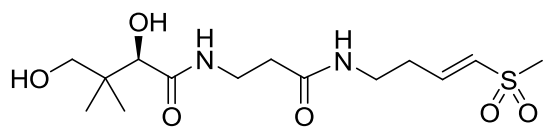
(DCM/methanol 19:1 to 9:1) to give **8b** (0.143 g, 59%) as a colorless viscous oil. ^1H NMR (CD_3OD , 400 MHz): δ = 0.92 (s, 6H), 1.46 (s, 9H), 2.39 (q, J = 6.7 Hz, 2H), 2.44 (t, J = 6.7 Hz, 2H), 3.29 (t, J = 7.0 Hz, 2H), 3.39 (d, J = 11.3 Hz, 1H), 3.45 (d, J = 10.9 Hz, 1H), 3.51 (t, J = 6.6 Hz, 2H), 3.95 (s, 1H), 5.80 (d, J = 15.6 Hz, 1H), 6.76–6.84 (d, J = 15.6, 7.0 Hz, 1H); ^{13}C NMR (CD_3OD , 75.5 MHz): δ = 20.6, 21.2, 27.8, 32.2, 35.8, 38.5, 39.7, 52.3, 69.6, 77.1, 81.1, 125.0, 145.6, 166.9, 173.2, 175.7; HRMS–ESI: m/z $[\text{M}+1]^+$ calcd. for $\text{C}_{18}\text{H}_{33}\text{N}_2\text{O}_6$: 373.2339; found: 373.2323.

(*R,E*)-2,4-Dihydroxy-3,3-dimethyl-*N*-(3-oxo-3-(5-oxo-5-phenylpent-3-enylamino)propyl)-butanamide (8c)

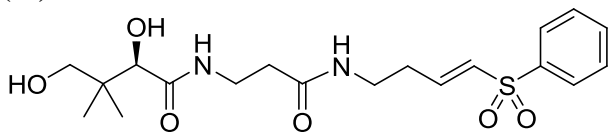


The Boc-protected ketone **4c** (0.327 g, 1.19 mmol) was dissolved in a solution of DCM/TFA (1:1) (7 mL) and stirred for 1 h at 0 °C. The solvent was removed *in vacuo* and under high vacuum to give the TFA salt of (*E*)-5-amino-1-phenylpent-2-en-1-one (0.346 g, >100%) as a dark red oil. ^1H NMR (CD_3OD , 400 MHz): δ = 2.71 (q, J = 7.1 Hz, 2H), 3.16 (t, J = 7.0 Hz, 2H), 6.96 (dt, J = 15.4, 7.1 Hz, 1H), 7.19 (d, J = 15.2 Hz, 1H), 7.50–7.54 (m, 2H), 7.60–7.64 (m, 1H), 7.98–8.00 (m, 2H); ^{13}C NMR (CD_3OD , 150 MHz): δ = 31.5, 39.3, 129.7, 129.8, 129.9, 134.5, 138.7, 144.1, 191.9. The above residue was taken up in DMF (6 mL) and added to a flask containing calcium pantothenate **7** (0.336 g, 1.39 mmol), HOBt (0.205, 1.52 mmol) and *N*-ethyl morpholine (177 μL , 1.39 mmol) dissolved in DMF (10 mL). After cooling to 0 °C, EDC (0.291 g, 1.52 mmol) was added and the mixture stirred for 1 h at 0 °C, after which it was warmed to room temperature and stirred overnight. The mixture was concentrated *in vacuo* and the residue was applied to a short silica gel column, eluting with DCM/methanol (9:1). The crude product was purified by flash chromatography (DCM/methanol 19:1 to 9:1) to give **8c** (0.263 g, 55%) as a dark red oil. ^1H NMR (CD_3OD , 400 MHz): δ = 0.92 (s, 6H), 2.47 (t, J = 6.7 Hz, 2H), 2.55 (q, J = 6.6 Hz, 2H), 3.37–3.45 (m, 4H), 3.51–3.57 (m, 2H), 3.97 (s, 1H), 6.95–7.02 (dt, J = 15.3, 6.6 Hz, 1H), 7.09 (d, J = 15.3 Hz, 1H), 7.50 (m, 2H), 7.61 (m, 1H), 7.96 (m, 2H); ^{13}C NMR (CD_3OD , 75.5 MHz): δ = 21.1, 22.0, 33.5, 36.4, 39.1, 40.2, 49.9, 70.1, 77.8, 128.5, 129.7, 129.8, 134.3, 138.7, 147.8, 173.9, 176.3, 192.6; HRMS–ESI: m/z $[\text{M}+\text{Na}]^+$ calcd. for $\text{C}_{20}\text{H}_{28}\text{N}_2\text{O}_5\text{Na}$: 399.1896; found: 399.1875.

(*R,E*)-2,4-Dihydroxy-3,3-dimethyl-*N*-(3-(4-(methylsulfonyl)but-3-enylamino)-3-oxopropyl)-butanamide (8d)



To a flask containing the Cbz-protected sulfone **6a** (0.592 g, 2.09 mmol) was added 6 M HCl (10 mL), and the solution was stirred under reflux for 3 h. The reaction mixture was diluted with H_2O (50 mL) and washed with DCM (3×10 mL). The aqueous layer was lyophilized to give the HCl salt of (*E*)-4-(methylsulfonyl)but-3-en-1-amine as a sticky yellow oil (0.359 g, >100%). A portion of this residue (0.146 g, 0.98 mmol) was taken up in DMF (3 mL) and added to a flask containing calcium pantothenate **7** (0.253 g, 1.06 mmol), HOBt (0.159, 1.17 mmol) and *N*-ethyl morpholine (137 μL , 1.08 mmol) dissolved in DMF (9 mL). After cooling to 0 °C EDC (0.225 g, 1.17 mmol) was added and the mixture stirred for 1 h at 0 °C, after which it was warmed to room temperature and stirred overnight. The mixture was concentrated *in vacuo* and the residue was applied to a short silica gel column, eluting with DCM/methanol (9:1). The crude product was purified by flash chromatography (DCM/methanol 19:1 to 9:1) which gave **8d** (0.174 g, 50%) as a colorless viscous oil. ^1H NMR (D_2O , 400 MHz): δ = 0.89 (s, 3H), 0.93 (s, 3H), 2.48–2.56 (m, 4H), 3.11 (s, 3H), 3.35–3.55 (m, 6H), 3.99 (s, 1H), 6.69 (d, J = 15.2 Hz, 1H), 6.93 (dt, J = 15.2, 7.0 Hz, 1H); ^{13}C NMR (D_2O , 75.5 MHz): δ = 23.6, 25.0, 35.3, 39.8, 40.0, 41.7, 43.2, 46.3, 72.9, 80.3, 134.1, 151.0, 178.4, 179.6; HRMS–ESI: m/z $[\text{M}+1]^+$ calcd. for $\text{C}_{14}\text{H}_{26}\text{N}_2\text{O}_6\text{S}$: 351.1590; found: 351.1578.

(*R,E*)-2,4-Dihydroxy-3,3-dimethyl-*N*-(3-oxo-3-(4-(phenylsulfonyl)but-3-enylamino)propyl)-butanamide (8e)

The Cbz-protected sulfone **6b** (119 mg, 0.345 mmol) was dissolved in methanol (2 mL) and conc. HCl (2 mL) was added. The mixture was brought to reflux and stirred overnight, after which the reaction was diluted with water (5 mL). The mixture was transferred to a

separatory funnel and the aqueous layer was washed with DCM (1×5mL). The aqueous layer was lyophilized to give the HCl salt of (*E*)-4-(phenylsulfonyl)but-3-en-1-amine (85 mg, 100%) as a yellow oil. ¹H NMR (D₂O, 400 MHz): δ = 2.68 (q, *J* = 7.1 Hz, 2H), 3.18 (t, *J* = 7.3 Hz, 2H), 6.78 (d, *J* = 15.6 Hz, 1H), 6.95–7.03 (dt, *J* = 15.2, 6.9 Hz, 1H), 7.61–7.65 (m, 2H), 7.73–7.77 (m, 1H), 7.87–7.94 (m, 2H); ¹³C NMR (D₂O, 75.5 MHz): δ = 27.0, 35.6, 125.5, 128.0, 129.9, 132.8, 136.2, 141.2. The above oil (85 mg, 0.34 mmol) was taken up in DMF (2 mL) and added to a flask containing calcium pantothenate **7** (91 mg, 0.38 mmol), HOBt (56 mg, 0.41 mmol) and *N*-ethyl morpholine (48 μL, 0.38 mmol) dissolved in DMF (2 mL). After cooling to 0 °C EDC (79 mg, 0.41 mmol) was added and the mixture stirred for 1h at 0 °C, after which it was warmed to room temperature and stirred overnight. The mixture was concentrated *in vacuo* and the residue was applied to a short silica gel column, eluting with DCM/methanol (9:1). The crude product was purified by flash chromatography (DCM/methanol 19:1 to 9:1) which gave **8e** (90 mg, 64%) as a colorless viscous oil. ¹H NMR (CD₃OD, 400 MHz): δ = 0.92 (s, 6H), 2.36 (t, *J* = 6.6 Hz, 2H), 2.46 (q, *J* = 6.7 Hz, 2H), 3.32–3.48 (m, 6H), 3.96 (s, 1H), 6.61 (d, *J* = 15.3 Hz, 1H), 6.92 (dt, *J* = 14.9, 7.0 Hz, 1H), 7.58–7.62 (m, 2H), 7.66–7.70 (m, 1H), 7.86–7.88 (m, 2H); ¹³C NMR (CD₃OD, 150 MHz): δ = 21.2, 21.8, 32.3, 36.4, 38.5, 40.2, 49.9, 70.1, 77.7, 128.6, 130.6, 133.2, 134.7, 141.8, 145.4, 173.8, 176.2; HRMS–ESI: *m/z* [M+1]⁺ calcd. for C₁₉H₂₉N₂O₆S: 413.1746; found: 413.1732.

Overexpression and purification of CoA biosynthetic enzymes

The *Staphylococcus aureus* pantothenate kinase (*SaPanK*) and dephospho-CoA kinase (*SaDPCK*) enzymes, and *Escherichia coli* PanK (*EcPanK*), phosphopantetheine adenylyltransferase (*EcPPAT*) and DPCK (*EcDPCK*) enzymes were expressed and purified according to published methods using BL21-star (DE3) (Invitrogen) as expression strain.³

Biotransformation of pantothenamides into CoA analogues

A 1500 μL reaction mixture contained one of the pantothenamides **8a–e** (5 mM), 8 mM ATP, 9 mM phosphoenolpyruvate (PEP), 5 mM MgCl₂, 30 mM NaOH, 5 units pyruvate kinase and 0.1 units inorganic pyrophosphatase in 50 mM Tris–HCl buffer (pH 7.6). The biosynthetic reaction was initiated by addition of 255 μg PanK, followed by 255 μg PPAT and 255 μg DPCK. The reaction mixture was subsequently incubated for 18 hours at 37 °C. The reaction was stopped by removing the enzymes by syringe filtration (GHP Acrodisc 13mm from PALL Life Sciences). The desired CoA analogue was subsequently purified using SPE cartridges (1 g). Prior to loading the reaction mixture, the cartridge was pre-conditioned with ~8 mL methanol followed by equilibration with ~8 mL of 10 mM NH₄OAc, pH 6.0. The crude reaction mixture was then loaded onto the column followed by washing with 8 mL of 10 mM NH₄OAc (pH 6.0). The products were eluted with 4 mL 20% acetonitrile in H₂O and concentrated using a Labconco Centrивap concentrator. The compounds were then re-dissolved in H₂O (5 mM stocks) and analyzed using HPLC, ¹H NMR and HRMS.

CoA analogue 2a

The biosynthesis reaction was performed according to the general procedure using **8a**, *SaPanK*, *EcPPAT* and *SaDPCK* and gave **2a** (3.9 mg, 62%) as a white powder. ¹H NMR (D₂O, 600 MHz): δ = 0.73 (s, 3H), 0.85 (s, 3H), 1.22 (t, *J* = 7.1 Hz, 3H), 2.36 (q, *J* = 6.7 Hz, 2H), 2.40 (t, *J* = 6.4 Hz, 2H), 3.24 (t, *J* = 6.7 Hz, 2H), 3.41 (t, *J* = 6.4 Hz, 2H), 3.54 (dd, *J* = 10.0, 4.7 Hz, 1H), 3.80 (dd, *J* = 9.9, 4.6 Hz, 1H), 3.98 (s, 1H), 4.14 (q, *J* =

7.1 Hz, 1H), 4.22 (br s, 2H), 4.56 (br s, 1H), 4.8 (m, 2H), 5.87 (d, $J = 15.8$ Hz, 1H), 6.13 (d, $J = 6.4$ Hz, 1H), 6.85 (dt, $J = 15.7$, 7.0 Hz, 1H), 8.22 (s, 1H), 8.51 (s, 1H), HRMS–ESI: m/z $[M+1]^+$ calcd. for $C_{26}H_{42}N_7O_{18}P_3$: 834.1877; found: 834.1862

CoA analogue 2b

The biosynthesis reaction was performed according to the general procedure using **8b**, *SaPanK*, *EcPPAT* and *EcDPCK* and gave **2b** (3.8 mg, 59%) as a white powder. 1H NMR (D_2O , 400 MHz): $\delta = 0.76$ (s, 3H), 0.89 (s, 3H), 1.45 (s, 9H), 2.37 (q, $J = 7.0$ Hz, 2H), 2.43 (t, $J = 6.7$ Hz, 2H), 3.27 (t, $J = 6.7$ Hz, 2H), 3.44 (t, $J = 7.1$ Hz, 2H), 3.65 (m, 1H), 3.84 (dd, $J = 9.7$, 4.7 Hz, 1H), 4.01 (s, 1H), 4.26 (br s, 2H), 4.59 (br s, 1H), 4.84 (m, 2H), 5.80 (d, $J = 15.6$ Hz, 1H), 6.17 (d, $J = 5.9$ Hz, 1H), 6.80 (dt, $J = 15.6$, 7.1 Hz, 1H), 8.26 (s, 1H), 8.54 (s, 1H); HRMS–ESI: m/z $[M+1]^+$ calcd. for $C_{28}H_{46}N_7O_{18}P_3$: 862.2190; found: 862.2172

CoA analogue 2c

The biosynthesis reaction was performed according to the general procedure using **8c**, *EcPanK*, *EcPPAT* and *EcDPCK*. While the presence of CoA analogue **2c** was confirmed by LC-MS analysis of the crude reaction mixture (peak at 10.4 min in HPLC chromatogram shown in figure S3 below), the analogue could not be purified using the general method as significant decomposition occurred during purification (as determined by HPLC analysis).

CoA analogue 2d

The biosynthesis reaction was performed according to the general procedure using **8d**, *SaPanK*, *EcPPAT* and *SaDPCK* and gave **2d** (3.6 mg, 57%) as a white powder. 1H NMR (D_2O , 400 MHz): $\delta = 0.76$ (s, 3H), 0.88 (s, 3H), 2.46 (m, 4H), 3.09 (s, 3H), 3.32 (t, $J = 6.3$ Hz, 2H), 3.44 (t, $J = 6.7$ Hz, 2H), 3.65 (m, 1H), 3.83 (dd, $J = 9.8$, 4.7 Hz, 1H), 4.01 (s, 1H), 4.26 (br s, 2H), 4.58 (br s, 1H), 4.82 (m, 2H), 6.18 (d, $J = 6.1$ Hz, 1H), 6.65 (d, $J = 15.2$ Hz, 1H), 6.89 (dt, $J = 15.3$, 7.8 Hz, 1H), 8.27 (s, 1H), 8.54 (s, 1H); HRMS–ESI: m/z $[M+1]^+$ calcd. for $C_{24}H_{40}N_7O_{18}P_3S$: 840.1442; found: 840.1425

CoA analogue 2e

The biosynthesis reaction was performed according to the general procedure using **8e**, *SaPanK*, *EcPPAT* and *EcDPCK* and gave **2e** (4.1 mg, 61%) as a white powder. 1H NMR (D_2O , 400 MHz): $\delta = 0.74$ (s, 3H), 0.87 (s, 3H), 2.18 (t, $J = 6.8$ Hz, 2H), 2.46 (q, $J = 7.0$ Hz, 2H), 3.21 (t, $J = 6.7$ Hz, 2H), 3.30 (t, $J = 6.7$ Hz, 2H), 3.64 (m, 1H), 3.82 (dd, $J = 9.7$, 4.6 Hz, 1H), 3.99 (s, 1H), 4.27 (br s, 2H), 4.58 (br s, 1H), 4.82 (br s, 2H), 6.14 (d, $J = 5.5$ Hz, 1H), 6.62 (d, $J = 14.5$ Hz, 1H), 6.93 (dt, $J = 14.5$, 6.9 Hz, 1H), 7.59 (m, 2H), 7.68 (m, 1H), 7.83 (m, 2H), 8.21 (s, 1H), 8.52 (s, 1H); HRMS–ESI: m/z $[M+1]^+$ calcd. for $C_{29}H_{42}N_7O_{18}P_3S$: 902.1598; found: 902.1577

HPLC chromatograms of purified CoA analogues 2a–e

Figure S1. HPLC chromatogram of **2a** using HPLC method A.

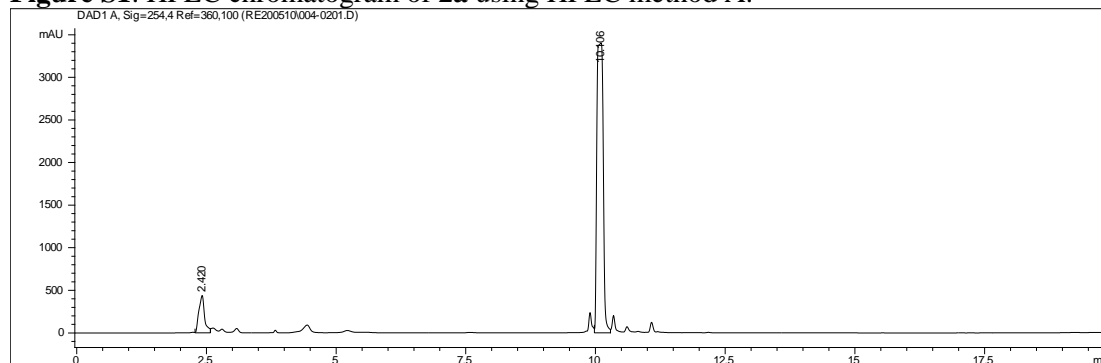


Figure S2. HPLC chromatogram of **2b** using HPLC method A.

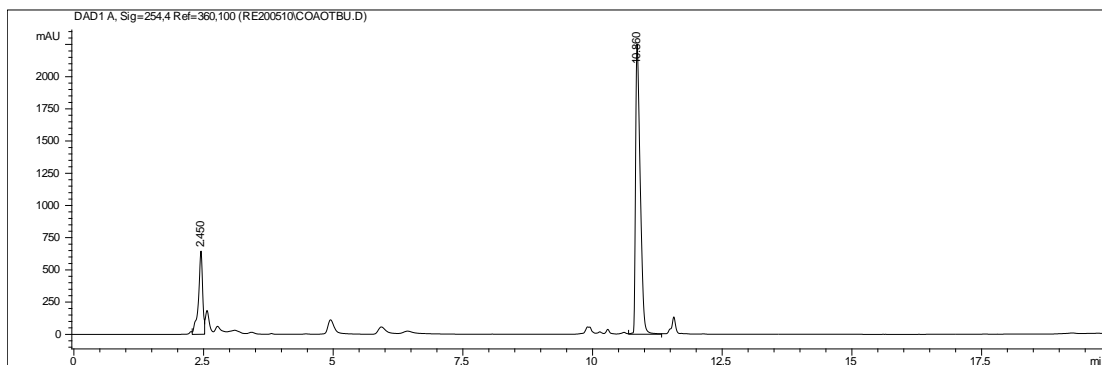


Figure S3. HPLC chromatogram of **2c** using HPLC method A.

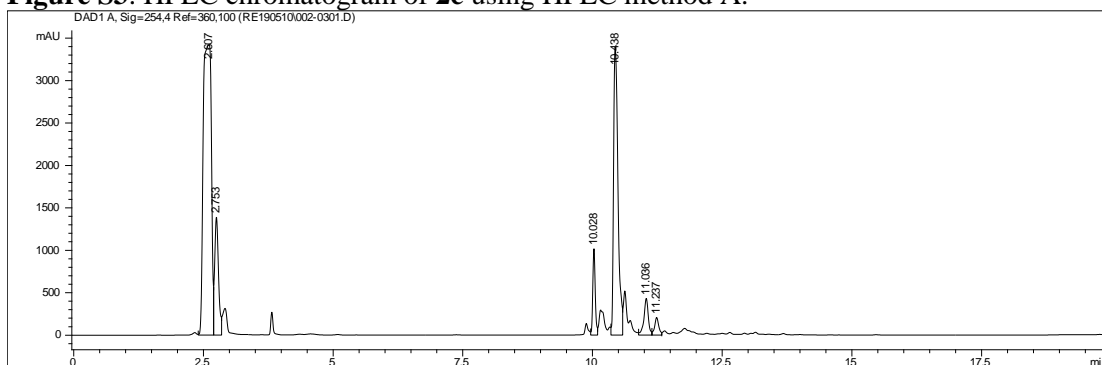


Figure S4. HPLC chromatogram of **2d** using HPLC method B.

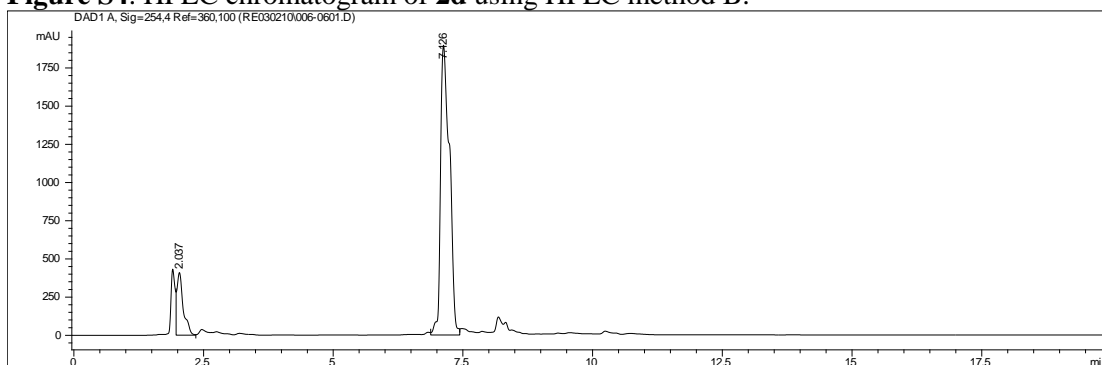
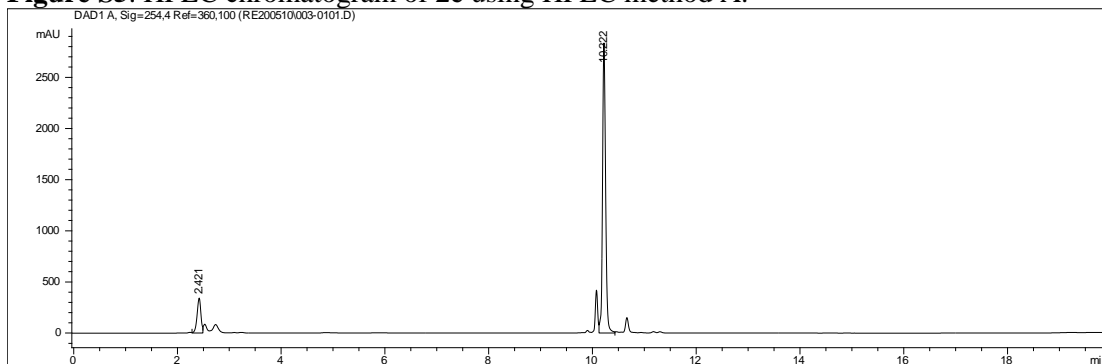


Figure S5. HPLC chromatogram of **2e** using HPLC method A.



Note: peaks at ~2.5 min represent residual ATP/ADP in the purified samples.

Cloning, expression and purification of SaCoADR

The expression and purification of recombinant SaCoADR was previously reported by delCardayre.⁴ In this study SaCoADR was cloned using a slightly modified strategy. Briefly, the *S. aureus cdr* gene was amplified from *S. aureus* (ATCC 35556) genomic DNA using primers which introduced an NdeI site at the 5'-end of the gene, and an XhoI site at its 3'-end (sites underlined):

Forward primer: 5'-GAGGAGGTAAGTTCATATGCCCAAATAGTCGTAGTCGG-3'

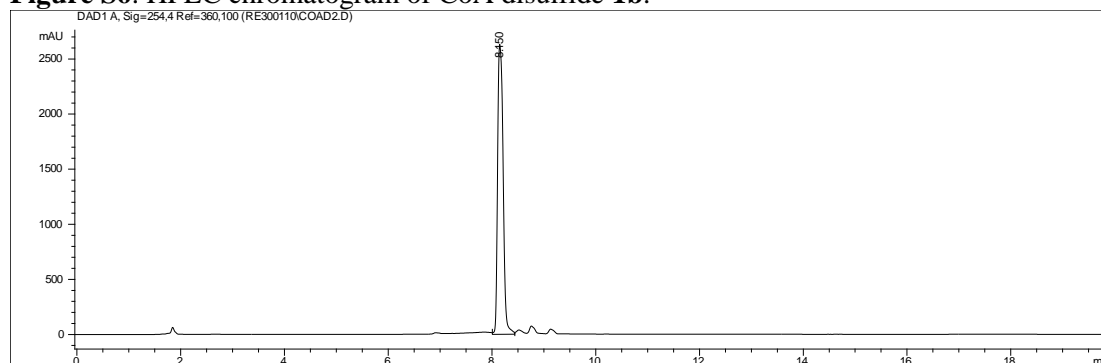
Reverse primer: 5'-GATTAGATTGAATCGCCTCGAGTCATTTATTAGCTTTG-3'

The amplified gene product was cut with NdeI and XhoI and ligated to a similarly cut pET-28a(+) vector. The resulting plasmid, pET-28a-SaCoADR, was sequenced to confirm the presence of the *cdr* gene and was transformed into *E. coli* BL21(Star)DE3 for expression. Expression was performed in Luria-Bertani broth supplemented with 30 mg/L kanamycin at 37 °C, and by induction with 1 mM IPTG at OD₆₀₀ = 0.6. Cell growth was continued for a further 3h at 37 °C post-induction, after which the cells were harvested by centrifugation. The obtained cell pellet was suspended in sonication buffer (5 mM imidazole, 500 mM NaCl and 20 mM Tris-HCl, pH 7.9; 10 mL/1 g cell paste) and subsequently sonicated to effect cell lysis. After centrifugation at 15 000×g for 30 min to collect cell debris, the crude extract (supernatant) was applied to a previously prepared 1 mL HisTrapFF metal affinity purification column using an ÄKTAprime purification system. Weakly bound proteins were removed by washing with sonication buffer, followed by sonication buffer containing 75 mM imidazole. SaCoADR was eluted by increasing the imidazole concentration to 500 mM. Elution was monitored at A₂₈₀. The purified protein was desalted using a 5 mL HiTrap desalting column (25 mM Tris, 5 mM MgCl₂, pH 8.0). Glycerol was added to the pure protein solution to a final concentration of 5%, after which the protein was aliquoted and stored at -80 °C.

Synthesis of the CoADR substrate

CoA disulfide (CoAS₂, **1b**) was prepared from CoA **1a** by using the established diamide-based oxidation of thiols.⁵ To a solution of 50 mM Tris-HCl (pH 7.6) in H₂O (13 mL) was added CoA (final concentration 2.0 mM), followed by diamide (final concentration 1.0 mM). The reaction mixture was stirred for 10 min at room temperature, followed by extraction of diamide with DCM (4×4 mL). The concentration of CoAS₂ in the final solution was determined by preparing five dilutions of the solution, which was each individually analyzed spectrophotometrically to determine the absorbance at 260 nm. The CoAS₂ concentration in each dilution was subsequently calculated using the reported extinction coefficient for CoA disulfide ($\epsilon_{260} = 33600 \text{ M}^{-1}\text{cm}^{-1}$).⁶ The average value was taken as the CoAS₂ concentration in the original solution. The purity of CoAS₂ **1b** was confirmed by HPLC analysis using HPLC method B. A typical chromatogram is shown below (Figure S6).

Figure S6. HPLC chromatogram of CoA disulfide **1b**.



CoADR activity and inhibition assay procedures

CoADR activity assay:

The CoADR reaction was monitored in the forward direction via a coupled assay procedure developed by Fairlamb⁷ for assaying trypanothione reductase. This assay relies on the reaction of the free thiol compound formed by reduction of its disulfide with 5,5'-dithiobis-(2-nitrobenzoic acid) (DTNB, Ellman's reagent) to form 2-nitro-5-thiobenzoate (NTB), which has a strong absorbance at 412 nm ($\epsilon_{412} = 13600 \text{ M}^{-1}\text{cm}^{-1}$). The assay was adapted and used in this study to determine the activity of *Sa*CoADR in the presence and absence of potential inhibitors. All measurements were corrected using a blank assay (no CoAS₂ present) to account for the possible direct reduction of DTNB by *Sa*CoADR, although it has been reported that DTNB is not a substrate for *Sa*CoADR.⁶ To further exclude DTNB-related effects, all inhibitors identified in the initial inhibition screen were also tested using the established NADPH-based CoADR assay.⁶ Exact reaction conditions for the assay depended on which test was being performed, and are given below.

Initial CoADR inhibitor screen:

The synthesized pantothenamides **8a–e** and CoA analogues **2a–e** were all first tested for inhibition at 200 μM to deduce if they inhibited CoADR in any manner (CoA analogue **2c** was tested using the crude, unpurified biosynthetic reaction product, see Figure S3 above).

Assay procedure: Reactions were performed by adding 225 μL of a reaction master mix to 25 μL containing CoAS₂ **1b** and inhibitor, and by monitoring the progress of the reaction at 37 °C over a period of 10 min. The final concentrations of all assay components were: 40 mM HEPES buffer (pH 7.5), 1.0 mM EDTA, 150 μM NADPH, 25 μM DTNB, 1% DMSO, either 2 or 20 nM CoADR, 60 μM CoAS₂ **1b** and 200 μM inhibitor.

None of the pantothenamides showed any inhibition, while all the CoA analogues showed inhibition of at least 25% based on the amount of product formed after 10 min. The inhibition of CoADR by **2a**, **2b**, **2d** and **2e** was subsequently characterized as described below.

Competitive inhibition of CoADR by CoA analogues 2a, 2b, 2d and 2e:

To analyze the inhibition of CoADR by the CoA analogues 10 nM CoADR was used in the assays, and the substrate (CoAS₂, **1b**) concentration was varied between 3 and 60 μM in the presence of four different inhibitor concentrations. All assays were performed in triplicate.

Assay procedure: Reactions were performed by adding 225 μL of a reaction master mix to 25 μL containing CoAS₂ **1b** and inhibitor, and by monitoring the progress of the reaction at 37 °C over a period of 10 min. The final concentrations of all assay components were: 40 mM HEPES buffer (pH 7.5), 1.0 mM EDTA, 150 μM NADPH, 25 μM DTNB, 1% DMSO, 10 nM CoADR, 3–60 μM CoAS₂ **1b** and inhibitor (see plots for values).

Data processing: The initial rate of each reaction was determined, and these values were plotted against the substrate concentration to give the plots shown below (Figures S7–S10, left panels). The mode of inhibition was deduced from the corresponding double reciprocal plots (Figures S7–S10, right panels) and was deemed to be competitive in nature in all cases.

Figure S7. Inhibition of CoADR by CoA analogue **2a**. Left panel, plots of initial rate against the concentration of CoAS₂ **1b** at various fixed concentrations of CoA analogue **2a** (concentrations indicated in the legend). All assays were performed in triplicate, with symbols representing the average value and errors bars showing the standard deviation. Right panel, double reciprocal plots of the same data.

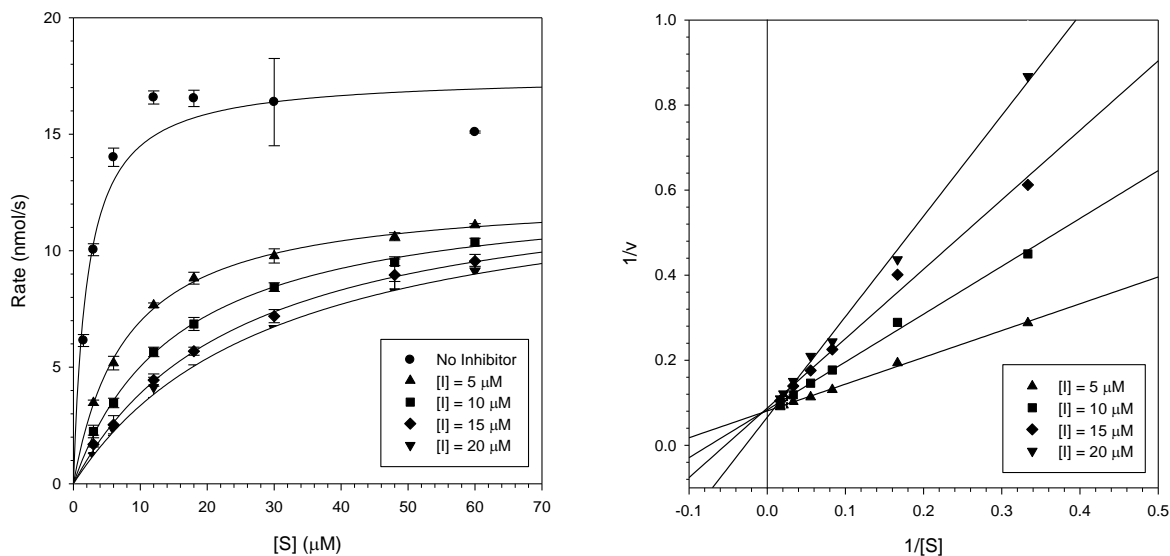


Figure S8. Inhibition of CoADR by CoA analogue **2b**. Left panel, plots of initial rate against the concentration of CoAS₂ **1b** at various fixed concentrations of CoA analogue **2b** (concentrations indicated in the legend). All assays were performed in triplicate, with symbols representing the average value and errors bars showing the standard deviation. Right panel, double reciprocal plots of the same data.

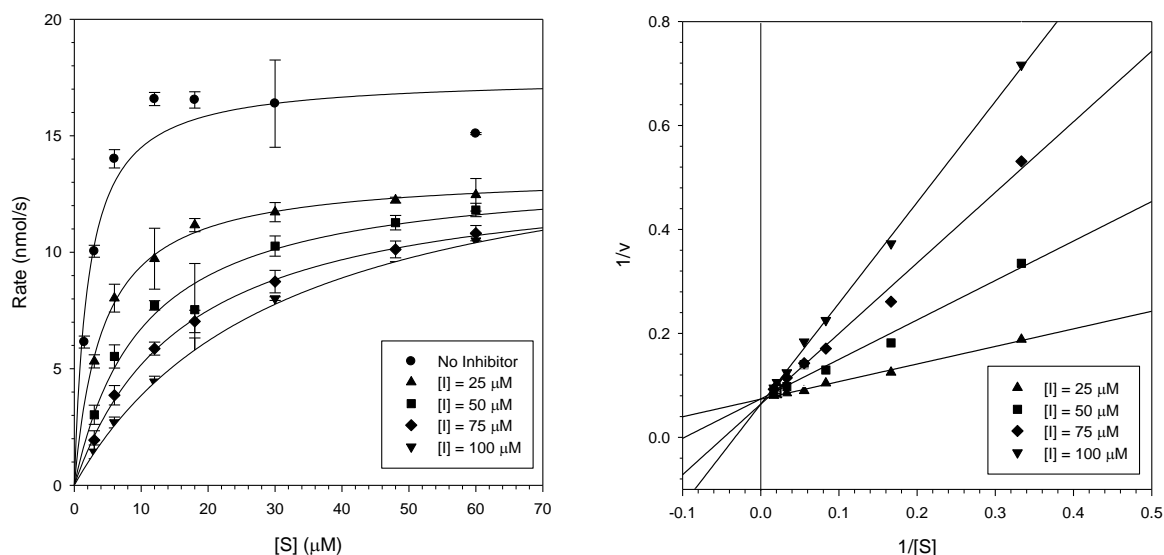


Figure S9. Inhibition of CoADR by CoA analogue **2d**. Left panel, plots of initial rate against the concentration of CoAS₂ **1b** at various fixed concentrations of CoA analogue **2d** (concentrations indicated in the legend). All assays were performed in triplicate, with symbols representing the average value and errors bars showing the standard deviation. Right panel, double reciprocal plots of the same data.

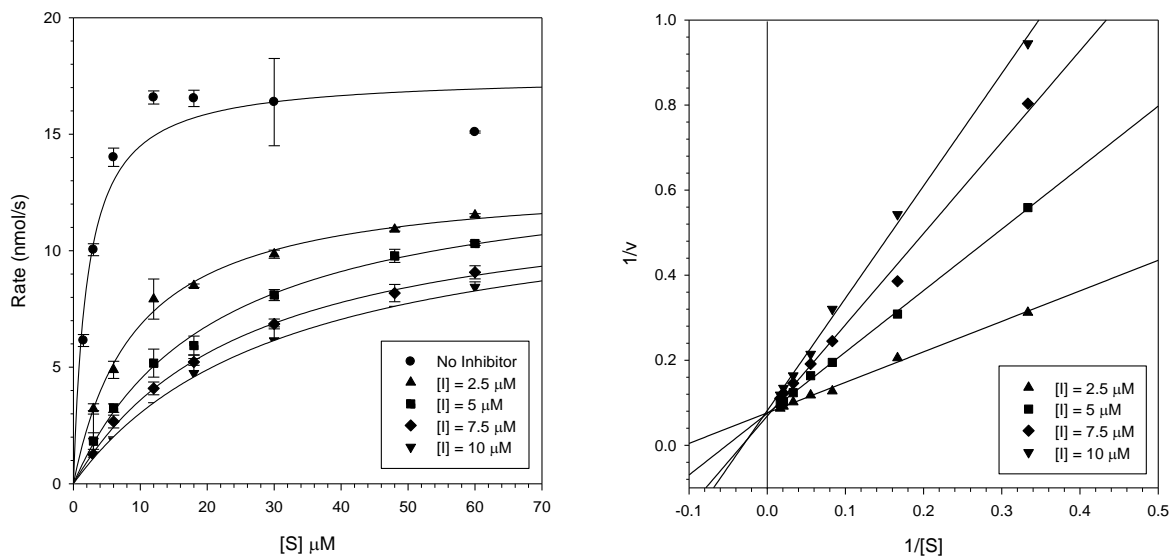
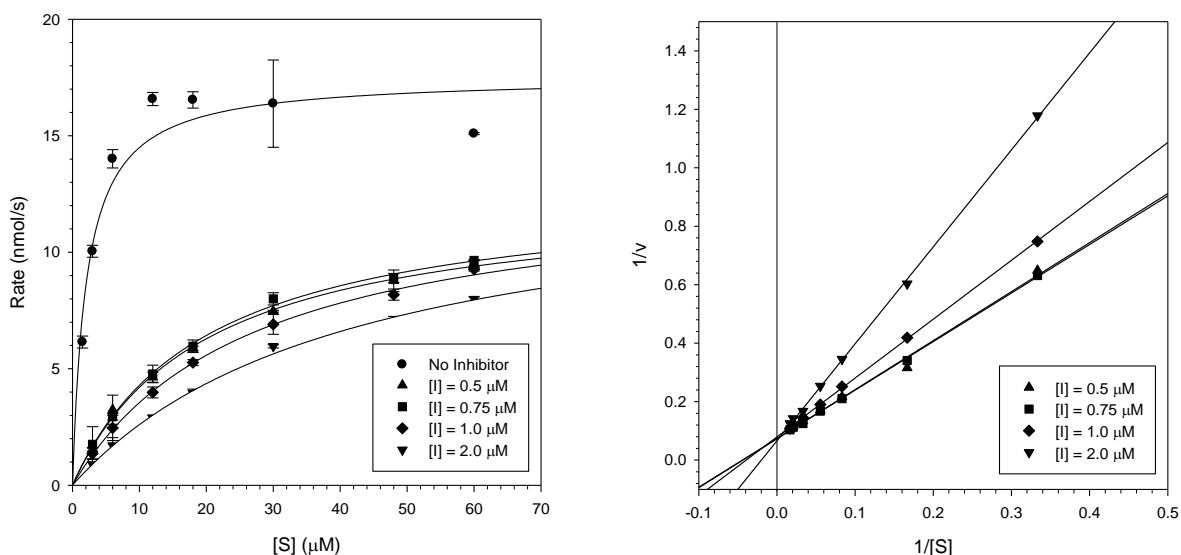


Figure S10. Inhibition of CoADR by CoA analogue **2e**. Left panel, plots of initial rate against the concentration of CoAS₂ **1b** at various fixed concentrations of CoA analogue **2e** (concentrations indicated in the legend). All assays were performed in triplicate, with symbols representing the average value and errors bars showing the standard deviation. Right panel, double reciprocal plots of the same data.



The kinetic parameters V_{\max} , K_M and K_i were subsequently determined in each case by non-linear regression analysis (using SigmaPlot 11.0) by fitting the data to equation (1). The results are summarized in Table S1.

$$v = \frac{V_{\max} [S]}{[S] + K_M \left(1 + \frac{[I]}{K_i} \right)} \quad (1)$$

Table S1. Kinetic parameters and dissociation constants determined from the characterization of the competitive inhibition of CoADR by CoA analogues **2a**, **2b**, **2d** and **2e**.

CoA analogue	V_{\max} (nmol/s)	K_M (μ M)	K_i (μ M)
2a	16.21 ± 0.56	1.62 ± 0.33	0.655 ± 0.121
2b	16.07 ± 0.50	1.51 ± 0.30	5.116 ± 0.962
2d	16.59 ± 0.52	1.73 ± 0.30	0.301 ± 0.047
2e	16.62 ± 0.72	1.76 ± 0.41	0.039 ± 0.008

Time-dependent inhibition of CoADR by CoA analogues **2a**, **2d** and **2e**:

To establish whether the most potent competitive inhibitors of CoADR also showed time-dependent inhibition of the CoADR enzyme, CoA analogues **2a**, **2d** and **2e** was analyzed by means of the progress curve method. At least six different concentrations were used for each inhibitor (with $[I] = \sim 20\text{--}125 \times K_i$, and $[I] > \sim 375 \times [E]$). All assays were performed in triplicate.

Assay procedure: Reactions were performed by adding 225 μ L of a reaction master mix to 25 μ L containing CoAS₂ **1b** and inhibitor, and by monitoring the progress of the reaction at 37 °C over a period of 30 min (a period over which the control reaction ($[I] = 0$) showed a linear increase in product formation). The final concentrations of all assay components were: 40 mM HEPES buffer (pH 7.5), 1.0 mM EDTA, 150 μ M NADPH, 25 μ M DTNB, 1% DMSO, 2 nM CoADR, 6 μ M CoAS₂ (for **2a** and **2d**) or 60 μ M CoAS₂ (for **2e**), and inhibitor (see plots for values).

Data processing: The resulting progress curves for each inhibitor are shown in the plots below (Figures S11-S13, left panels). Since all these plots showed that the steady state velocity (v_s) of the enzyme reaction in the presence of inhibitor approached zero, the first order rate constant for the onset of inhibition (k_{obs}) was determined by non-linear regression analysis (using SigmaPlot 11.0) by fitting the data to equation (2).

$$P = \frac{v_i}{k_{\text{obs}}} \left[1 - e^{-k_{\text{obs}} t} \right] \quad (2)$$

(where P = product formed, v_i = initial rate, t = time, and k_{obs} = the first-order rate constant).

The first-order rate constants (k_{obs}) were subsequently plotted against the inhibitor concentration (Figures S11-S13, right panels). If k_{obs} varied linearly with $[I]$ as in the case of **2a** and **2d**, then the second-order rate of inactivation constant k_{inact}/K_i was determined from the slope of the line fitted to the data by linear regression analysis using equation (3), after correction for zero substrate concentration by using $[S] = 6 \mu$ M and the K_M -value determined in the presence of the specific inhibitor (Table S1).

$$k_{obs} = \frac{k_{inact}[I]}{K_I \left(1 + \frac{[S]}{K_M}\right)} \quad (3)$$

If k_{obs} varied hyperbolically with $[I]$ as in the case of **2e**, then non-linear regression analysis was performed to determine k_{inact} and K_I using equation (4), with $[S] = 60 \mu\text{M}$ and a K_M -value of 1.76 ± 0.41 (Table S1). The resulting inhibition parameters are given in Table S2.

$$k_{obs} = \frac{k_{inact}[I]}{[I] + K_I \left(1 + \frac{[S]}{K_M}\right)} \quad (4)$$

Note: It is possible that k_{obs} may vary linearly with $[I]$ even in the case of a two-step mechanism, even though this is normally indicated by a hyperbolic curve. For example, this would occur if $[I] < K_I^{app}$. For a more detailed explanation of this phenomenon, see ref. 8a.

Figure S11. Time-dependent inhibition of CoADR by CoA analogue **2a**. Left panel, reaction progress in the presence of increasing amounts of inhibitor. Right panel, rate constants for the onset of inhibition (k_{obs}) as determined from the progress curves plotted against the concentration of **2a**. Error bars indicate the standard error.

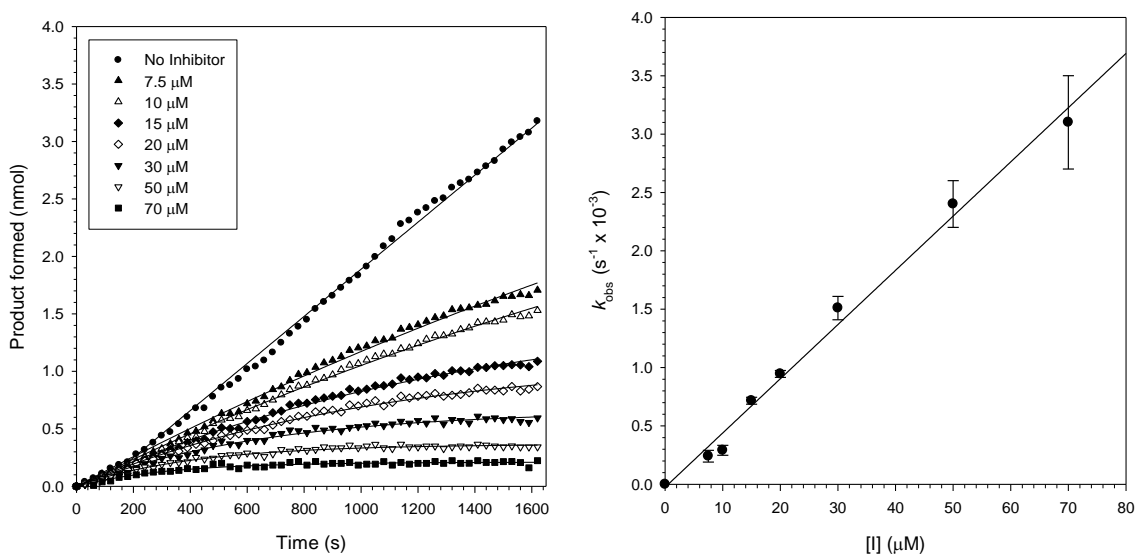


Figure S12. Time-dependent inhibition of CoADR by CoA analogue **2d**. Left panel, reaction progress in the presence of increasing amounts of inhibitor. Right panel, rate constants for the onset of inhibition (k_{obs}) as determined from the progress curves plotted against the concentration of **2d**. Error bars indicate the standard error.

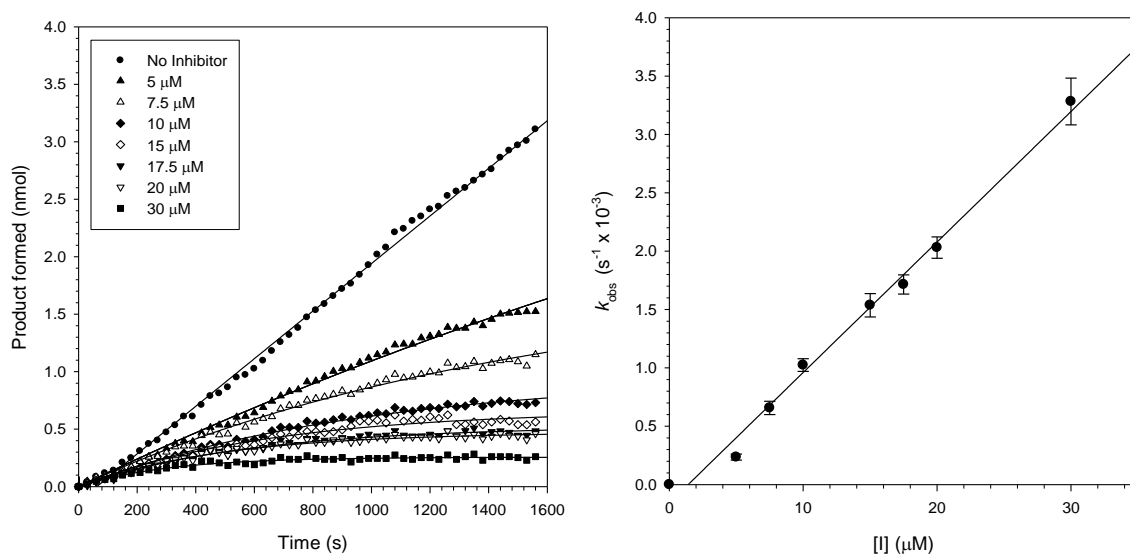


Figure S13. Time-dependent inhibition of CoADR by CoA analogue **2e**. Left panel, reaction progress in the presence of increasing amounts of inhibitor. Right panel, rate constants for the onset of inhibition (k_{obs}) as determined from the progress curves plotted against the concentration of **2e**. Error bars indicate the standard error.

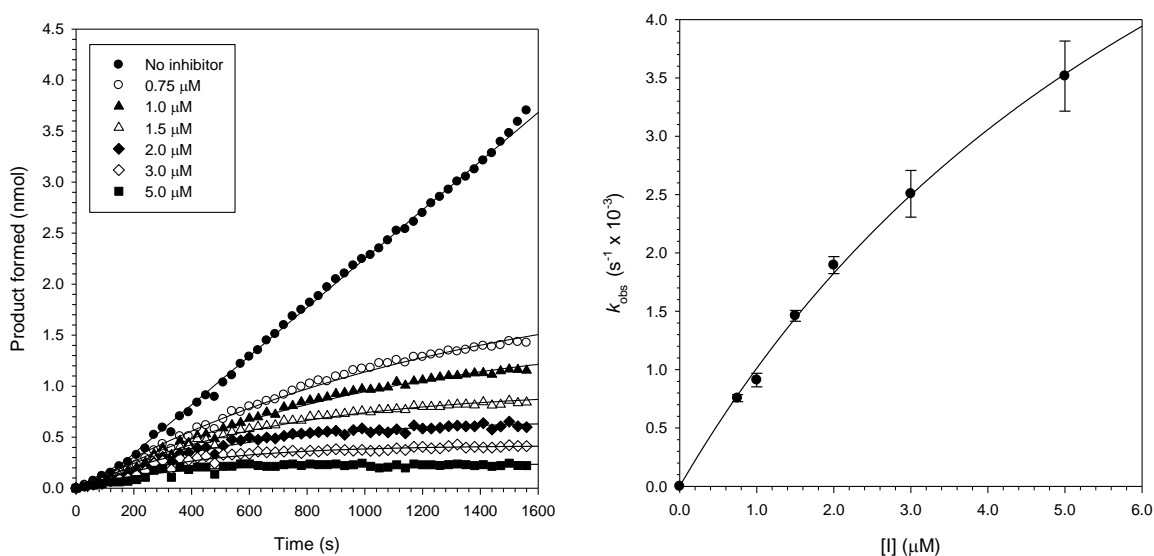


Table S2. Second-order rate of inactivation constants determined from the characterization of the time-dependent inhibition of CoADR by CoA analogues **2a**, **2b** and **2e**.

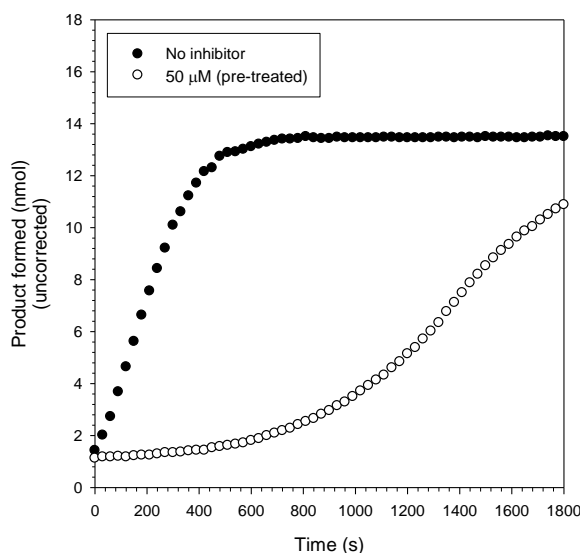
CoA analogue	k_{inact}/K_i ($\text{s}^{-1}\cdot\text{M}^{-1}$)	k_{inact} ($\text{s}^{-1}\times 10^{-3}$)	K_i (μM)
2a	219.1 ± 45.5	nd	nd
2b	500.2 ± 89.8	nd	nd
2e	39690 ± 10980	9.38 ± 0.80	0.236 ± 0.062

Note: A correlation between the values of K_i determined here in and K_i determined in the previous experiment should not be expected, as they are constituted of different sets of rate constants (see refs. 8b and 8c).

Determination of the irreversibility of inhibition of CoADR by CoA analogue **2e**:

To determine whether the time-dependent inhibition exhibited by the CoA analogues is indeed irreversible, CoADR enzyme samples were pre-treated with CoA analogue **2e** and subsequently gel-filtered to remove all unbound small molecules from the sample. Solutions contained 40 mM HEPES buffer (pH 7.5), 1.0 mM EDTA, 150 μM NADPH, 0.74 μM CoADR and 50 μM **2e** in a total volume of 100 μL , and were pre-incubated at 37 °C for 10 min. A portion of the treated samples (70 μL) were subsequently loaded onto micro-gelfiltration spin columns containing Biogel P-6 (0.7 mL slurry loaded per column) equilibrated in 50 mM Tris-HCl (pH 7.6), followed by centrifugation at 3500 rpm for 4 min. A portion of the eluate (25 μL) was subsequently used to assay for CoADR activity as above by adding 225 μL of assay mixture. A substrate (CoAS₂, **1b**) concentration of 85 μM was used, and the final CoADR concentration was estimated to be 740 nM. A control sample, treated in the same manner but in the absence of inhibitor, was used as reference. The progress of the reactions was subsequently monitored at 37 °C over a period of 30 min. All assays were performed in triplicate, and the results are shown in Figure S14. The pre-treated sample showed no signs of activity during the first 5-10 min of the reaction, although activity did slowly return over time as shown. Note, however, that the maximum rate of the regenerated enzyme is still less than that of the control.

Figure S14. Determination of the irreversibility of inhibition. Reaction progress of CoADR samples pre-treated with water or CoA analogue **2e**, which was subsequently gel-filtered and analyzed for remaining activity. Note that the amount of product formed is uncorrected; the background activity was similar to that obtained in other assays.



Staphylococcus aureus growth assays

To determine whether the pantothenamide precursors of the CoA analogues **2a–e** showed any inhibition of *S. aureus* growth, growth inhibition assays were performed. A starter culture of *S. aureus* RN4220 was prepared by inoculating 1% tryptone broth with four colonies from cultures grown on LB agar plates. The starter culture was subsequently diluted 30-fold in the same medium and grown at 37 °C until the OD₆₀₀ reached 1.0. It was then diluted 10 000-fold, and 10 μL of the diluted cell suspension was used to inoculate each well of a 96-well flat-bottomed plate containing 110 μL 1% tryptone broth and one of the pantothenamides **8a–e** in final concentration of 200 μM. The plates were subsequently incubated without shaking at 37 °C for 20 h, and the amount of growth inhibition was subsequently assessed by determination of the OD₆₀₀. At this concentration, only pantothenamides **8a** and **8b** were found to affect *S. aureus* growth; a full dose-response analysis was therefore performed on each of these compounds. This was done by inoculation of 110 μL 1% tryptone broth in the wells of a 96-well flat-bottomed plate containing increasing concentrations of either **8a** or **8b** (0.39–200 μM) with 10 μL of the 10 000-fold diluted starter culture. The plate was subsequently incubated for 20 h at 37 °C, after which the cell density was measured by determining the OD₆₀₀ of the cell suspension in each well. The extent of growth was normalized to the OD₆₀₀ values of a negative growth control which contained only 1% tryptone medium (no cells) as 0% growth, and a negative inhibition control which did not contain any compound as 100% growth. Data analyses were subsequently performed by plotting the % growth against the logarithm of the compound concentration, fitting the data to equation (5) by non-linear regression analysis and by estimating the minimum inhibitory concentration (MIC) from the concentration-response curves as the minimum amount of inhibitor that gave 100 % inhibition of cell growth. The results (Table S3) represent the average of two separate experiments, each performed in triplicate.

$$\%Growth = \frac{a}{1 + \left(\frac{x}{x_0}\right)^b} \quad (5)$$

Table S3. Minimum inhibitory concentration (MIC) values determined for the two pantothenamides that exhibited *S. aureus* growth inhibition at 200 μ M.

Pantothenamide	MIC – Exp.		Ave MIC (μ M)
	#1 (μ M)	#2 (μ M)	
8a	35.1	74.0	54.6 \pm 27.6
8b	51.2	53.5	52.4 \pm 1.7

References

- (1) Henderson, J. A.; Phillips, A. J. *Angew. Chem. Int. Ed.* **2008**, *47*, 8499-8501.
- (2) Zhu, X.; Stolz, F.; Schmidt, R. R. *J. Org. Chem.* **2004**, *69*, 7367-7370.
- (3) (a) Strauss, E.; Begley, T. P. *J. Biol. Chem.* **2002**, *277*, 48205-48209. (b) Virga, K. G.; Zhang, Y.-M.; Leonardi, R.; Ivey, R. A.; Hevener, K.; Park, H.-W.; Jackowski, S.; Rock, C. O.; Lee, R. E. *Bioorg. Med. Chem.* **2006**, *14*, 1007-1020. (c) Rootman, I.; de Villiers, M.; Brand, L. A.; Strauss, E. *ChemCatChem* **2010**, *2*, DOI: 10.1002/cctc.201000197.
- (4) delCardayre, S. B.; Davies, J. E. *J. Biol. Chem.* **1998**, *273*, 5752-5757.
- (5) Kosower, N. S.; Kosower, E. M. *Methods Enzymol.* **1995**, *251*, 123-133.
- (6) delCardayre, S. B.; Stock, K. P.; Newton, G. L.; Fahey, R. C.; Davies, J. E. *J. Biol. Chem.* **1998**, *273*, 5744-5751.
- (7) Hamilton, C. J.; Saravanamuthu, A.; Eggleston, I. M.; Fairlamb, A. H. *Biochem. J.* **2003**, *369*, 529-537.
- (8) (a) Bieth, J. G. In *Methods Enzymol.*; Alan, J. B., Ed.; Academic Press: 1995; Vol. Volume 248, p 59-84. (b) Copeland, R. A. *Evaluation of Enzyme Inhibitors in Drug Discovery*; John Wiley & Sons, Inc.: Hoboken, NJ, 2005. (c) Silverman, R. B. *Methods Enzymol.* **1995**, *249*, 240-283

Chapter 2 (continued)

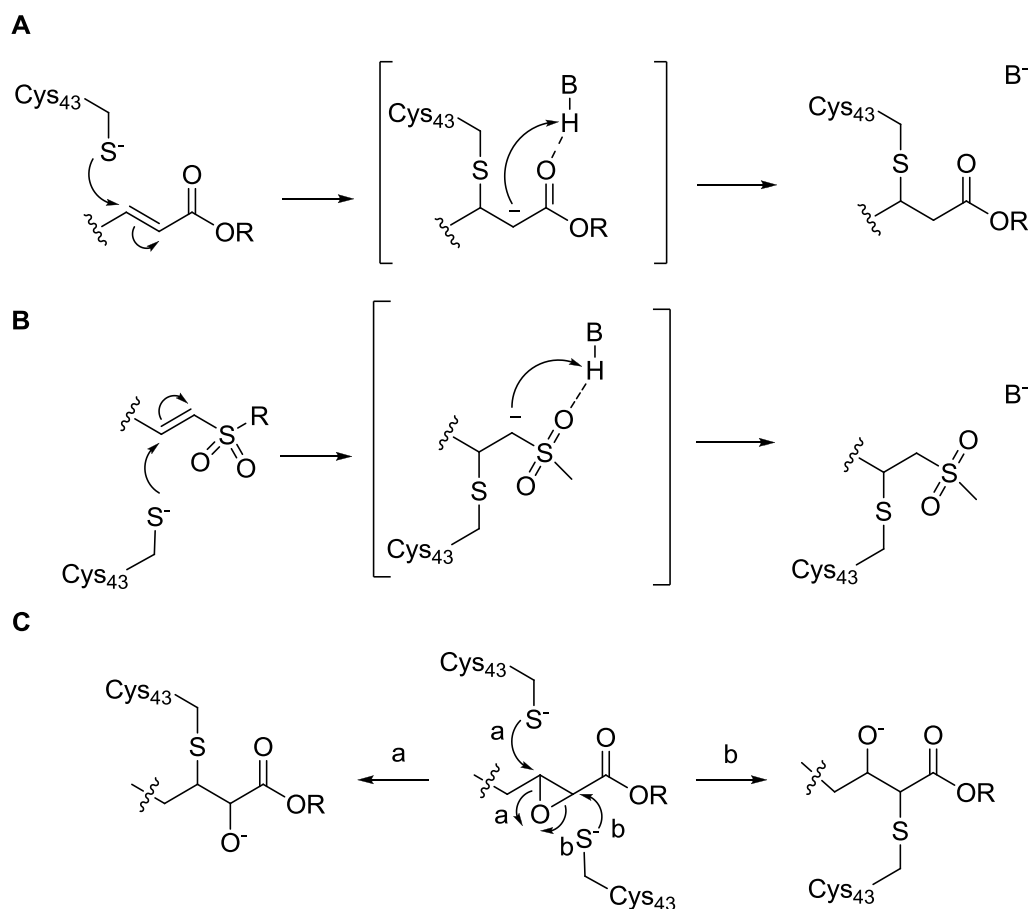
CoADR inhibitors - Additional information

2.2 Synthesis of inhibitors of SaCoADR

Apart from the results reported in accompanying manuscript, some additional studies were also carried out which are presented here.

2.2.1 Inhibitor design

During our initial inhibitor design we envisaged employing three electrophilic warheads towards the alkylation of the catalytic Cys of CoADR, namely α,β -unsaturated esters and ketones, alkyl vinylsulfones (all of which are described in the accompanying manuscript), and epoxides. These warheads are commonly used for inhibition of cysteine proteases as discussed in Powers' recent review of irreversible protease inhibitors.^{1,2,3} Our motivation for the addition of an epoxide-containing warhead was mainly based on this moiety's ability to give irreversible inhibition of CoADR after addition of the thiol of Cys₄₃ (Scheme 2.1). At the same time, involvement of an active site base is also not required, which we envisaged may enlarge the scope of potential inhibitors that could be used, and since a lack of protonation of the other electrophilic inhibitors may lead to reversal of the inhibitory complex by expulsion of the nucleophile. However, the results presented in the manuscript showed that this was not the case, and that the inhibition seen for α,β -unsaturated carbonyl and vinylsulfone inhibitors was only slowly reversed after gel-filtration treatment of the enzyme (Figure S14 of Supplementary information).

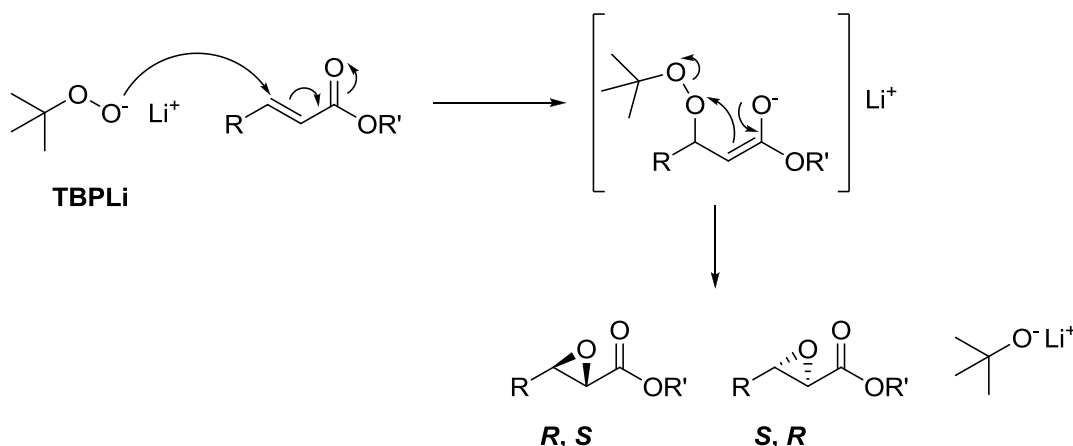


Scheme 2.1. Nucleophilic addition of the active site thiol of Cys₄₃ to α,β -unsaturated esters (**A**), vinylsulfone (**B**) and epoxide (**C**) functionalities rendering CoADR inactive. In the case of the epoxide an active site base (BH) is not required for protonation of the enolate intermediate.

2.2.2 Synthesis of epoxide-containing pantothenamides

A literature search revealed that epoxides can be introduced onto α,β -unsaturated esters and vinylsulfone moieties using tertiary butylhydroperoxide (TBHP) and *n*-BuLi.⁴ Since the preliminary results indicated that only the α,β -unsaturated esters inhibited *S. aureus* growth we focused on transforming these compounds to epoxides.

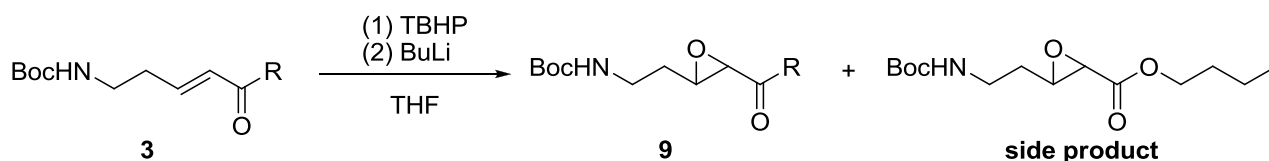
Since we already had the α,β -unsaturated carbonyl pantothenamides (**8a-8b**) in hand we decided to use the methodology of Meth-Cohn⁴ to introduce the epoxide (Scheme 2.2) via nucleophilic epoxidation. This method yields the *trans* epoxides by nucleophilic addition of the deprotonated tertiary butylhydroperoxide (TBPLi) to the α,β -unsaturated ester functionality. To confirm that this strategy would yield the epoxide we firstly investigated the epoxidation of Boc-protected α,β -unsaturated esters (**3a-3b**) as a model system.



Scheme 2.2. Mechanism of nucleophilic epoxidation of enoates yielding *trans* epoxides.

2.2.2.1 Synthesis of protected epoxides 9a-c as a model system

Initially the epoxidation of **3a** was performed at room temperature (rt) which yielded the epoxide in 10% yield (Scheme 2.3). A second product was also isolated (~10% yield) which was found to be the corresponding *n*-butyl ester of **9a** based on NMR and MS spectroscopic analysis. In a description of this method, Meth-Cohn *et. al.* also mentions that transesterification with *n*-butanol (formed as a side product when BuLi reacts with TBHP) takes place in some cases, but that the extent of esterification could be reduced by either working at lower temperatures or increasing the size of the ester substituent. The latter strategy presumably protects the carbonyl by hindering the attack of the incoming alcohol. Accordingly, the epoxidation of **3a** at lower temperature and with the bulkier *t*-butyl ester **3b** was investigated. The yield of **9a** increased to 34% when the epoxidation was performed at -45 °C, while the yield of *t*-butyl epoxide **9b** was 53% when the reaction was performed at rt. Interestingly, the epoxidation of *t*-butyl ester **3b** conducted at -45 °C did not take place and only starting material was recovered, albeit at a reduced amount suggesting that decomposition is a significant factor in this reaction. To further investigate this epoxidation approach, the epoxidation of phenyl ketone **3c** was also attempted, although we were aware that this reaction could potentially also lead to a Baeyer-Villiger-type oxidation of the ketone. The results indicated that the epoxide was formed in 36% yield and that a by-product formed which could not be identified using ^1H NMR spectroscopy.

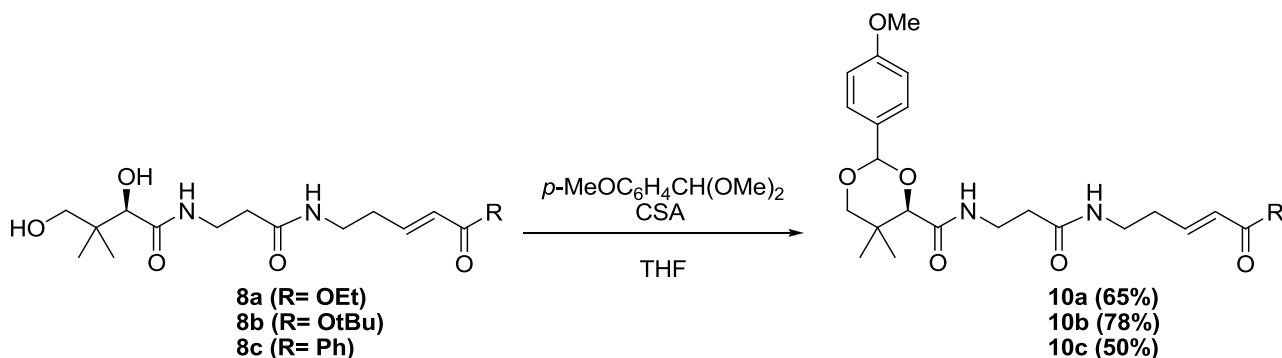


Alkene	R	Conditions	Epoxide	Yield (%)	Side product (%)
3a	OEt	2 h, rt	9a	14	10
3a	OEt	18 h, -45 °C	9a	34	< 5
3b	OtBu	18 h, -45 °C	9b	0	0
3b	OtBu	3 h, rt	9b	53	0
3c	Ph	2 h, rt	9c	36	0

Scheme 2.3. Synthesis of Boc-protected epoxides.

2.2.2.2 Epoxidation of protected pantothenamides

With the knowledge gained on the model system, we attempted the epoxidation of protected pantothenamides. In order to protect the 1,3-diol of pantothenamides (**8a-c**) we used *p*-methoxybenzaldehyde dimethylacetal and a catalytic amount of 10-camphorsulfonic acid (CSA) which gave the *p*-methoxybenzylidene (PMB)-protected pantothenamides in good yield (Scheme 2.4).



Scheme 2.4. Synthesis of PMB-protected pantothenamides.

The epoxidation of PMB-protected pantothenamide **10a** was first attempted using three sets of conditions, of which none gave the epoxide in significant yield (Scheme 2.5). According to TLC analysis of the epoxidation of **10a** performed using the first set of conditions (rt, 2h) a new compound did form with the expected polarity of the epoxide, but it seemed to decompose during purification by flash chromatography as no product could be isolated. Upon purification, 10% of the starting material (**10a**) was also recovered. Prolonging the time of the reaction, or lowering the

clear that the product of the reaction is the expected PMB-protected epoxide **11c**. This was also confirmed by HRMS analysis. During the measurement of the ^{13}C NMR spectrum in CDCl_3 it was found that **11c** decomposed over time, and therefore no ^{13}C NMR spectrum could be obtained.

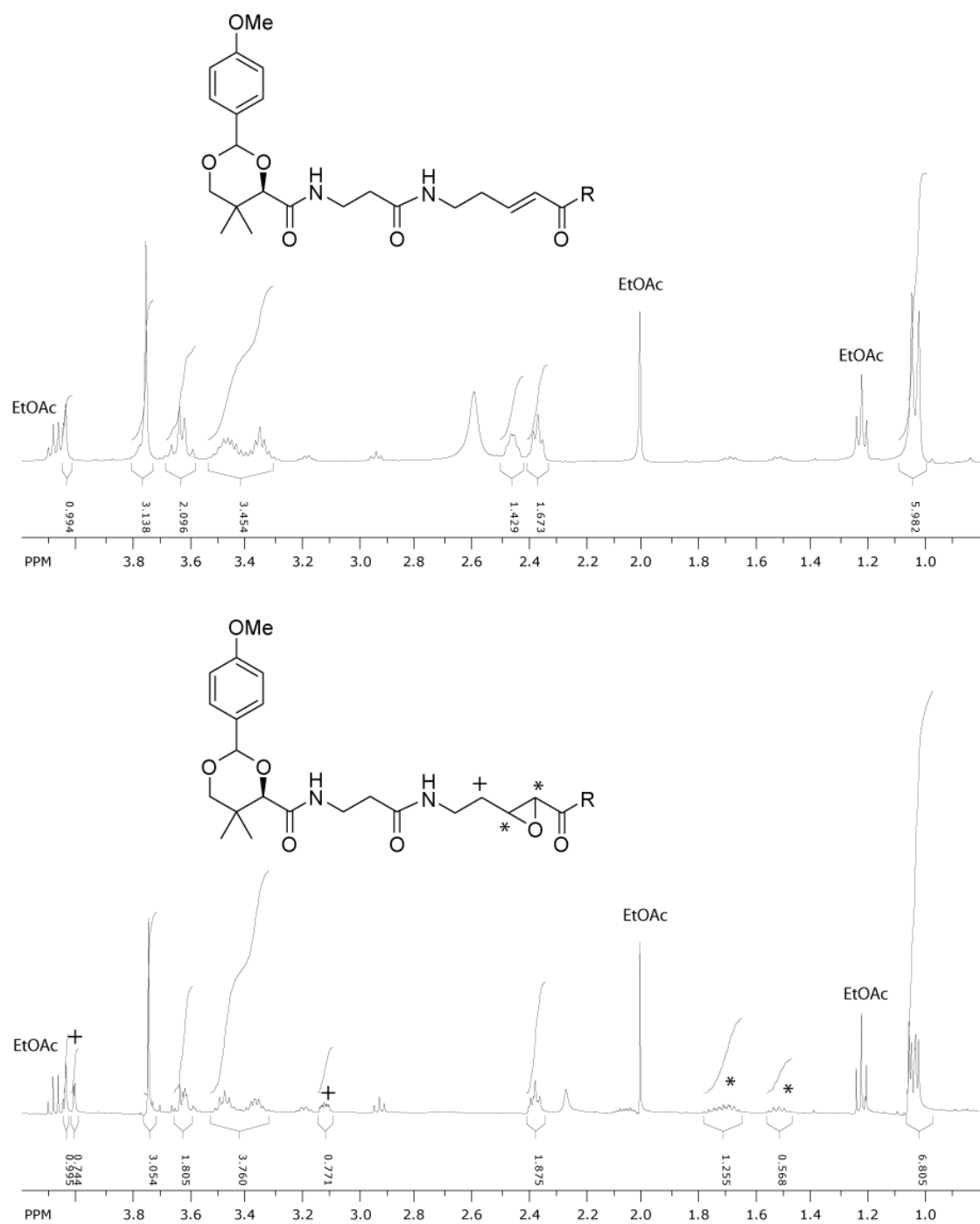
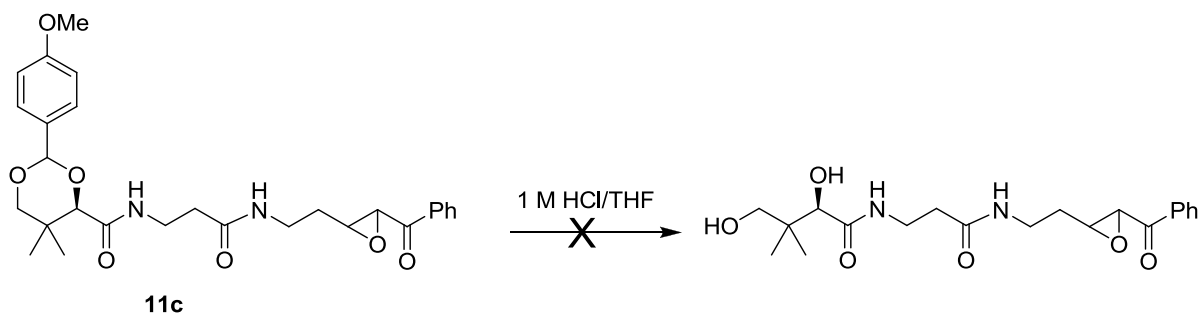


Figure 2.1. Comparison of up field region of ^1H NMR of α,β -unsaturated ketone **10c** (top) and epoxide **11c** (bottom). The * denotes epoxide protons, + denotes protons α to the epoxide and R = Ph.

2.2.2.4 Attempted deprotection of epoxide **11c**

With the diastereomeric mixture of **11c** in hand, the deprotection of the PMB group was attempted using 0.5 M aqueous HCl in THF at rt (Scheme 2.6). Unfortunately, extensive decomposition of **11c** was noted on TLC and none of the desired epoxide-containing pantothenamide could be isolated. In the literature, numerous ways of deprotecting the PMB group are reported, and it may therefore be possible that a milder deprotection procedure could potentially be utilized to obtain the desired epoxy-pantothenamide. However, in light of the successful demonstration of the inhibition of CoADR by the other Michael acceptor-containing CoA analogues our attempts at preparing an epoxide-containing CoADR inhibitor were abandoned. It is worth noting that the instability of epoxides was also noted in the synthesis of a epoxide-containing trypanothione reductase inhibitor, and that this also prevented the authors of this study to use it as an inhibitor of the enzyme.⁵



Scheme 2.6. Attempted deprotection of PMB-protected epoxide **11c**.

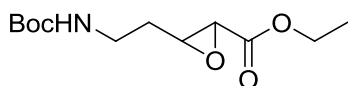
2.3 Conclusion

To supplement the Michael acceptor-based warheads of the published CoADR inhibitors we attempted the synthesis of an epoxide-containing pantothenamide. Apart from being used extensively in the development of cysteine proteases inhibitors, epoxides have the additional advantage that they do not require a base for protonation after nucleophilic attack by the active site Cys. Although epoxides are attractive warheads for this type of inhibition, its introduction into pantothenamides were hampered by instability and low yields. We were eventually successful in the synthesis of a PMB-protected pantothenamide precursor, but its deprotection was unsuccessful due to decomposition of the epoxide. With numerous other reagents available for synthesizing epoxides the required epoxide-containing pantothenamide could possibly be prepared. However, with similar problems with the introduction of epoxides being reported by other groups, the epoxide synthesis was abandoned and was therefore not included in the accompanying manuscript.

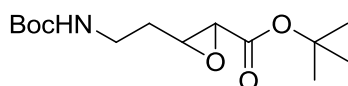
2.4 Experimental Section

All *trans*-epoxides were synthesized using a general procedure for the stereocontrolled epoxidation of α,β -unsaturated esters, which was similar to the method previously described by Meth-Cohn.⁴

2.4.1 Ethyl 3-(2-(*tert*-butoxycarbonylamino)ethyl)oxirane-2-carboxylate (**9a**)



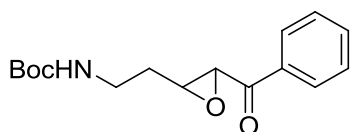
To a solution of TBHP (638 μ L of a 5.5 M anhydrous solution in decane, 3.51 mmol) in anhydrous THF (5.5 mL) at -78°C was added BuLi (1.72 mL of a 1.50 M solution in hexane, 2.58 mmol). The solution was stirred for 5 min, after which **3a** (0.570 g, 2.34 mmol) in THF (23 mL) was added. The reaction was allowed to warm to -45°C and stirred overnight followed by the addition of solid Na_2SO_3 (0.230 g) and stirring for a further 10 min. The reaction mixture was transferred to a separatory funnel containing EtOAc (100 mL) and washed with 1 M HCl (2 x 20 mL) and brine (2x20 mL). After drying the organic layer over Na_2SO_4 , filtration and concentration *in vacuo* the crude product was purified using flash chromatography (Hexane/EtOAc 3:1) which afforded the *trans* epoxide **9a** (0.208 g, 34%). ^1H NMR (CDCl_3 , 400MHz): δ = 1.29 (t, J = 6.9 Hz, 3H), 1.43 (s, 9H), 1.68 (m, 1H), 2.00 (m, 1H), 3.21 (m, 1H), 3.25 (d, J = 1.9 Hz, 1H), 3.29 (m, 2H), 4.23 (dq, J = 7.0 Hz, 2H); MS (ESI^+): m/z (%) = 260 (50) $[\text{M}+1]^+$.



2.4.2 *tert*-Butyl 3-(2-(*tert*-butoxycarbonylamino)ethyl)oxirane-2-carboxylate (**9b**)

To a solution of TBHP (322 μ L of a 5.5 M anhydrous solution in decane, 1.77 mmol) in anhydrous THF (2.8 mL) at -78°C was added BuLi (0.975 mL of a 1.33 M solution in hexane, 1.30 mmol). The solution was stirred for 5 min, after which **3b** (0.320 g, 1.18 mmol) in THF (2 mL) was added. The reaction was allowed to warm to rt and stirred for 2h followed by the addition of solid Na_2SO_3 (0.110 g) and stirring for a further 10 min. The reaction mixture was transferred to a separatory funnel containing EtOAc (80 mL) and washed with 1 M HCl (2 x 20 mL) and brine (20 mL). After drying the organic layer over Na_2SO_4 , filtration and concentration *in vacuo* the crude product was purified using flash chromatography (Hexane/EtOAc 4:1) which afforded the *trans* epoxide **9b** (0.178 g, 53%). ^1H NMR (CDCl_3 , 400MHz): δ = 1.45 (s, 9H), 1.49 (s, 9H), 1.66 (m, 1H), 2.0 (m, 1H), 3.13–3.32 (m, 4H); MS (ESI^+): m/z (%) = 310.2 (40) $[\text{M}+\text{Na}]^+$.

2.4.3 *tert*-Butyl 2-(3-benzoyloxiran-2-yl)ethylcarbamate (**9c**)

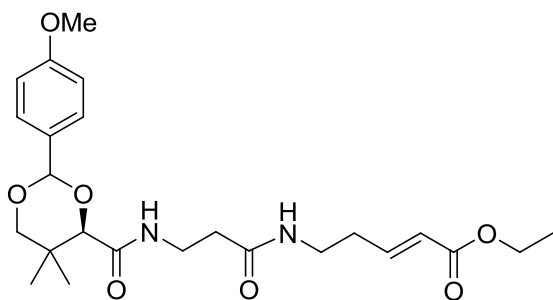


To a solution of TBHP (101 μ L of a 5.5 M anhydrous solution in decane, 0.588 mmol) in anhydrous THF (1.5 mL) at -78°C was added BuLi (0.319 mL of a 1.35 M solution in hexane, 0.431 mmol). The solution was stirred for 5 min, after which **3c** (0.320 g, 1.18 mmol) in THF (2.0 mL) was added. The reaction was allowed to warm to rt and stirred for 2h followed by the addition of solid Na_2SO_3 (70 mg) and stirring for a further 10 min. The reaction mixture was transferred to a separatory funnel containing EtOAc (10 mL) and washed with 1 M HCl (2 x 10 mL) and brine (10 mL). After drying the organic layer over Na_2SO_4 , filtration and concentration *in vacuo* the crude product was purified using flash chromatography (Hexane/EtOAc 2:1) which afforded the *trans* epoxide **9c** (0.33 g, 36%). ^1H NMR (CDCl_3 , 400MHz): δ = 1.41 (s, 9H), 1.80 (m, 1H), 2.11 (br s, 1H), 3.20 (m, 1H), 3.33 (m, 2H), 4.06 (d, J = 2.0 Hz, 1H), 7.48 (m, 2H), 7.61 (m, 1H), 7.98 (m, 2H); ^{13}C NMR (CDCl_3 , 150MHz): δ = 24.0, 27.9, 34.0, 54.8, 56.3, 79.6, 132.8, 133.4, 138.9, 140.5, 162.8, 204.5; HRMS–ESI: m/z $[\text{M}+1]^+$ calcd for $\text{C}_{16}\text{H}_{21}\text{NO}_4$: 292.1549; found: 292.1529.

2.4.4 General procedure for PMB protection of pantothenamides (**10a-c**)

An oven-dried Schlenk tube was charged with a 0.2 M solution of pantothenamide in THF. The solvent was removed under reduced pressure while maintaining anhydrous conditions, followed by re-dissolution of the amide in THF. This cycle was repeated three times to render the pantothenamide completely anhydrous. The pantothenamide was again dissolved in anhydrous THF and CSA (0.1 eq) and *p*-methoxybenzaldehyde dimethyl acetal (2.0 eq) was added. The reaction was stirred at room temperature for 24h. The reaction mixture was concentrated *in vacuo* and the resulting residue was purified using flash chromatography.

2.4.5 (*E*)-Ethyl 5-{3-[(4*R*)-2-(4-methoxyphenyl)-5,5-dimethyl-1,3-dioxane-4-carboxamido] propanamido} pent-2-enoate (**10a**)

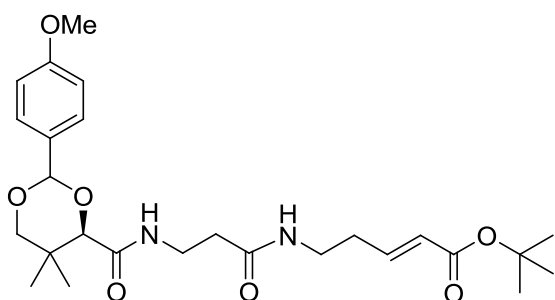


The reaction was conducted as in the general procedure using **8a** (0.342 g, 0.993 mmol), CSA (23 mg, 0.099 mmol), *p*-methoxybenzaldehyde dimethyl acetal (0.338 mL, 1.99 mmol). The product was purified using flash chromatography (100% EtOAc) which gave **10a** (0.300 g, 65%) as a white sticky oil.

^1H NMR (CD_3OD , 400MHz): δ = 1.02 (s, 3H), 1.09 (s, 3H), 1.25 (t, J = 7.0 Hz, 3H), 2.34 (q, J = 7.0 Hz, 2H), 2.40 (t, J = 6.3 Hz, 2H), 3.26 (m, 2H), 3.49

(m, 2H), 3.66 (d, $J = 11.3$ Hz, 1H), 3.72 (d, $J = 11.4$ Hz, 1H), 3.78 (s, 3H), 4.16 (m, 3H), 5.52 (s, 1H), 5.84 (d, $J = 15.6$ Hz, 1H), 6.86 (dt, $J = 15.6, 7.0$ Hz, 1H), 6.91 (d, $J = 8.4$ Hz, 2H), 7.44 (d, $J = 8.6$ Hz, 2H); ^{13}C NMR (CD_3OD , 75.5MHz): $\delta = 14.5, 19.7, 22.1, 32.9, 36.1, 36.4, 39.0, 40.2, 55.7, 61.5, 79.2, 85.0, 102.6, 114.5, 123.9, 128.8, 131.7, 147.2, 161.7, 168.0, 171.7, 173.9$; MS (ESI $^+$): m/z (%) = 463.2 (30) $[\text{M}+1]^+$.

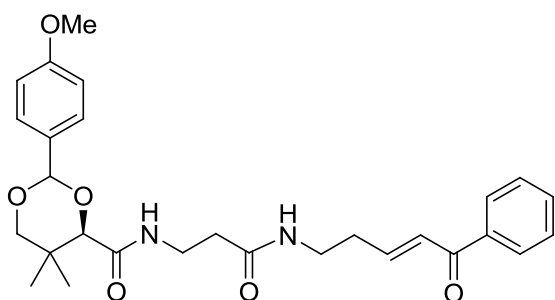
2.4.6 (*E*)-*tert*-Butyl 5-{3-[(4*R*)-2-(4-methoxyphenyl)-5,5-dimethyl-1,3-dioxane-4-carboxamido] propanamido} pent-2-enoate (**10b**)



The reaction was conducted as in the general procedure using **8b** (0.471 g, 1.27 mmol), CSA (29 mg, 0.13 mmol), *p*-methoxybenzaldehyde dimethyl acetal (0.431 mL, 2.53 mmol). The product was purified using flash chromatography (100% EtOAc) which gave **10b** (0.488 g, 78%) as a yellow paste. ^1H

NMR (CD_3OD , 400MHz): $\delta = 1.03$ (s, 3H), 1.09 (s, 3H), 1.46 (s, 9H), 2.31 (q, $J = 6.9$ Hz, 2H), 2.39 (t, $J = 6.7$ Hz, 2H), 3.24 (m, 2H), 3.46 (t, $J = 6.7$ Hz, 2H), 3.67 (d, $J = 11.3$ Hz, 1H), 3.72 (d, $J = 11.4$ Hz, 1H), 3.79 (s, 3H), 4.15 (s, 1H), 5.53 (s, 1H), 5.75 (d, $J = 15.6$ Hz, 1H), 6.76 (dt, $J = 15.6, 7.1$ Hz, 1H), 6.91 (d, $J = 9.1$ Hz, 2H), 7.44 (d, $J = 8.9$ Hz, 2H); HRMS–ESI: m/z $[\text{M}+1]^+$ calcd for $\text{C}_{26}\text{H}_{39}\text{N}_2\text{O}_7$: 491.2757; found: 491.2744.

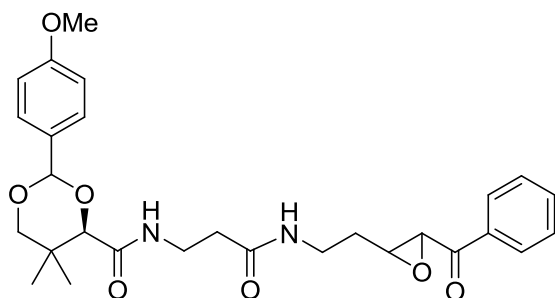
2.4.7 (4*R*)-2-(4-Methoxyphenyl)-5,5-dimethyl-N-{3-oxo-3-[(*E*)-5-oxo-5-phenylpent-3-enylamino] propyl}-1,3-dioxane-4-carboxamide (**10c**)



The reaction was conducted as in the general procedure using **8c** (0.223 g, 0.592 mmol), CSA (14 mg, 0.059 mmol), *p*-methoxybenzaldehyde dimethyl acetal (0.202 mL, 1.18 mmol). The product was purified using flash chromatography (EtOAc/Hexane 3:1 to EtOAc) which gave **10c** (0.146 g, 50%) as a

yellow paste. ^1H NMR (CD_3OD , 400MHz): $\delta = 1.02$ (s, 3H), 1.08 (s, 3H), 2.42 (t, $J = 6.8$ Hz, 2H), 2.48 (q, $J = 6.3$ Hz, 2H), 3.35 (t, $J = 5.1$ Hz, 2H), 3.42–3.55 (m, 2H), 3.65 (d, $J = 11.3$ Hz, 1H), 3.69 (d, $J = 11.2$ Hz, 1H), 3.75 (s, 3H), 4.13 (s, 1H), 5.49 (s, 1H), 6.89 (d, $J = 9.0$ Hz, 2H), 6.93 (dt, $J = 15.5, 6.3$ Hz, 1H), 7.03 (d, $J = 15.7$ Hz, 1H), 7.43 (d, $J = 9.0$ Hz, 2H), 7.5 (m, 2H), 7.6 (m, 1H), 7.94 (m, 2H); ^{13}C NMR (CDCl_3 , 100MHz): $\delta = 18.9, 21.5, 32.4, 32.9, 35.0, 35.8, 37.9, 55.2, 78.3, 83.6, 101.3, 113.6, 126.8, 127.3, 128.5, 129.2, 129.6, 133.0, 137.3, 146.0, 160.2, 171.4, 171.5, 191.0$; MS (ESI $^+$): m/z (%) = 495.2 (20) $[\text{M}+1]^+$.

2.4.8 (4*R*)-N-{3-[2-(3-Benzoyloxiran-2-yl)ethylamino)-3-oxopropyl]-2-(4-methoxyphenyl)}-5,5-dimethyl-1,3-dioxane-4-carboxamide (**11c**)



To a solution of TBHP (81 μ L of a 5.5 M anhydrous solution in decane, 0.44 mmol) in anhydrous THF (2.2 mL) at -78°C was added BuLi (241 μ L of a 1.35 M solution in hexane, 0.33 mmol). The solution was stirred for 5 min, after which **10c** (0.146 g, 0.295 mmol) in THF (1 mL) was added. The reaction was allowed to warm to room temperature and stirred for 2h followed by the addition of solid Na_2SO_3 (70 mg) and stirring for a further 10 min. The reaction mixture was transferred to a separatory funnel containing EtOAc (10 mL) and washed with water (10 mL). After drying the organic layer over Na_2SO_4 , filtration and concentration *in vacuo* the crude product was purified using flash chromatography (EtOAc/Hexane 3:1 to EtOAc) which afforded the *trans* epoxide **11c** (71 mg, 47%). HRMS–ESI: m/z $[\text{M}+1]^+$ calcd for $\text{C}_{28}\text{H}_{35}\text{N}_2\text{O}_7$: 511.2444; found: 511.2427

2.5 References

1. Powers, J. C.; Asgian, J. L.; Ekici, O. D.; James, K. E., Irreversible inhibitors of serine, cysteine, and threonine proteases. *Chem. Rev.* **2002**, *102* (12), 4639-4750.
2. Asgian, J. L.; James, K. E.; Li, Z. Z.; Carter, W.; Barrett, A. J.; Mikolajczyk, J.; Salvesen, G. S.; Powers, J. C., Aza-Peptide Epoxides: A New Class of Inhibitors Selective for Clan CD Cysteine Proteases. *J. Med. Chem.* **2002**, *45* (23), 4958-4960.
3. James, K. E.; Asgian, J. L.; Li, Z. Z.; Ekici, O. D.; Rubin, J. R.; Mikolajczyk, J.; Salvesen, G. S.; Powers, J. C., Design, Synthesis, and Evaluation of Aza-Peptide Epoxides as Selective and Potent Inhibitors of Caspases-1, -3, -6, and -8. *J. Med. Chem.* **2004**, *47* (6), 1553-1574.
4. Meth-Cohn, O.; Moore, C.; Taljaard, H. C., A stereocontrolled approach to electrophilic epoxides. *J. Chem. Soc., Perkin Trans. 1* **1988**, (9), 2663-2674.

Determination of the mechanism of action of CJ-15,801[†]

3.1 Discovery of CJ-15,801 as an antistaphylococcal agent

In 2001 it was reported by Sugie *et al.* that a compound isolated from fermenting cultures of the fungus *Seimatosporium* sp. potently inhibits the growth of three multi-drug resistant strains of *S. aureus* with MIC values ranging from 6.25 to 50 µg/mL (28.8-230 µM).¹ The structure of this compound was identified to be the pantothenic acid analogue **3.1**, and it was named CJ-15,801 (Figure 3.1). Structural analysis of CJ-15,801 showed that it contained a novel *trans* enamide functionality replacing the β-alanine moiety of pantothenic acid (PanCOOH) **1.1**.

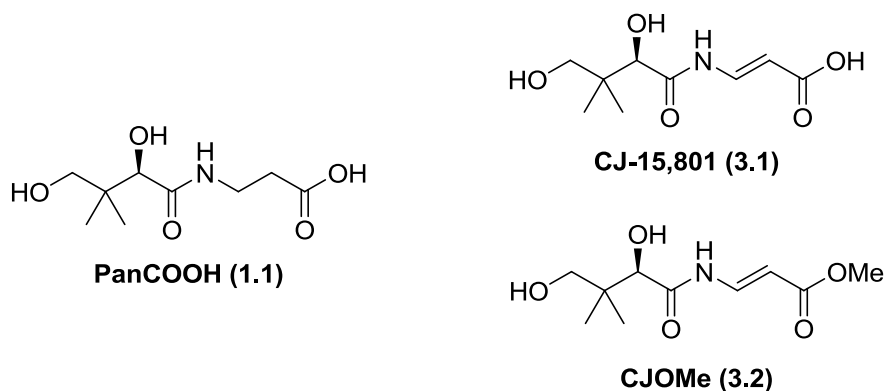


Figure 3.1. Comparison of the structures of pantothenic acid, CJ-15,801 and its methyl ester analogue.

The only additional biological study of CJ-15,801 that has been conducted to date was done by Saliba *et al.* who investigated its effect on the proliferation of the malaria parasite *Plasmodium falciparum*.² They showed that CJ-15,801 is a potent inhibitor of parasite growth ($IC_{50} = 39 \mu M$) and concluded that it exerts its effect by inhibiting the utilisation of PanCOOH. This was based on the finding that increased concentrations of PanCOOH reversed the antiplasmodial effect of CJ-15,801. However, to date no definitive study has surfaced on the mechanism of action (MOA) of this compound in *S. aureus* or in any other bacterium, and its antibiotic mechanism and biological target still remains unknown. We therefore set out to determine the molecular target for the

[†] Parts of the study described in this chapter were conducted in collaboration with the group of Prof. Michael Burkart at University of California, San Diego, USA. The data obtained in his group that are reported here are clearly indicated.

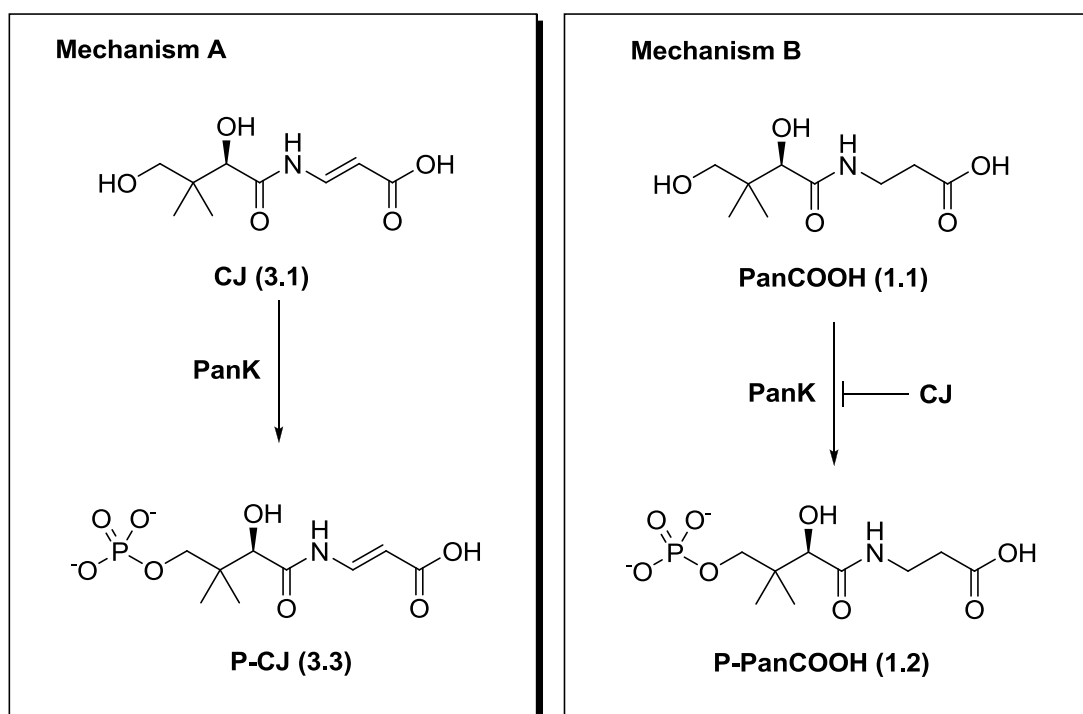
reported growth inhibition caused by CJ-15,801. In the rest of this dissertation CJ-15,801 will be referred to only as CJ.

3.2 Potential targets for the antibiotic action of CJ

Since the structures of PanCOOH (which is the natural substrate of PanK) and CJ bear significant similarity, it is most probable that its target would be found among the CoA biosynthetic enzymes, or enzymes that utilize CoA. We have identified the following potential targets for CJ action that are involved in CoA biosynthesis and metabolism.

3.2.1 Competitive inhibition of PanK

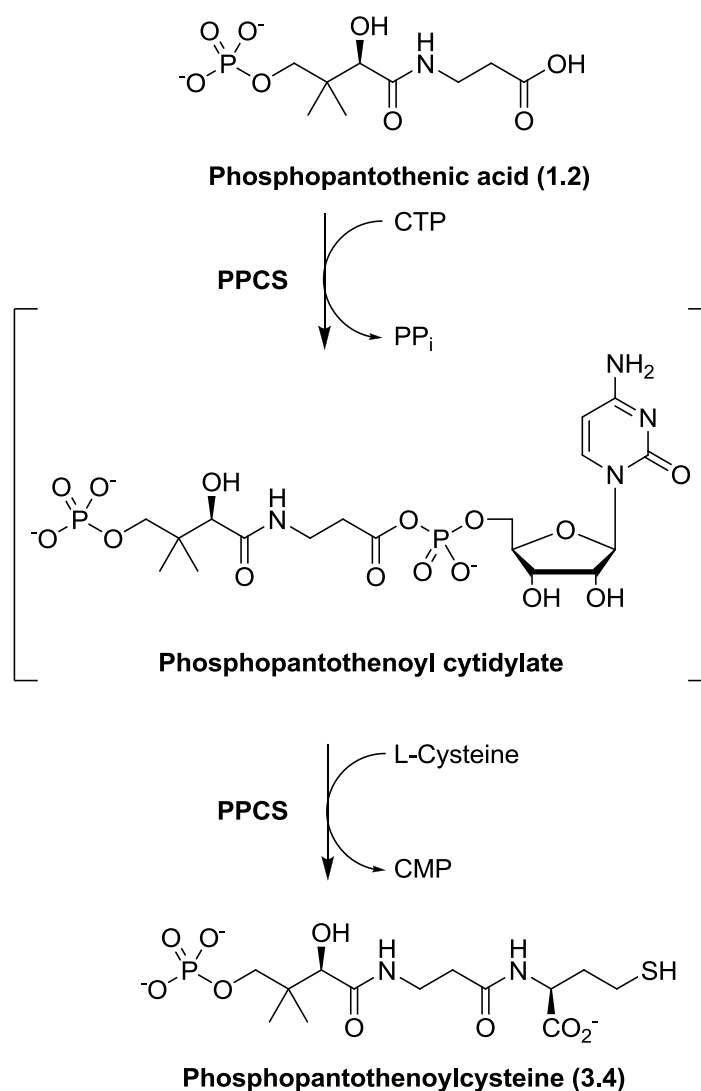
The first potential target through which CJ could exert its effect is by inhibition of PanK, the first enzyme in the CoA biosynthetic pathway (Scheme 1.1). This could take place by CJ either competing with PanCOOH by acting as a substrate of PanK (Scheme 3.1, Mechanism A) or by acting as a competitive inhibitor of PanK (Scheme 3.1, Mechanism B). An important difference between these two mechanisms is that in the case of mechanism A CJ will be consumed over time, thereby reducing its effective concentration, while in the case of mechanism B the inhibitory effect of CJ will only be reduced by its removal or degradation. Moreover, acting as a substrate like in mechanism A will transform CJ into phosphorylated CJ (P-CJ) which may exert down-stream effects similar to the pantothenamides (See Chapter 1 section 1.3.2), while this cannot be the case if mechanism B is in operation.



Scheme 3.1. Possible PanK inhibition mechanisms by CJ. In mechanism A CJ acts as an alternate substrate to PanCOOH for phosphorylation by PanK. In mechanism B CJ is a competitive inhibitor of PanK.

3.2.2 Inhibition of PPCS

The second step in the CoA biosynthetic pathway (Scheme 1.1) is catalysed by phosphopantothenoylcysteine synthetase (PPCS) and involves the coupling of Cys to phosphopantothenic acid (P-PanCOOH) **1.2** via an amide linkage to form phosphopantothenoylcysteine **3.4** (Scheme 3.2). This reaction proceeds in two steps, where in the first step P-PanCOOH is activated by transfer of a cytidyl group from CTP to the carboxylate of **1.2** to give an intermediate phosphopantothenoyl cytidylate and pyrophosphate (PP_i) as products. In the second step the amide bond is introduced via the nucleophilic attack of the amino group of Cys on the activated acyl cytidylate intermediate with the concomitant release of CMP.



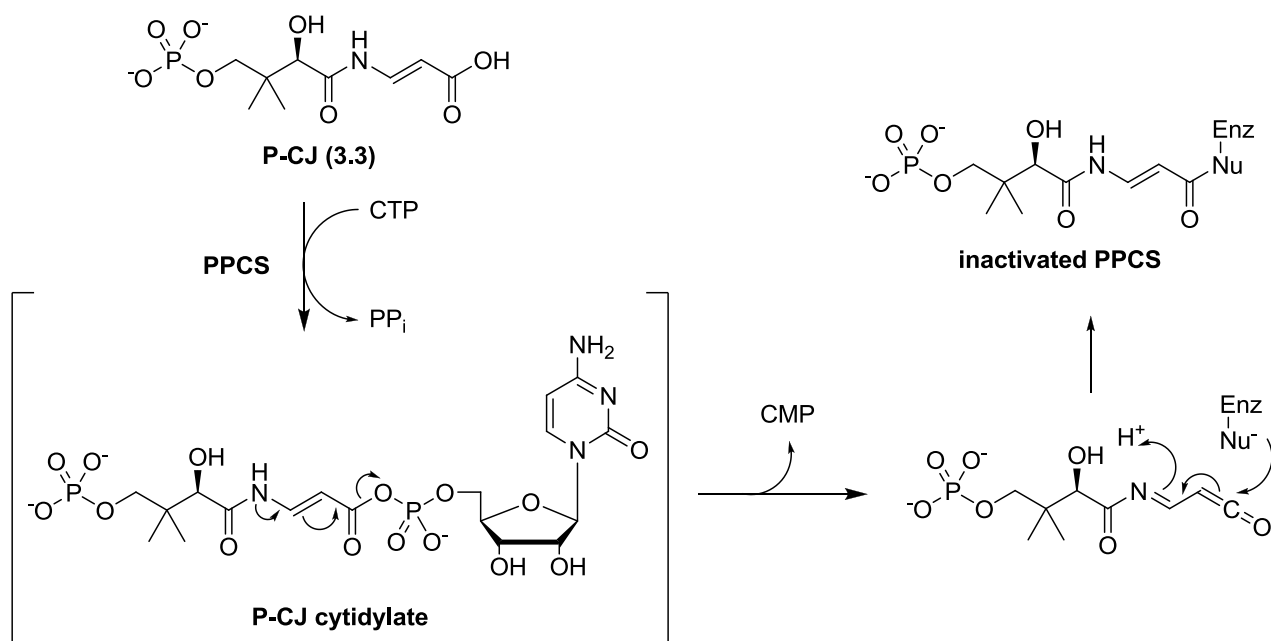
Scheme 3.2. Mechanism of the reaction catalysed by PPCS.

Should CJ act as a substrate of PanK to form P-CJ, this compound could potentially inhibit PPCS by one of two distinct mechanisms that can be differentiated based on the reversibility of the inhibition, as detailed below.

3.2.1.1 Irreversible inhibition of PPCS

A mechanism for the potential irreversible inhibition of PPCS by CJ can be proposed based on the close structural similarity of CJ to PanCOOH, and on the inherent reactivity of its enamide moiety. Specifically, if PPCS accepts P-CJ as an alternate substrate and activates it as an acyl cytidylate in a manner similar to the native reaction, subsequent rearrangement of the enamide moiety could lead to expulsion of CMP, and formation of a reactive ketene intermediate as set out in Scheme 3.3. Such a ketene could react with closely positioned nucleophiles in the active site of PPCS to cause irreversible inhibition of the enzyme. This type of inhibition, also known as mechanism-

based inhibition, occurs when the enzyme transforms the inhibitor into a chemically reactive species which acts as (1) an affinity label, (2) a transition state analogue, or (3) a very tight binding reversible inhibitor prior to release from the enzyme active site.³ The proposed ketene-based mechanism for P-CJ shown in Scheme 3.3 would turn it into an affinity label.



Scheme 3.3. Proposed ketene-based inhibition mechanism. A ketene could form after PPCS-mediated activation of the carboxylate of CJ by CTP, followed by rearrangement and expulsion of CMP. Nu represents an active-site nucleophile.

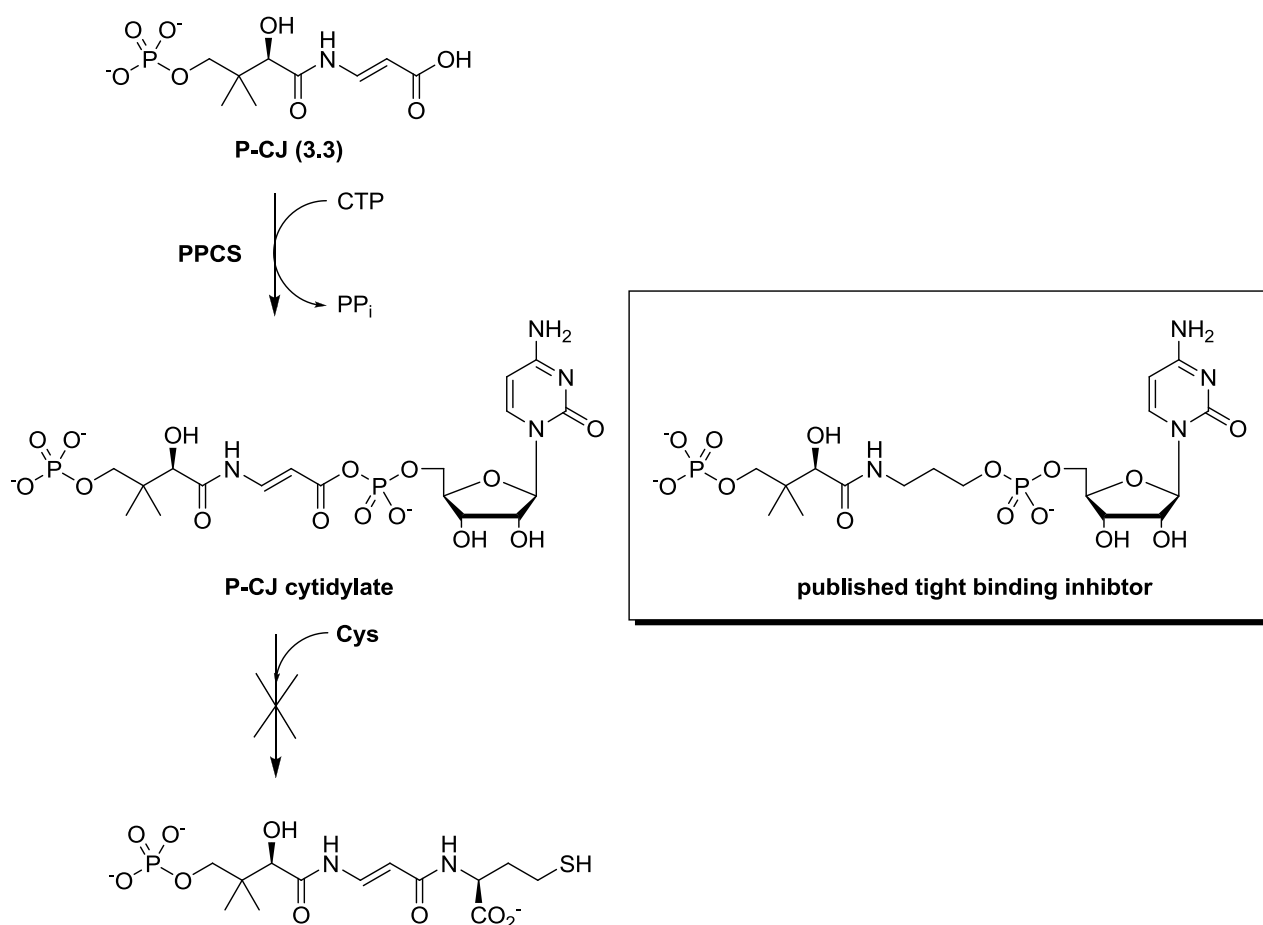
3.2.1.2 Reversible inhibition of PPCS

A second possible mechanism for PPCS inhibition would also entail formation of an activated P-CJ cytidylate. However, instead of this intermediate undergoing rearrangement to give an affinity label, the structurally more rigid double bond modifies its bonding and reactivity in such a manner that it becomes a reversible, albeit potentially tight-binding, inhibitor (Scheme 3.4). This activated cytidylate would be unreactive towards cysteine, most probably because it is not correctly positioned for nucleophilic attack.

Support for an inhibition mechanism that involves the transformation of P-CJ into a reaction intermediate that is also a tight binding inhibitor can be found in a recent study by Patrone *et al.* which showed that non-reactive analogues of the acyl cytidylate are indeed potent tight-binding inhibitors of PPCS enzymes.⁴ The compounds, previously referred to in chapter 1 (see section 1.3.2.2), are the only published inhibitors of PPCS enzymes and showed potent broad spectrum activity against a wide range of PPCSs from Enterobacteria. The most potent inhibitor (structure

shown in Scheme 3.4) had the mixed phospho-anhydride of the intermediate phosphopantothenoil cytidylate replaced by a phosphodiester moiety.

Further support for the P-CJ cytidylate adduct potentially occupying the active site in an inhibitory fashion can be found in the crystal structure of the *EcPPCS* Asn210Asp mutant, which is defective in cysteine binding or impairs its ability to attack the acyl cytidylate.⁵ The structure of the phosphopantothenoil cytidylate intermediate was found to occupy the active site of this mutant even after purification and crystallization.^{6,7} It may therefore be that the introduction of the *E*-double bond into phosphopantothenoil cytidylate may lead to a structure that similarly impairs cysteine binding or attack.

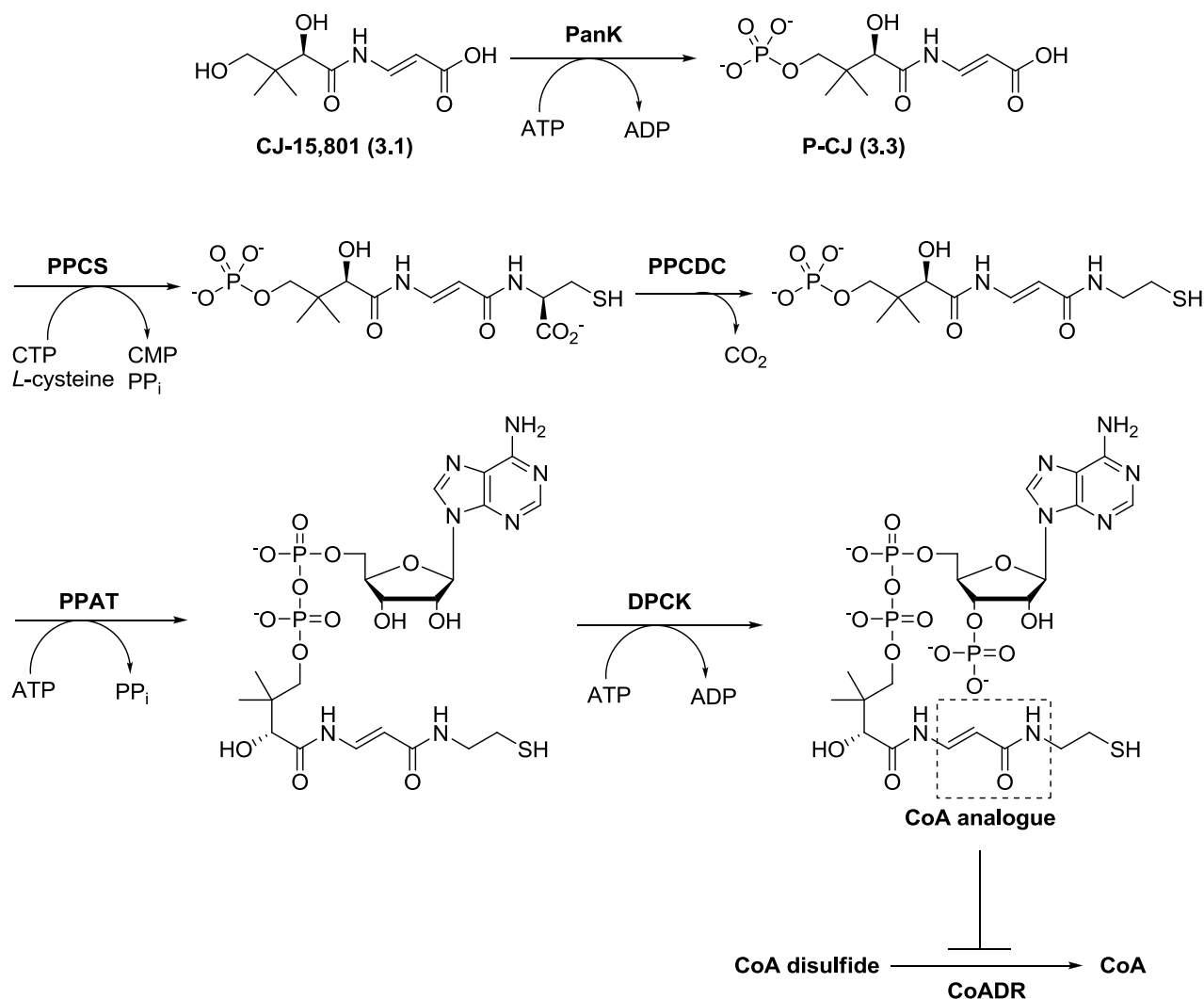


Scheme 3.4. Proposed mechanism of inhibition of PPCS by the formed P-CJ cytidylate intermediate. The insert shows the structure of the most potent tight binding inhibitor reported in a previous study.

3.2.3 CoADR as target

Another potential target for CJ-15,801 could be CoADR, the subject of the study described in the previous chapter. Such inhibition would be possible if instead of inhibiting PPCS, CJ acts as an alternative substrate of this and subsequent CoA biosynthetic enzymes to form a CoA analogue

(Scheme 3.5). The CoA analogue produced in this manner would have an incorporated α,β -unsaturated amide moiety that could act as a Michael-acceptor that may inhibit CoADR by alkylation of the active-site cysteine of CoADR in a manner similar to that described for the Michael acceptor-containing analogues described in the previous chapter.



Scheme 3.5. The conversion of CJ-15,801 to a CoA analogue by CoA biosynthetic enzymes which could potentially inhibit CoADR. The Michael-acceptor of the formed CoA analogue is enclosed by a box of dashed lines.

Based on these proposals we set out to determine the actual mechanism of action of the antibiotic CJ.

3.3 Results: CJ acts as a substrate, not an inhibitor, of PanK[§]

To determine if CJ is an inhibitor or a substrate of PanK a kinetic investigation was performed using the *EcPanK* and *SaPanK* enzymes. The results of this study (Table 3.1) showed that CJ is not an inhibitor of *SaPanK*, but rather acts as an alternate substrate. Furthermore, they found that the methyl ester of CJ was also a substrate for *SaPanK*. From the data in Table 3.1 it can be seen that CJ is a very good substrate for *SaPanK* since it has a k_{cat}/K_M value half of the value of natural substrate PanCOOH. The methyl ester was a much poorer substrate. Our collaborators also did similar experiments on *EcPanK* which found that CJ is not a substrate for *EcPanK*. This result is significant since CJ showed no inhibitory activity against *E. coli* growth at a concentration of 250 μ M, suggesting that when CJ cannot be phosphorylated by PanK (as in the case of this organism) it has no antibiotic activity. With the knowledge that CJ is a substrate for *SaPanK* we turned our attention towards the possible inhibition of PPCS by P-CJ.

Tabel 3.1. Kinetic parameters of *E. coli* and *S. aureus* PanK's with **1.1**, **3.1** and **3.2**.

Substrate	PanK enzyme	K_M (μ M)	k_{cat} (s^{-1})	k_{cat}/K_M ($mmol^{-1}s^{-1}$)	MIC (μ M)
Pantothenate (1.1)		25 ± 7.5	0.95 ± 0.03	38.4 ± 4.60	^a
CJ-15,801 (3.1)	<i>EcPanK</i>	n/a	n/a	n/a	>250
CJOMe (3.2)		n/a	n/a	n/a	n/a
Pantothenate (1.1)		31.8 ± 6.8	0.96 ± 0.07	30.2 ± 10.1	^a
CJ-15,801 (3.1)	<i>SaPanK</i>	66.0 ± 14.1	0.91 ± 0.08	13.8 ± 5.72	120
CJOMe (3.2)		314 ± 48.0	2.21 ± 0.23	7.50 ± 4.80	n/a

^a = is the natural substrate of PanK. n/a = no activity.

[§] The kinetic study described in this section was performed by Jordan Meier from the Burkart group at UCSD using CJ he prepared synthetically following a published procedure.⁸

3.4 Results: PPCS is the main target inhibited by CJ

3.4.1 *In situ* generation of P-CJ

In order to test for inhibition of PPCS by P-CJ, the phosphorylated version of the natural product was required. While the synthetic preparation of P-CJ was being undertaken by our collaborators, we decided to generate P-CJ *in situ* in our assays. We used SaPanK and ATP and CJ provided to us by the Burkart group to achieve this.

To ensure that **3.1** is fully converted to P-CJ under our assay conditions and within a short time we studied this reaction by following the formation of P-CJ at 254 nm using HPLC. The HPLC analysis of the SaPanK reaction with **3.1** showed that 0.5 mM CJ is quantitatively converted to P-CJ in 10 min (Figure 3.2). Unfortunately, it also showed that the polarity of ATP and P-CJ are similar - this would make their separation and hence the purification of P-CJ difficult. We therefore concluded that the conversion of CJ to P-CJ by SaPanK is sufficiently fast to use the *in situ* generation of P-CJ in all the PPCS assays described in this chapter.

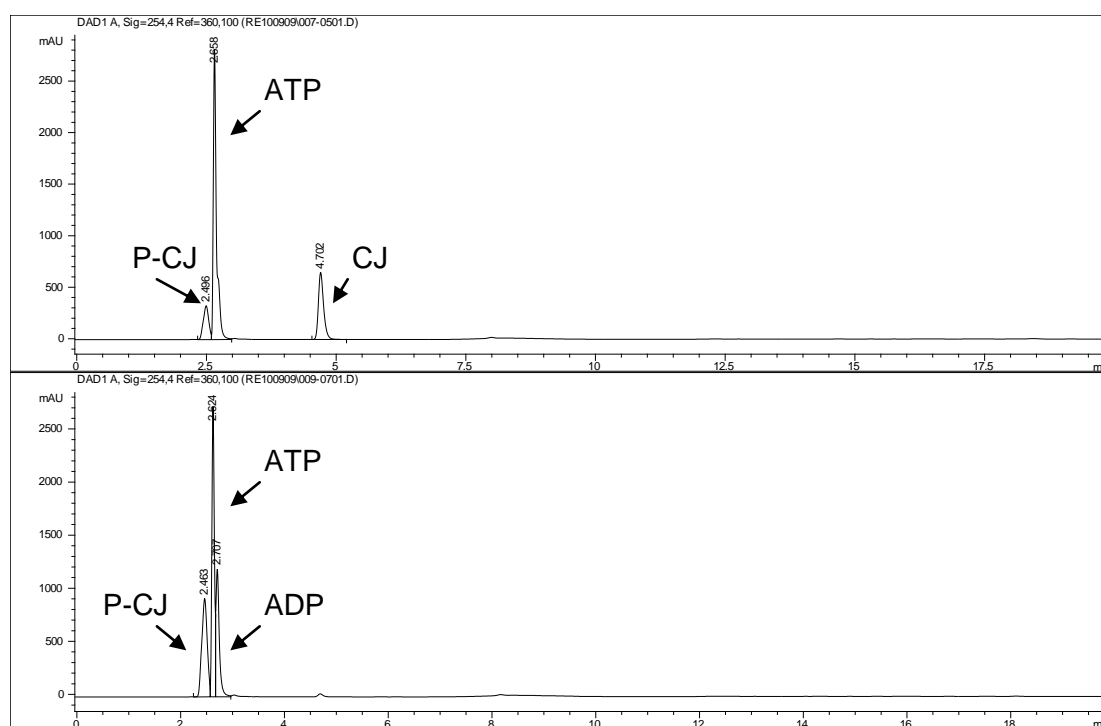


Figure 3.2. HPLC analysis of the conversion of CJ to P-CJ by SaPanK. Top chromatogram shows the reaction after 1 min and the bottom chromatogram shows the reaction after 10 min. Peaks at 2.5 and 4.7 min are P-CJ and CJ respectively and other peaks represent ATP and ADP.

3.4.2 PPCS inhibition assay

The PPCS enzyme from *E. coli* (*EcPPCS*) is well characterized and was available in our lab. Therefore it was used as a model to characterize the inhibition of PPCS enzymes by P-CJ. We used P-PanCOOH as substrate, which was prepared according to published methods, in all PPCS assays.⁹ In the literature and in this study pyrophosphate (PP_i) which is produced during the first step of the PPCS reaction, was measured using a commercial kit that couples the production of PP_i to the depletion in NADPH.^{4,10}

3.4.3 PPCS is inhibited by P-CJ, but not by its ester

An initial screen for PPCS inhibition by CJ, the methyl ester of CJ (CJOMe), the phosphorylated version of CJOMe (P-CJOMe) and P-CJ was performed at a concentration of 100 μ M. P-CJOMe was prepared by enzymatic conversion of CJOMe using the same procedure described in the previous section, and its formation was confirmed by HPLC (see experimental). The results of the assay showed that while CJ, CJOMe and P-CJOMe did not show any inhibition of *EcPPCS*, P-CJ significantly reduced its activity. The inactivity of the methyl ester analogues is consistent with the requirement of a free carboxylate group for inhibition to take place by any of the proposed mechanisms. The lack of inhibition seen for CJ also indicated the necessity of the phosphate group for binding and inhibition. With this exciting result we set out to first quantify the extent of inhibition and secondly to determine its mechanism.

3.4.4 Determining the IC_{50} of *EcPPCS* inhibition by P-CJ

The IC_{50} was determined by comparing the activity of *EcPPCS* with 250 μ M P-PanCOOH as substrate to its activity under the same conditions, but in the presence of increasing amounts of P-CJ prepared by the *in situ* conversion of CJ. The percentage activity was calculated by dividing the initial rate at each inhibitor concentration by the rate of the reaction without inhibitor. A potential problem with the *in situ* preparation of P-CJ is that the rate of conversion of CJ into P-CJ at high concentrations (\sim 100 μ M) might not be high enough, and that the observed inhibition would not be truly reflective of inhibition of P-CJ at such a concentration. In such a case the observed inhibition would be less than expected if actual P-CJ was used directly.

The resulting concentration-activity profile (Figure 3.3) shows the IC_{50} of P-CJ for *EcPPCS* (concentration of 240 nM) to be 3.3 ± 0.36 μ M. Since this value is close to 10-fold the enzyme concentration, it suggests that tight binding inhibition, rather than simple reversible inhibition, might be at play.¹¹ From the profile it can also be seen that the data recovered at concentrations of P-CJ higher than 10 μ M do not converge to 0% activity (100% inhibition), since in the assays conducted

at these inhibitor concentrations some initial *EcPPCS* activity could be detected during the first minute of the reaction, after which it slowly disappeared. This suggests that conversion of CJ to P-CJ may indeed be limiting at high concentrations as discussed above. This indicates that the availability of pure P-CJ would be an essential requirement for accurate IC_{50} determinations. The IC_{50} value of 3.3 μM can therefore be seen as an upper limit, since the actual value will in all likelihood be lower.

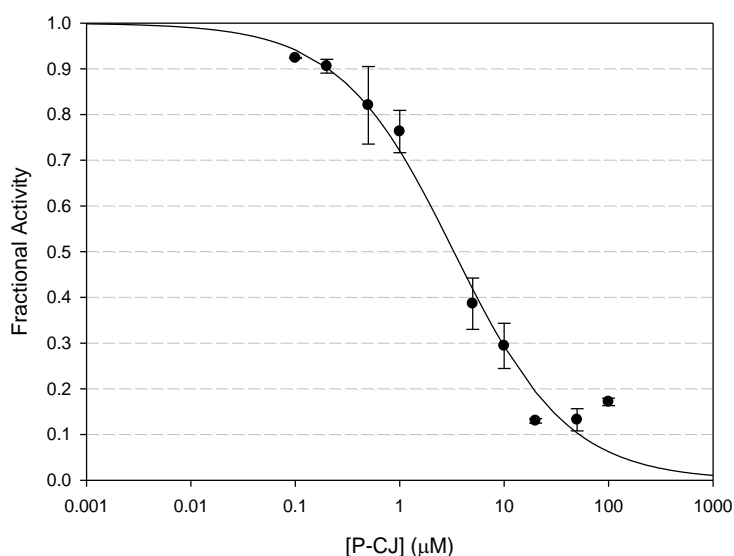


Figure 3.3. Concentration-activity profile of P-CJ-mediated inhibition of *EcPPCS* to determine the IC_{50} value.

3.4.5 Determining the reversibility of inhibition of PPCS by P-CJ

To distinguish between the two proposed inhibition mechanisms of PPCS (Section 3.1.2) two tests were performed. First, the irreversibility of inhibition was investigated by performing a test for irreversibility as described by Copeland.³ Second, the inhibitor treated enzyme was gel-filtered and subsequently assayed to establish if its activity returned upon removal of the inhibitor.

3.4.5.1 Determining reversibility by dilution

A reversibility test to determine if an enzyme's activity returns once the inhibitor is removed by dilution should be able to indicate if inhibition is reversible, slowly reversible or irreversible. We performed a reversibility test by pre-incubating CJ, SaPanK, *EcPPCS* and other assay components at 37 °C for 15 min. During pre-incubation [CJ] was 3-fold the IC_{50} of [P-CJ] (10 μM) and the [*EcPPCS*] was 100-fold the concentration used in the standard kinetic assays, i.e. 925 nM. After 15 minutes of incubation the pre-incubated mixture was diluted 100-fold and assayed. The obtained progress curves were compared to a control experiment without CJ.

Since the $[CJ]$ in the assay mixtures should be $\sim 0.1 \mu M$, or $\sim 3\%$ of the IC_{50} after dilution, one would expect a linear progress curve with a slope of roughly 97% of the control reactions rate if the inhibition is rapidly reversible. For a completely irreversible inhibitor, the expected progress curve would also be linear, but would be much lower and would reflect the extent of enzyme inactivation during pre-incubation. Since P-CJ was used at 3-fold IC_{50} the remaining (uninhibited) activity is expected to be about 9.7% of the control. A third possible progress curve with a curvilinear shape results from a slowly reversible inhibitor. This curvature is the result of the slow recovery of activity of the enzyme as the inhibitor dissociates from the target enzyme.

Unfortunately none of the above mentioned 3 possibilities were observed when the results of the dilution experiment were plotted (Figure 3.4). Instead, the observed activity is about 70% of the control reaction in the beginning, and then slowly decreases until it reaches about 33% towards the end. This result is therefore inconclusive in regards to the mechanism of inhibition, although it does rule out rapid reversible inhibition as a possibility.

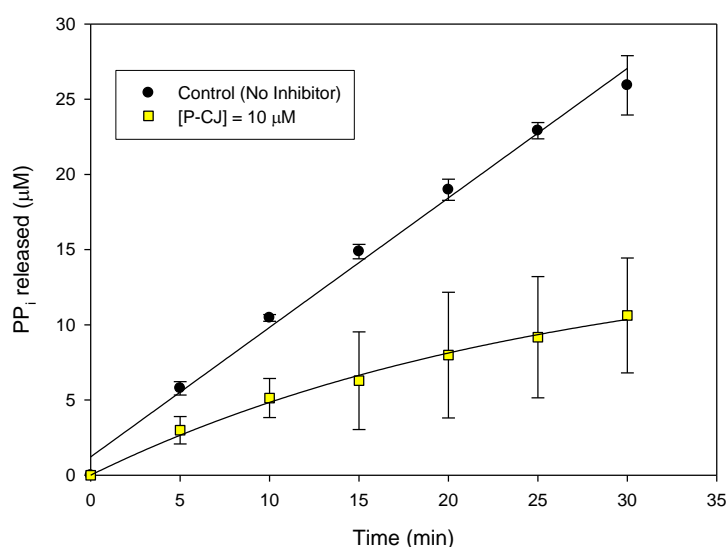


Figure 3.4. Test for reversibility of inhibition by 100-fold dilution and subsequent activity analysis of a PPCS sample pre-treated with P-CJ at a concentration of $10 \mu M$.

3.4.5.2 Determining reversibility by gel-filtration

To further investigate the mechanism of inhibition a mixture of *EcPPCS* and P-CJ was pre-incubated for 15 min (similar to above experiment), and was subsequently subjected to immediate gel filtration followed by a 100-fold dilution. Since gel filtration should remove all non-covalently-bound small compounds, such an experiment can be used to determine if *EcPPCS* and P-CJ forms a stable covalent bond. The enzyme was assayed to measure the remaining activity as

described above, and the percentage activity was calculated, using initial rates, relative to *EcPPCS* which was gel-filtered but not treated with P-CJ. The results showed that *EcPPCS* pre-treated with 100 μ M inhibitor had no reduced activity (Table 3.2). *EcPPCS* was therefore treated with higher inhibitor concentrations (0.5 mM and 1 mM) which resulted in reduced activities of 39% and 9% respectively. These results are surprising, and seem to indicate that inhibition of *EcPPCS* is irreversible at high P-CJ concentrations, but reversible at lower concentrations. However, such a conclusion would not be in agreement with the results of the previous experiment, which indicated reversible inhibition does not take place when even less (10 μ M vs 100 μ M) P-CJ was used. Currently this discrepancy cannot be explained.

Table 3.2. Remaining activity after gel-filtration of PPCS pre-incubated at different P-CJ concentrations.

P-CJ (mM)	% remaining activity
0.1	100
0.5	39
1	9

3.4.6 Progress curve analysis of the inhibition of *EcPPCS* by CJ

The inhibition of *EcPPCS* by P-CJ was subsequently studied by the progress curve method. The progress curves were generated by following the PPCS reaction by monitoring the production of PP_i as above, but by using an *EcPPCS* concentration of 9.3 nM. To ensure that substrate depletion would not significantly affect the reaction rate, a low enzyme concentration and high substrate concentration (P-PanCOOH = 250 μ M) were used, which allowed the control experiment (without inhibitor) to proceed linearly over 30 min. Such a procedure should allow any divergence from linearity, caused by slow onset or irreversible inhibition, to be clearly observable. The obtained results are shown in Figure 3.5.

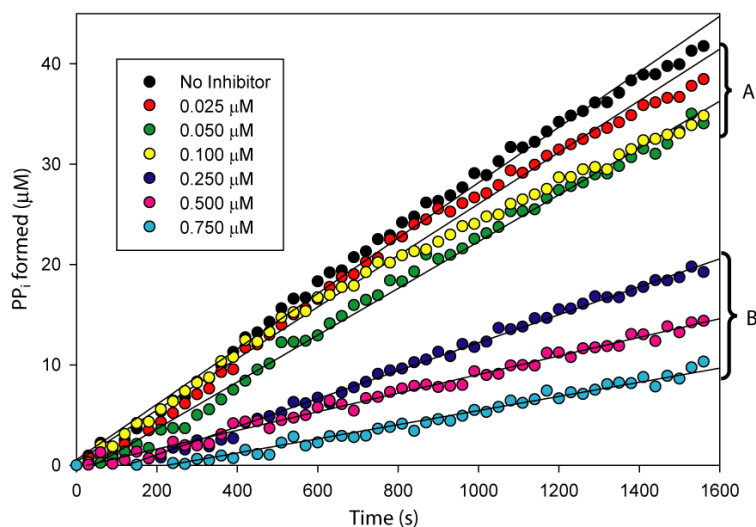


Figure 3.5. Progress curves obtained for the inhibition of PPCS by various P-CJ concentrations. The curves marked with A slightly deviate from linearity, where the curves donated by B are linear. The data points represent the average of an assay performed in triplicate.

The data again shows a distinction between results obtained at higher and lower concentrations of P-CJ. At lower inhibitor concentrations the progress curves deviated slightly from linearity (bracketed by A in Figure 3.5), which is indicative of slow onset inhibition. This is often found for tight binding inhibitors and causes the initial rate of the reaction and the steady state rate to differ.³ In contrast, at higher inhibitor concentrations (bracketed by B in Figure 3.5) the progress curves were linear.

Despite the slight deviation from linearity seen at lower inhibitor concentrations it was still possible to accurately determine the slopes of the progress curves presented in Figure 3.5 by linear regression. This was done for five inhibitor concentrations, since the slope of the line obtained at an inhibitor concentration of 0.100 μM could not be determined due to the hyperbolic shape of this curve. The calculated slopes, the substrate concentration and inhibitor concentrations were used to calculate the value of K_i^{app} by fitting the Morrison equation for tight binding inhibitors (Equation 3.1) to this data using SigmaPlot. The valued for K_i^{app} obtained in this manner was 282 nM.

$$\frac{v_i}{v_o} = 1 - \frac{([E] + [I] + K_i^{\text{app}}) - \sqrt{([E] + [I] + K_i^{\text{app}})^2 - 4[E][I]}}{2[E]} \quad 3.1$$

$$K_i^{\text{app}} = K_i \left(1 + \frac{[S]}{K_M} \right) \quad 3.2$$

The K_i^{app} was then converted to K_i by using Equation 3.2, which adjusts the K_i^{app} for competitive inhibitors for the substrate concentration used. Using a K_M value of 109 μM (calculated from the same data) for P-PanCOOH a K_i value of 85.5 ± 6.5 nM for the inhibition of EcPPCS by P-CJ was obtained in this manner. A graphical representation of the data used to calculate the value of K_i and K_M (i.e. the activity of the enzyme at each inhibitor concentration relative to the uninhibited reaction) is given in Figure 3.6.

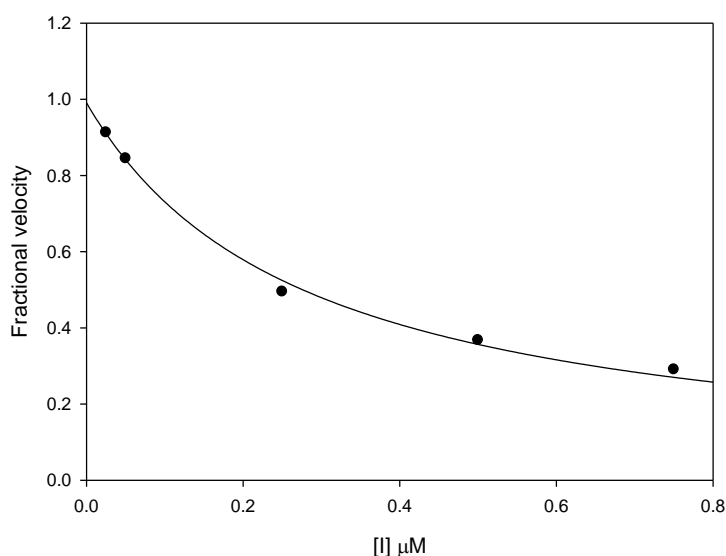


Figure 3.6. Concentration-response plot for the data presented in figure 3.5.

3.5 Discussion: Mechanism of EcPPCS inhibition by CJ

The lack of inhibition observed after gel filtration of enzyme treated at 100 μM inhibitor concentration, the regained activity seen after dilution of the pre-treated enzyme, and the absence of hyperbolic progress curves with steady state rates equal to 0 ($v_s = 0$) all indicate that P-CJ does not inhibit EcPPCS by a completely irreversible mechanism. This would suggest that inhibition does not proceed via the proposed ketene mechanism shown in Scheme 3.3, or that the ketene – if it forms – does not lead to irreversible inhibition. We have shown that the inhibited reaction proceeds linearly and is inhibited by inhibitor concentrations that approach the enzyme concentration. These observations lead us to believe that P-CJ is converted to a reaction intermediate that acts as a tight binding inhibitor of PPCS as shown in Scheme 3.4. However, in an attempt to gain support for such a proposal conflicting results were obtained, with different results being seen at high and low inhibitor concentrations. This has made it difficult to deduce the mechanism of inhibition with certainty. As we do not currently know whether the use of *in situ*

generated P-CJ in our assays contributes to these contrasting results, the confirmation of the inhibition mechanism of P-CJ on PPCS therefore awaits the preparation of pure of P-CJ.

3.6 Results: Cloning, expression and purification of SaCoaBC

With significant evidence that CJ exerts its antibiotic activity through the inhibition of PPCS, we wanted to determine if it shows the same level of inhibition against SaPPCS as that exhibited against EcPPCS. The native, bifunctional PPCS/PPCDC enzyme (SaCoaBC) from *S. aureus* was therefore produced by cloning the respective gene and by heterologous expression of the protein in *E. coli* with an N-terminal His-tag.

We found that conducting expressions at 37 °C did not yield any soluble protein, but that lowering the temperature of expression to 25 °C gave sufficient soluble protein to allow purification by immobilized metal affinity chromatography (IMAC). Subsequent analyses indicated that the expression yielded 3.5 mg of pure protein from 1 L of culture. The SDS page gel of purified SaCoaBC (figure 3.7) shows a band at 50 KDa which is in accordance with the predicted size of 48.2 KDa of SaCoaBC.

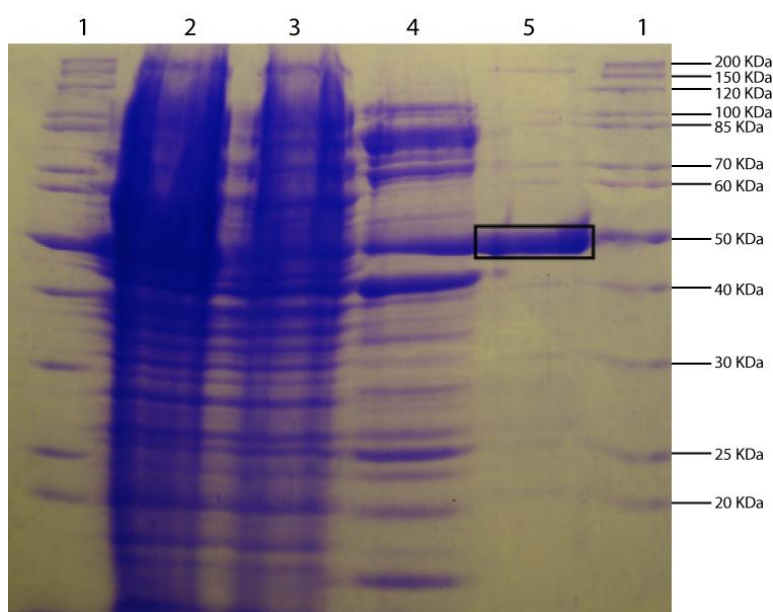


Figure 3.7. The 12% SDS PAGE gel of the purification of SaCoaBC. The lanes contain the following samples: Lane 1- marker, lane 2-His-SaCoaBC crude extract (total cell lysate), lane 3-SaCoaBC flow through, lane 4-SaCoaBC wash peak, lane 5-Purified SaCoaBC.

3.7 Results: The PPCS activity of SaCoaBC is also inhibited by P-CJ

An initial screen showed the newly expressed SaCoaBC was active under the same conditions used to conduct the various EcPPCS assays described above. With SaPPCS therefore available in

the form of the bifunctional enzyme SaCoaBC the protein was tested for inhibition by P-CJ. The results showed that no PPCS activity could be detected when 104 nM SaCoaBC was assayed in the presence of 100 μ M *in situ* generated P-CJ suggesting that the *S. aureus* enzyme is probably inhibited in a similar manner to EcPPCS.

3.8 Conclusion

In this chapter we presented the results of our efforts to elucidate the mechanism of action of CJ, which was found to display potent antibacterial activity toward MRSA. Our results indicated that CJ is converted to P-CJ by SaPanK, after which it is converted by SaPPCS to form a P-CJ-CMP adduct which inhibits SaPPCS. Kinetic studies performed on EcPPCS indicated that the P-CJ-CMP adduct has a K_i of ~85 nM, and that it may act as a tight binding inhibitor. However, this preliminary assessment will have to be confirmed by repeating the assays using pure P-CJ, as the effect of generating the inhibitor *in situ* has on the assays is currently not known.

In spite of the experimental difficulties that was encountered, it must be highlighted that the K_i of the most potent inhibitor of PPCS (structure in Scheme 3.4) previously discovered was found to be 24 nM on *E. faecalis* PPCS. This is only ~3-fold less than the K_i determined for P-CJ on EcPPCS in this study.⁴ However, since the previously reported inhibitors were all highly polar structural analogues of the acyl cytidylate intermediate, none of these compounds shows any inhibition in whole cell assays as expected. In contrast, CJ acts as a precursor to the actual inhibitor that can cross the cell membrane, and shows potent inhibitory activity against *S. aureus* growth. Moreover, since CJ has been reported not to inhibit the growth of mammalian cells, it is also a selective inhibitor.² This selectivity is most probably based on CJ not being a substrate for the human PanK enzyme.

CJ and its basic structural scaffold therefore presents an ideal starting point for the development of selective PPCS inhibitors. Our efforts towards the synthesis of such compounds are described in the next chapter.

3.9 Experimental

3.9.1 Materials and methods

All chemicals were purchased from Sigma-Aldrich (Aldrich, Sigma or Fluka). HisTrapTM Chelating and Desalting Columns (Amersham Biosciences) were from Supelco (Sigma). A Quick Start Bradford Protein Assay Kit was purchased from Bio-rad and contained Bradford reagent and a Bovine Serum Albumin standard set. Large-scale centrifugation was done on a Heraeus

Multifuge® 3S/3S-R. Centrifugation on a smaller scale was conducted on a Heraeus Biofuge pico centrifuge. PPCS enzyme assays were monitored via an enzyme-linked assay which couples the production of pyrophosphate to the oxidation of NADH. This is available commercially as the pyrophosphate reagent kit from sigma and each vial of the PR was initially suspended in 4.0 mL dH₂O. A assay procedure similar to the published PPCS assay was followed.⁴ Enzyme assays were performed on a Varioskan multiplate spectrophotometer (ThermoLabsystems). All curve-fitting analysis was performed using SigmaPlot 11.0 (Systat software).

HPLC analysis was performed on an Agilent 1100 instrument using a Supelcosil LC-18-T 3 μ C18 column (150 x 4.6 mm) from Supelco. The column was equilibrated in 95% solution A (100 mM potassium phosphate, pH 6.5) and 5% solution B (methanol), followed by elution with 95% A (0–3 minutes, isocratic), a linear gradient increasing solution B to 30% (5–7 minutes) and by an isocratic elution at 30% B (7–20 minutes). A flow rate of 1 mL.min⁻¹ was maintained throughout.

3.9.2 HPLC analysis of the conversion reaction by SaPanK under assay conditions.

A 1000 μ L reaction mixture contained either CJ or CJOMe (0.5 mM) and 1.5 mM ATP, 50 mM Tris buffer (pH 7.6), 2.5 mM MgCl₂ and 20 mM KCl. The biosynthetic reaction was initiated by addition of 10 μ g SaPanK. The reaction mixture was subsequently incubated at 37 °C and 150 μ L aliquots were removed after 1, 5, 10 min. The enzyme was removed by precipitation at 95 °C followed by centrifugation at 13 000 x g for 5 min. Then the supernatant was analysed by HPLC for each sample. The HPLC chromatograms of the biosynthesis reaction with CJOMe after 1 and 10 min are shown in figure 3.8.

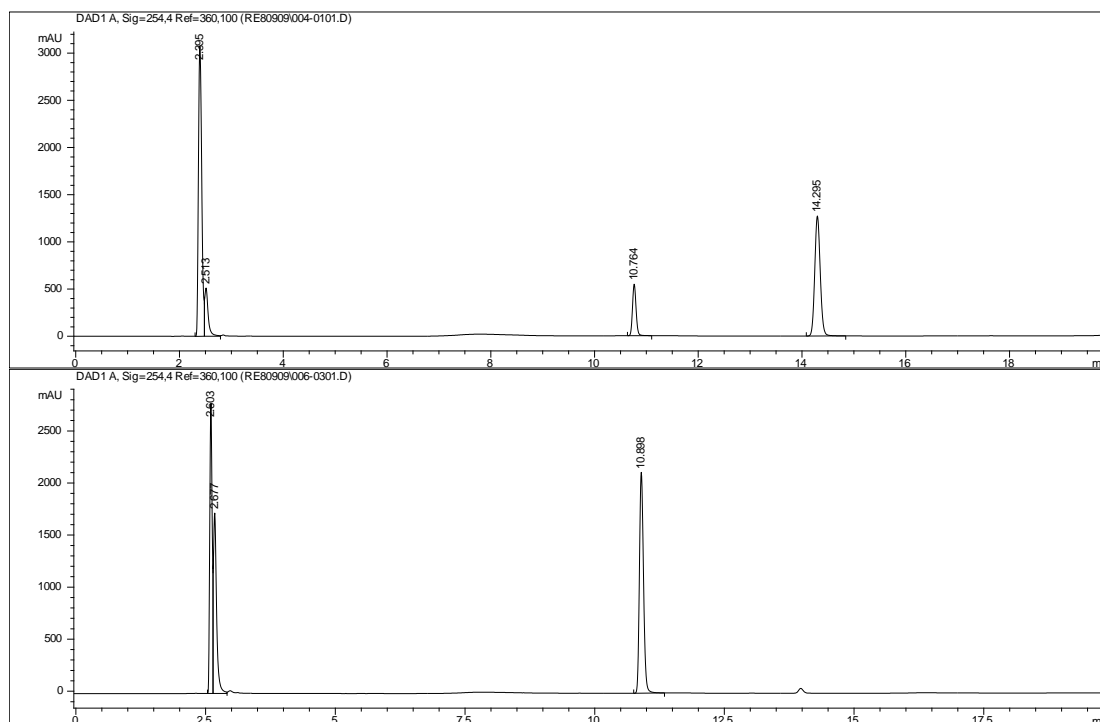


Figure 3.8. HPLC analysis of the conversion of CJOME to P-CJOME by SaPanK. Top chromatogram shows the reaction after 1 min and the bottom chromatogram shows the reaction after 10 min. Peaks at 10.8 and 14.3 min are P-CJOME and CJOME respectively and other peaks represent ATP and ADP.

3.9.3 Preliminary tests for inhibition of *EcPPCS* by CJ compounds:

To screen for inhibition of *EcPPCS* by CJ, CJOME, P-CJ and P-CJOME the compounds were individually added to assay mixtures containing P-PanCOOH, which was synthesized according to the literature procedure.⁹ In all cases the concentration of the CJ test compound was 100 μM , while the substrate concentration [P-PanCOOH] was 100 μM in the case of CJ and P-CJ, and 250 μM in the case of CJOME and P-CJOME. In the tests with CJ and CJOME SaPanK and ATP were omitted from the assay mixture. The rate of each of these reactions was subsequently compared to a control reaction that contained only substrate.

Assay mixtures contained 50 mM Tris buffer (pH 7.6), 2.5 mM MgCl_2 , 20 mM KCl, 1.0 mM CTP, 1.5 mM ATP, 1.0 mM Cys, 2.5 mM DTT, 100 μM or 250 μM P-PanCOOH, 100 μM of the test compound, 1.5 μg SaPanK, 9.25 nM *EcPPCS* and 60 μL pyrophosphate reagent in a total assay volume of 150 μL per well in 96-well plates. *EcPPCS* activity was determined by following the production of pyrophosphate, which was continuously monitored at 340 nm.

3.9.4 Determination of IC₅₀

A master assay mix containing 50 mM Tris buffer (pH 7.6), 2.5 mM MgCl₂, 20 mM KCl, 1.5 mM ATP, 1.0 mM CTP, 1.0 mM Cys, 2.5 mM DTT, 1.5 µg SaPanK, 240 nM EcPPCS and 60 µL pyrophosphate reagent was added to a 96-well plate containing 250 µM P-PanCOOH and CJ at concentrations between 0.1 µM to 100 µM in different wells to give a final assay volume of 150 µL. Control samples contained only P-PanCOOH, not inhibitor. The percentage activity at each inhibitor concentration was calculated by comparing the initial rate of a reaction with inhibitor with the initial rate of the control.

3.9.5 Test for irreversibility

A solution containing 50 mM Tris buffer (pH 7.6), 2.5 mM MgCl₂, 20 mM KCl, 1.5 mM ATP, 1.0 mM CTP, 1.0 mM Cys, 2.5 mM DTT, 10 µM CJ, 1.0 µg/100µL SaPanK and 925 nM EcPPCS in a total volume of 1000 µL was preincubated at 37 °C for 15 min. Subsequently the solution was diluted 10-fold by adding 10 µL of the preincubated mixture to 90 µL dH₂O. A master reaction mix (135 µL) containing 50 mM Tris buffer (pH 7.6), 2.5 mM MgCl₂, 20 mM KCl, 1.0 mM CTP, 1.0 mM Cys, 2.5 mM DTT, 250 µM P-PanCOOH and 60 µL pyrophosphate reagent was then added to 15 µL of the diluted preincubated mixture to give a total assay volume of 150 µL per well and overall a 100-fold dilution of the preincubated mixture. The final EcPPCS concentration was therefore 9.25 nM.

3.9.6 Test for irreversibility using gel filtration

Solutions containing 50 mM Tris buffer (pH 7.6), 2.5 mM MgCl₂, 20 mM KCl, 1.5 mM ATP, 1.0 mM CTP, 1.0 mM Cys, 2.5 mM DTT, CJ at different concentrations, 1.0 µg/100 µL SaPanK and 24.4 µM EcPPCS in a total volume of 100 µL were pre-incubated at 37°C for 15 min. The samples were subsequently loaded onto micro-gelfiltration spin columns of Biogel P-6 equilibrated (0.7 mL slurry loaded per column) in 50 mM Tris buffer (pH 7.6), followed by centrifugation at 3500 x g for 4 min. The eluate (60 µL) was diluted 10-fold with dH₂O, and 15 µL of the diluted solution was transferred to 96-well plate. Finally a master assay mix containing 50 mM Tris buffer (pH 7.6), 2.5 mM MgCl₂, 20 mM KCl, 1.0 mM CTP, 1.0 mM Cys, 2.5 mM DTT, 250 µM P-PanCOOH and 60 µL pyrophosphate reagent was added to give a total assay volume of 150 µl per well. The final EcPPCS concentration was estimated to be 244 nM.

3.9.7 Progress curve analysis

A master assay mix containing 50 mM Tris buffer (pH 7.6), 2.5 mM MgCl₂, 20 mM KCl, 1.5 mM ATP, 1.0 mM CTP, 1.0 mM Cys, 2.5 mM DTT, 1.5 µg SaPanK, 9.25 nM EcPPCS and 60 µL pyrophosphate reagent was added to a 96-well plate containing 250 µM P-PanCOOH and CJ at

concentrations between 25 nM to 750 nM in different wells, followed by determination of the rate of activity over 30 min.

3.9.8 Cloning, overexpression and purification of SaCoaBC

The amplified gene product was cut with NcoI and XhoI and ligated to a similarly cut PROEX vector. The resulting plasmid, PROEX-SaCoaBC, was sequenced to confirm the presence of the SaCoaBC gene and was transformed into *E. coli* BL21(Star)DE3 for expression. Expression was performed in Luria-Bertani broth supplemented with 100 mg/L ampicillin at 37 °C and grown until OD₆₀₀= 0.6. Then, the culture was cooled to 25 °C and induced with 0.1 mM IPTG and cell growth was continued overnight at 25 °C post-induction, after which the cells were harvested by centrifugation. The obtained cell pellet was suspended in sonication buffer (5 mM imidazole, 500 mM NaCl and 20 mM Tris–HCl, pH 7.9; 10 mL/1 g cell paste) and subsequently sonicated to effect cell lysis. After centrifugation at 25 000 rpm for 20 min to collect cell debris, the crude extract (supernatant) was applied to a previously prepared 1 mL HisTrapFF metal affinity purification column using an ÄKTAprime purification system. Weakly bound proteins were removed by washing with sonication buffer, followed by sonication buffer containing 75 mM imidazole. SaCoaBC was eluted by increasing the imidazole concentration to 500 mM. Elution was monitored at A₂₈₀. The purified protein was desalted using a 5 mL HiTrap desalting column (25 mM Tris, 5 mM MgCl₂, pH 8.0). Glycerol was added to the pure protein solution to a final concentration of 5%, after which the protein was aliquoted and stored at -80°C. The protein concentration was determined to be 0.5 mg/ml using a Bradford procedure.

3.9.9 PPCS inhibition assays with SaCoaBC

An initial screen for inhibition was conducted using the procedure described in section 3.9.3 and replacing *EcPPCS* with 104 nM SaCoaBC.

3.10 References

1. Sugie, Y.; Dekker, K. A.; Hirai, H.; Ichiba, T.; Ishiguro, M.; Shiomi, Y.; Sugiura, A.; Brennan, L.; Duignan, J.; Huang, L. H.; Sutcliffe, J.; Kojima, Y., CJ-15,801, a novel antibiotic from a fungus, *Seimatosporium* sp. *J. Antibiot.* **2001**, *54* (12), 1060-1065.
2. Saliba, K. J.; Kirk, K., CJ-15,801, a fungal natural product, inhibits the intraerythrocytic stage of *Plasmodium falciparum* *in vitro* via an effect on pantothenic acid utilization. *J. Molbiopara.* **2005**, *141* (1), 129-131.
3. Copeland, R. A., *Evaluation of Enzyme Inhibitors in Drug Discovery* John Wiley & Sons, Inc.: Hoboken, NJ, 2005.
4. Patrone, J. D.; Yao, J.; Scott, N. E.; Dotson, G. D., Selective Inhibitors of Bacterial Phosphopantothenoylecysteine Synthetase. *J. Am. Chem. Soc.* **2009**, *131* (45), 16340-16341.
5. Stanitzek, S.; Augustin, M. A.; Huber, R.; Kupke, T.; Steinbacher, S., Structural Basis of CTP-Dependent Peptide Bond Formation in Coenzyme A Biosynthesis Catalyzed by *Escherichia coli* PPC Synthetase. *Structure* **2004**, *12* (11), 1977-1988.
6. Kupke, T., Molecular Characterization of the 4'-Phosphopantothenoylecysteine Synthetase Domain of Bacterial Dfp Flavoproteins. *J. Biol. Chem.* **2002**, *277* (39), 36137-36145.
7. Kupke, T., Active-site residues and amino acid specificity of the bacterial 4'-phosphopantothenoylecysteine synthetase CoaB. *Eur. J. Biochem.* **2004**, *271* (1), 163-172.
8. Villa Mathew, V. J.; Targett Sarah, M.; Barnes John, C.; Whittingham William, G.; Marquez, R., An efficient approach to the stereocontrolled synthesis of enamides. *Org. Lett.* **2007**, *9* (9), 1631-1633.
9. Strauss, E.; Kinsland, C.; Ge, Y.; McLafferty, F. W.; Begley, T. P., Phosphopantothenoylecysteine synthetase from *Escherichia coli*. Identification and characterization of the last unidentified coenzyme A biosynthetic enzyme in bacteria. *J. Biol. Chem.* **2001**, *276* (17), 13513-13516.
10. Yao, J.; Patrone, J. D.; Dotson, G. D., Characterization and Kinetics of Phosphopantothenoylecysteine Synthetase from *Enterococcus faecalis*. *Biochemistry* **2009**, *48* (12), 2799-2806.
11. Copeland, R. A., *Enzymes*. Second ed.; John Wiley & Sons, Inc.: Hoboken, NJ, 2000.

Chapter 4

Synthesis of CJ-15,801 and its analogues[‡]

4.1 Introduction

The previous chapter gave a detailed account of the studies that have been performed to elucidate the mechanism of action of the natural product CJ-15,801. An important component of any future studies on this compound would require its synthetic preparation in larger quantities than have been accomplished to date. In this chapter we disclose our findings on the use of a methodology that has not previously been used to introduce the enamide functionality into CJ-15,801, and show that this same methodology can also be used in the syntheses of various ester and amide analogues of CJ-15,801. The results described here provide an alternative to the limited number of published methodologies on the synthesis of CJ-15,801 and its analogues.

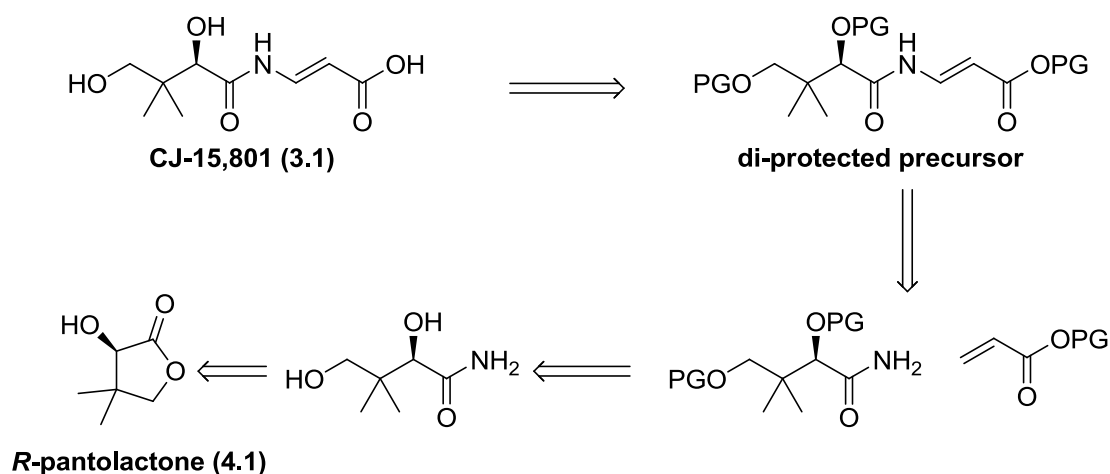
The CJ-15,801 analogues described in this chapter were prepared prior to our discovery that the PPCS enzyme is the main target of the inhibitory action exhibited by CJ-15,801. In fact, these analogues were synthesized as Michael acceptor-containing precursors of CoA analogues that we proposed could potentially inhibit the *S. aureus* CoADR enzyme in a manner similar to the compounds described in Chapter 2. However, the results detailed in Chapter 3 shows that the free carboxylate of CJ-15,801 is required for this compound to exert its inhibitory effect, indicating that analogues in which this group is modified may not function as whole cell inhibitors. Nonetheless, the CJ-15,801 analogues described here may still potentially act as enhanced cell membrane-permeable precursors that could be transformed into the natural product *in vivo*, depending on the nature of the modification made to the core of the CJ-15,801 structure. For example, esters and amides of CJ-15,801 may be converted into free CJ-15,801 by action of any number of hydrolytic enzymes, where after it may exert its effect in a manner similar to that described in the previous chapter.

4.2 Overview of published syntheses of CJ-15,801 and its precursors

A retrosynthetic analysis of CJ-15,801 shows that the overall efficiency of the synthesis will most probably rely on the method used to introduce the enamide functionality (Scheme 4.1), since (*R*)-pantolactone is commercially available, and several of its amides have been prepared before.

[‡] The contents of this chapter will be submitted in modified format for publication in the journal *Organic Letters*.

However, enamides are uncommon, difficult to handle synthetically and, in the case of CJ-15,801, also has to be introduced with stereocontrol so that predominantly the *E*-enamide functionality is obtained. Interestingly, enamides, and in particular *N*-acyl vinylogous carbamates and ureas, are present in various natural products including palytoxin and enamidonin,^{1,2} and therefore methodologies for their synthetic preparation have undergone considerable investigation in recent years.³ More specifically, a literature search reveals that CJ-15,801, or one of its protected precursors, have been prepared in four separate studies. A short discussion of each of these methodologies follows below.



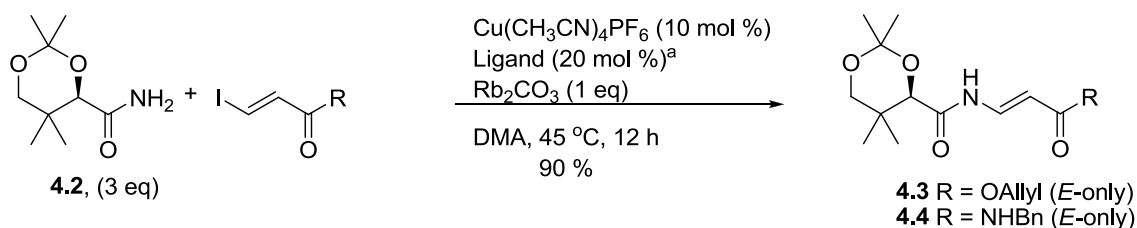
Scheme 4.1. Retrosynthesis of CJ-15,801. *R*-Pantolactone is commercially available. PG = protecting groups.

4.2.1 Methodology 1: Cu-catalyzed synthesis of *N*-acyl vinylogous carbamates and ureas via amidation of β -iodoacrylates and β -iodoacrylamides

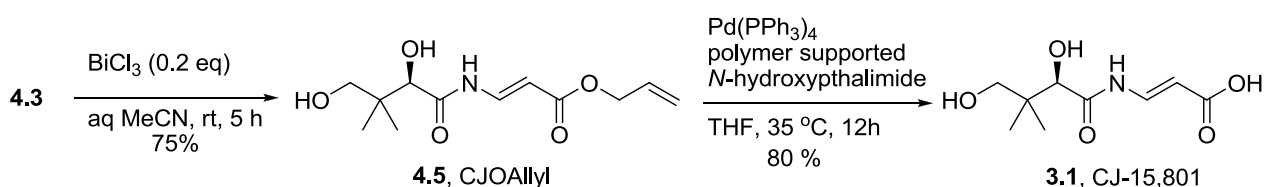
The first methodology for introducing the enamide functionality of CJ-15,801 was published by Han *et al.*⁴ These researchers used a Cu-catalyst and a 3,4,7,8-tetramethyl-1,10-phenanthroline ligand for amidation of β -iodoacrylates which afforded only the *E*-isomer of *N*-acyl vinylogous carbamates and ureas in good yields (Scheme 4.2A). They found that $\text{Cu}(\text{CH}_3\text{CN})_4\text{PF}_6$ was the most efficient Cu source in these syntheses. The reaction was conducted in the presence of several bases, including K_2CO_3 , Cs_2CO_3 and Rb_2CO_3 . It was found that when Rb_2CO_3 was employed that conversion was the highest, although no rationalisation of this result was provided. This study subsequently used this same methodology to accomplish the first total synthesis of CJ-15,801. An important consideration in the planning of the total synthesis of CJ-15,801 is the choice of protecting groups, as the enamide functionality is both acid- and base-sensitive. Therefore, it is essential that protecting groups that can be removed under mild and neutral conditions are employed. In the total synthesis described by Han *et al.* an acetonide acetal was used for the protection of the 1,3 diol, while an allyl ester protected the carboxylic acid of CJ-15,801. These

protecting groups were subsequently removed using BiCl_3 and $\text{Pd}(\text{PPh}_3)_4$ respectively, both of which satisfy the requirement of mild reaction conditions. Using this method CJ-15,801 was prepared from amide **4.2** with an overall yield of 54% over three steps (Scheme 4.2B).

A



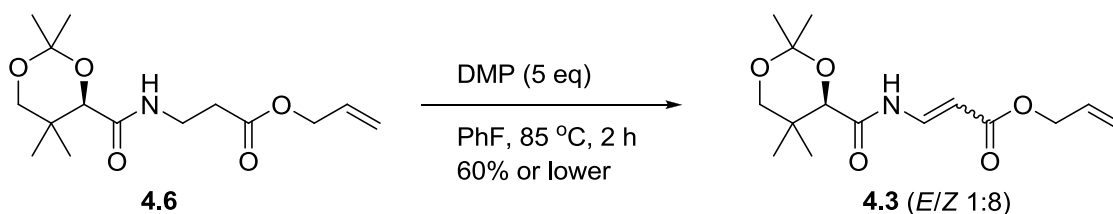
B



Scheme 4.2. Reported synthesis of antibiotic CJ-15,801. (A) Cu-catalyzed amidation of β -iodoacrylates and β -iodoacrylamides to yield *N*-acyl vinylogous carbamate **4.3** and urea **4.4**. (B) Deprotection of di- and mono- protected CJ-15,801 precursor under neutral conditions to yield CJ-15,801. ^aThe ligand employed was 3,4,7,8-tetramethyl-1,10-phenanthroline.

4.2.2 Methodology 2: Synthesis of *N*-acyl vinylogous carbamates and ureas via oxidation of amides with Dess-Martin periodinane

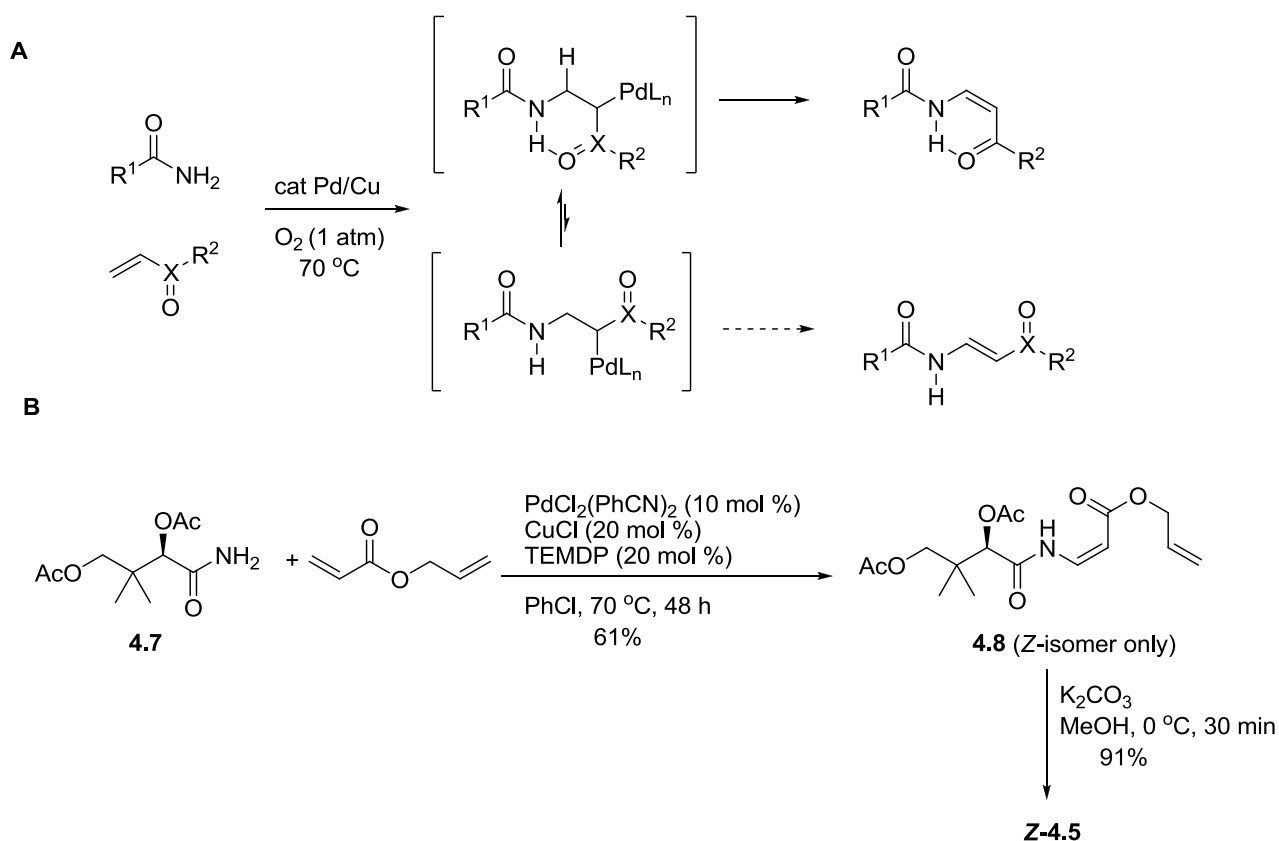
The second methodology for the synthesis of CJ-15,801 was developed by the group of Nicolaou. In this protocol the enamide functionality is introduced by oxidation of the amide moiety using the reagent Dess–Martin periodinane (DMP) (Scheme 4.3).⁵ Using this procedure the same di-protected precursor **4.3** used in *Methodology 1* was obtained in 60% or lower yield (the reported yield of 93% was based on the recovery of 39% of the starting material) with an *E/Z* ratio of 1:8. The same deprotecting procedure as described in the previous methodology was then used to give the unnatural *Z*-isomer of CJ-15,801 in an overall yield of 45% over three steps from amide **4.6**.



Scheme 4.3. Synthesis of the di-protected precursor of CJ-15,801 by oxidation of **4.6** with DMP.

4.2.3 Methodology 3: Pd-catalyzed synthesis of *Z*-enamides via oxidative amidation of conjugated olefins

The third published method on the synthesis of the title compound uses a Pd/Cu co-catalyst under oxidative conditions to introduce the enamide.⁶ The methodology gives good yields with excellent stereocontrol, although only the *Z*-isomer is produced. Nonetheless, this method is attractive since the enamide is introduced by using the alkene instead of vinyl halides, as in the case of *Methodology 1*, which could be difficult to obtain in some cases. The authors attributed the excellent stereocontrol that favours the *Z*-isomer to a hydrogen bond forming between the hydrogen of the enamide and the oxygen of the carbonyl in the reaction intermediate (Scheme 4.4A). The same study also demonstrated that *Z*-enamides could be converted to *E*-enamides using photoisomerization, although aliphatic enamides was shown to be less effectively isomerized than aromatic enamides. Using this methodology, *Z*-CJ-15,801 precursor **Z-4.5** was prepared with an overall yield of 56%, over two steps from amide **4.7** (Scheme 4.4 B). The deprotection and preparation of free *Z*-CJ-15,801 was not reported.

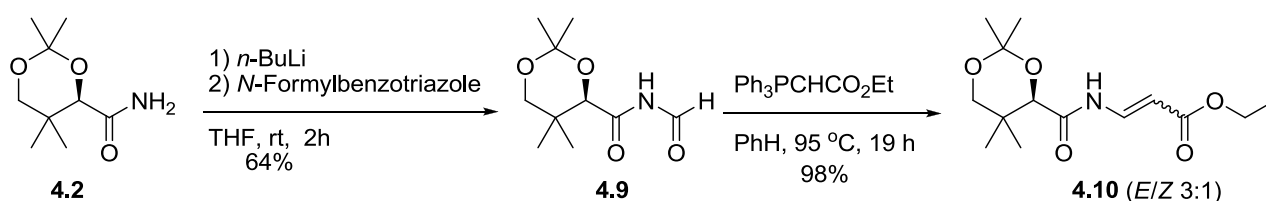


Scheme 4.4. Introduction of the enamide functionality into *Z*-CJ-15,801 by oxidative coupling of vinyl esters to protected pantoic amide. (A) The general methodology leads to the selective formation of the *Z*-isomer of the enamide based on

stabilization of the one transition state by means of a hydrogen bond. (B) Synthesis of a protected precursor of Z-CJ-15,801 using this coupling methodology

4.2.4 Methodology 4: Synthesis of enamides via Wittig-olefination of imides

The last reported methodology for the synthesis of a di-protected precursor of CJ-15,801 was published by Villa *et al.*⁷ It involves a two-step approach, in which the amide **4.2** is formylated in the first step to produce the imide **4.9**, followed by Wittig-olefination in the second step to yield the enamide (Scheme 4.5). The di-protected CJ-15,801-precursor **4.10** was obtained in this way from amide **4.2** in 63% yield over these two steps. The products had an *E/Z* ratio of 3:1. In this strategy the removal of the protecting groups of **4.10** was not attempted.



Scheme 4.5. Two step synthesis of the di-protected precursor of CJ-15,801 by Wittig olefination of an *N*-formyl imide.

4.2.5 Evaluation of the suitability of Methodologies 1-4 for the synthesis of CJ-15,801

Careful consideration of the suitability of the four procedures discussed above for the synthesis of the title compound lead us to believe that none of them satisfied our criteria for a scalable, stereocontrolled synthesis that gave predominantly the *E*-isomer and used mainly commercially-available starting materials. Although *Methodology 1* nearly satisfies these requirements, it and the other methodologies suffer from certain shortcomings that can be summarized as follows:

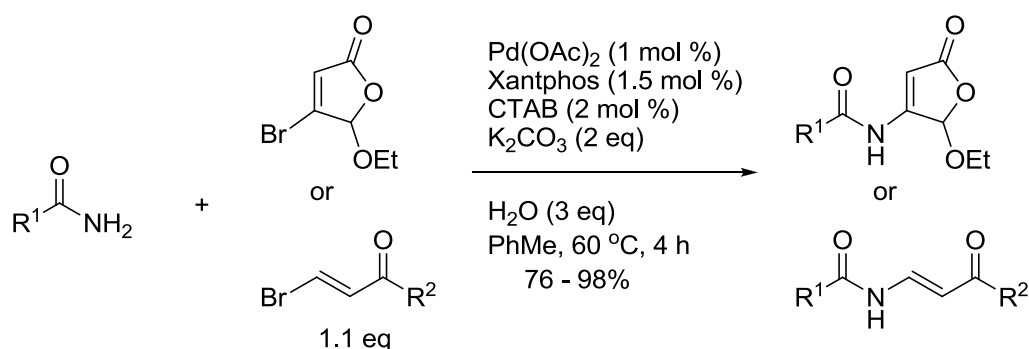
- *Methodology 1*: the reported reaction was conducted on a scale of less than 100 mg and three equivalents of the amide **4.2** was used. The yield of the coupling reaction is ~90%, but the scalability of the reaction remains untested.
- *Methodology 2*: predominantly yields the *Z*-isomer in moderate yield (<60%) and uses five equivalents of the expensive reagent DMP.
- *Methodology 3*: only the *Z*-isomer is formed in moderate yield (~60%).
- *Methodology 4*: the enamide is introduced in two steps as the CJ-15,801 precursor protected as the ethyl ester with an overall yield of ~60%. This synthesis is probably most suited to our needs, although the use of other esters as protecting groups would have to be explored as

very few if any methodologies exist to remove the ethyl ester protecting group under neutral conditions.

Taken together, it is clear that none of the published methodologies fully satisfy our requirements for the synthesis of CJ. These factors therefore prompted us to search for an alternative approach for the synthesis of this natural product.

4.3 Proposed novel methodology: Pd-catalyzed synthesis of *N*-acyl vinylogous carbamates and ureas via amidation of β -bromoacrylates and β -bromoacrylamides

After an extensive literature search was conducted, a fifth and potentially more suitable methodology for the introduction of the enamide moiety was uncovered. In this method a Pd-catalyzed reaction is used to stereoselectively prepare enamides in excellent yield from amides using commercially available reagents and β -bromoacrylic esters and β -bromoacrylamides (Scheme 4.6).⁸ Apart from the Pd-catalyst an appropriate ligand, a base (K_2CO_3) to neutralize the HBr that forms during the course of the reaction and a phase transfer-catalyst (cetyltrimethylammonium bromide, CTAB) is also required. The ligand employed in this methodology was the bisphosphine ligand Xantphos (4,5-Bis(diphenylphosphino)-9,9-dimethylxanthene), a ligand often employed in Pd-catalysed C-N bond formation systems. Although the report made no mention of the stereoselectivity of the methodology, all prepared compounds were named as having *E*-geometry.



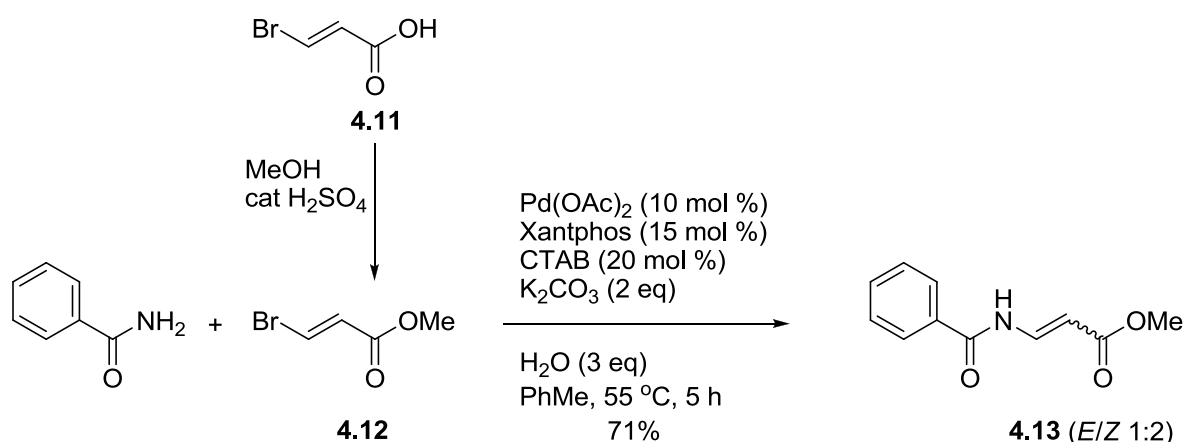
Scheme 4.6. Pd-catalyzed coupling reaction of amides and carbamates to β -bromoacrylates and β -bromoacrylamides. R^1 = aliphatic, aromatic or carbamate and R^2 = OEt, or NHBn.

While this methodology is similar to *Methodology 1*, it differs in that the authors demonstrated that the reaction can be performed on up to a 1 kg scale. However, the authors did not attempt the synthesis of CJ-15,801 or any of its precursors using this protocol. We envisaged that it could be

adapted for its preparation by coupling β -bromoacrylic esters to amide **4.2**, and therefore set out to demonstrate its feasibility in this regard.

4.4 Results: Applying *Methodology 5* on a model system

The coupling of benzamide and methyl (*E*)- β -bromoacrylate **4.12** using *Methodology 5* was first attempted to verify that the published protocol could be repeated in our hands (Scheme 4.7). Methyl β -bromoacrylate **4.12** was synthesized by esterification of **4.11** (**4.11** was prepared by bromination of propiolic acid) according to the literature procedure and yielded only the *E*-product as determined by ^1H NMR spectroscopic analysis (more specifically based on the coupling constants of the alkene protons).⁹ The Pd-catalyzed coupling of **4.12** to benzamide proceeded cleanly to then yield the enamide **4.13** (both *E* and *Z* isomers) in good yield (71%). NMR spectroscopic analysis showed that the products were formed with an *E/Z* ratio of 1:2. While this was surprising, considering that the Pd-catalyzed reaction is supposed to proceed with high stereospecificity, we decided to investigate the reasons for this isomerization in subsequent studies. The synthesis of a protected CJ-precursor was therefore subsequently attempted..

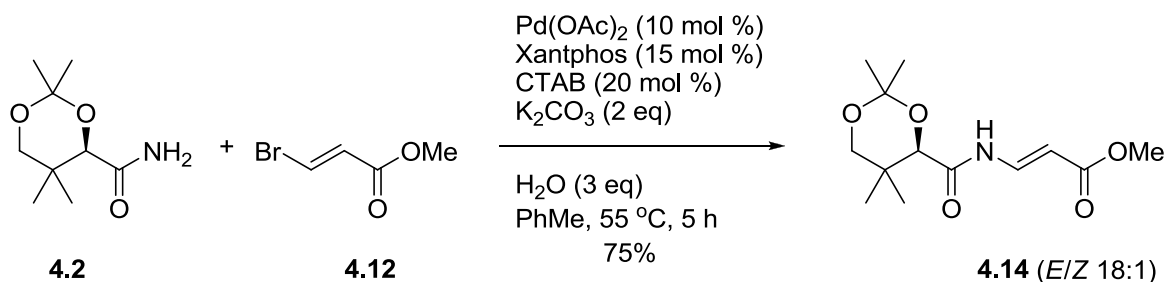


Scheme 4.7. Pd catalyzed coupling of methyl bromoacrylate **4.12** and benzamide.

4.5 Results: Applying *Methodology 5* in the synthesis of di-protected CJ-15,801

Next we proceeded with the coupling of protected pantoic amide **4.2** to **4.12** under the same conditions (Scheme 4.8). Amide **4.2** was synthesized in two steps from pantolactone **4.1** in a manner similar to those previously published in literature.¹⁰ Gratifyingly, the reaction proceeded cleanly to give the desired product **4.14** in a 75% yield that predominantly had the expected *E*-stereochemistry (*E/Z* ratio of 18:1). Next, the same reaction was performed in the presence of 10-fold less catalyst. This was done to evaluate whether the relatively high amount of catalyst reported in *Methodology 5* was a necessary requirement in the reaction. Under such conditions the reduced

amount of catalyst (1 mol % Pd(OAc)₂ and 1.5 mol % Xantphos) resulted in a reduced yield (58% vs 75% obtained previously). Longer reaction times at this lower catalyst load did not increase the yield. While it is possible that intermediate amounts of catalyst may be sufficient to give a good balance between catalyst load and final yield, this was not investigated. We therefore decided to use 10 mol % Pd(OAc)₂ and 15 mol % Xantphos in all subsequent coupling reactions.

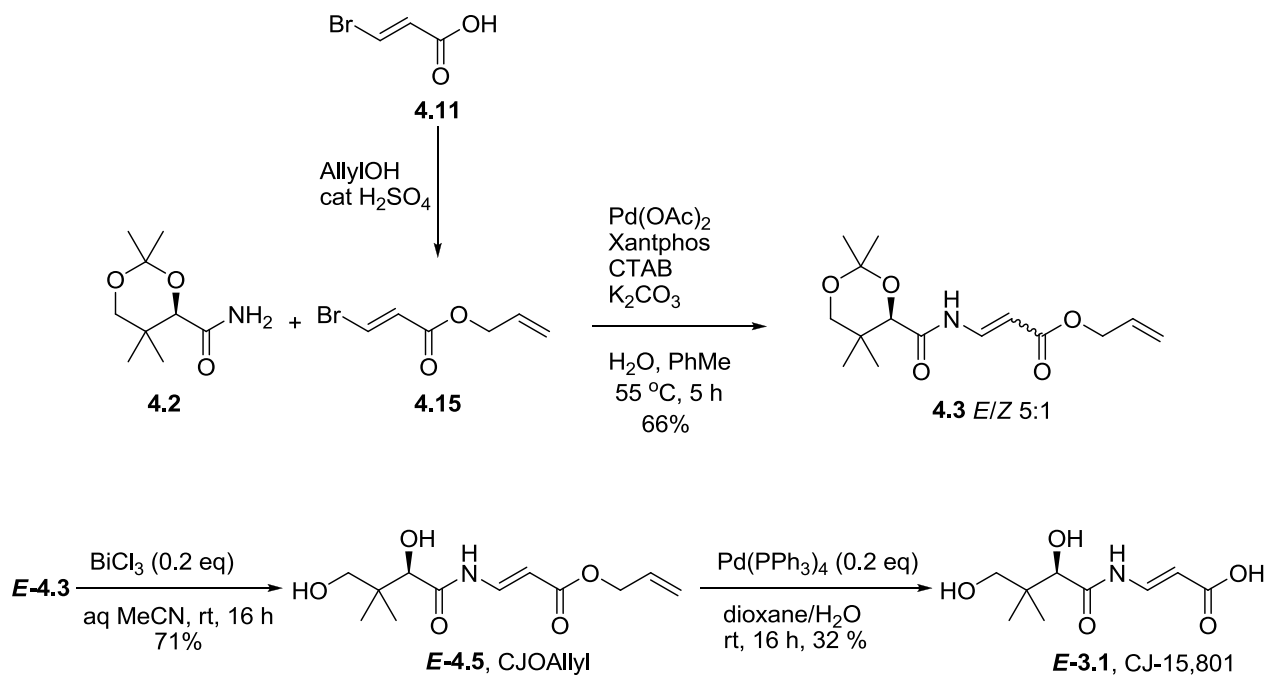


Scheme 4.8. Pd-catalyzed coupling of methyl β-bromoacrylate **4.12** and amide **4.2**. The *E*-isomer was favored in this case.

4.6 Results: A new total synthesis of CJ-15,801

With the new procedure in hand we set out to synthesize the title compound using the Pd-catalyzed coupling reaction of *Methodology 5*. As mentioned previously, the enamide functionality is extremely acid-sensitive and the deprotection need to be carried out using mild conditions at neutral pH. We therefore decided on using a deprotection strategy similar to the one employed in *Methodology 1* (Scheme 4.2B), in which an allyl ester protects the carboxylate, and an acetonide protects the 1,3-diol of the pantoate moiety. Initially we had some concerns regarding the use of an allyl ester, since the Pd(OAc)₂ employed in the coupling reaction is also routinely used for the deprotection of allyl esters.¹¹ Nevertheless, we found that (*E*)-allyl β-bromoacrylate **4.15** (prepared as for methyl β-bromoacrylate **4.12**) was efficiently coupled to protected pantoic amide **4.2** to give the allyl-protected enamide **4.3** in good yield (66%) (Scheme 4.9). Moreover, the preferred *E*-isomer was formed preferentially in this reaction (*E/Z* 5:1). As noted previously, the formation of the *Z*-olefin is surprising, since it is expected that these coupling reactions should be stereospecific and should retain the configuration of the bromoacrylate starting material. The formation of the *Z*-isomer was therefore mainly attributed to *E* to *Z* isomerization after product formation, which would be agreement with the previous studies of enamides by Tanoury *et al*⁸ who also observed heat-induced isomerization of the enamide products. However, isomerisation of the β-bromoacrylate prior to coupling cannot be excluded, although this has not been observed in previous studies. Subsequent deprotection of the acetonide and allyl esters of **E-4.3** using published procedures was achieved in yields of 71% and 32% respectively and no isomerization was found during deprotection. The yield of the allyl-deprotection step of **E-4.5** is much lower than that reported by

Han *et al.*, and may be attributed to the fact that unlike them we did not use a polymer-supported *N*-hydroxyphthalimide allyl scavenger (which is not commercially available) in the workup of the reaction.⁴ This also complicates the purification of the acid to some extent, due to the formation of significant amounts of side-products in the absence of allyl scavenger.



Scheme 4.9. Total synthesis of CJ-15,801. The di-protected precursor **4.3** was synthesized using adapted Pd-catalyzed methodology. The protecting groups of the *E*-isomer were subsequently removed using established methods.

These results demonstrate that the Pd-catalyzed methodology (*Methodology 5*) used for the synthesis of the *N*-acyl vinylogous carbamates **4.3** can successfully be applied in the total synthesis of CJ-15,801. Importantly, the yield of the key coupling step of this reaction (66-75% depending on the ester moiety) compares favorably to the yields of ~60% obtained for most of the other coupling reactions, although it is significantly lower than the yield of ~90% obtained in *Methodology 1*. However, unlike *Methodology 1* this modified methodology allows protected precursors of CJ-15,801 such as **4.14** and **4.5** to be prepared on a gram scale if necessary. The biggest single stumbling block to the preparation of free CJ-15,801 at these scales remains the final deprotection of the ester. Due to the low yield of this step, the overall yield for the synthesis of CJ-15,801 by the new method is only 15 % over three steps, starting from amide **4.2**. However, this same stumbling block will be encountered regardless of the strategy followed to prepare the enamide, and will be addressed in future studies.

4.7 Results: Heat-induced isomerization of enamides

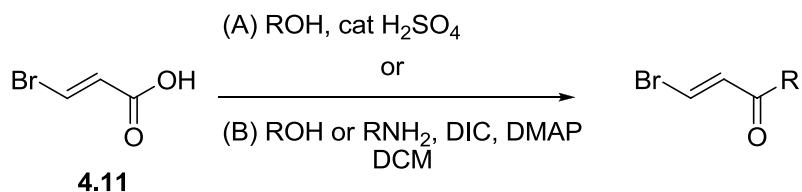
As mentioned earlier, it would be advantageous to have both the natural *E*- and unnatural *Z*-isomers of CJ-15,801, and its analogues in hand for biological testing purposes. In the original publication describing *Methodology 5* the authors noted that the enamide products formed by the coupling reaction were susceptible to isomerization if left at elevated temperatures. This phenomenon was also investigated in the synthesis of the CJ-15,801 analogues by performing the Pd-catalyzed coupling of amide **4.2** and acrylate **4.15** at a temperature of 80 °C, instead of at 55 °C. Interestingly, this reaction returned only the *Z*-isomer, albeit in a significantly lower yield (43% compared to 66% for the reaction conducted at lower temperature). This result indicates that the *Z*-isomers of the CJ analogues can successfully be synthesized by conducting the coupling reactions at elevated temperatures, although this may negatively impact on the yield of the reaction.

4.8 Results: Synthesis of CJ analogues using newly established methodology

With the new coupling conditions in hand we wanted to determine how the reaction would perform when other vinyl bromide substrates are coupled to amide **4.2**, with the goal to prepare additional CJ analogues for biological testing. We therefore set out to synthesize several other ester and amide analogues of CJ.

4.8.1 Synthesis of (*E*)- β -bromoacrylic ester and (*E*)- β -bromoacrylamide substrates

The required acrylic ester and acrylamides were synthesized by one of two general procedures (Table 4.1). In procedure A, acrylates **4.12**, **4.15** and **4.16** were prepared by esterification of the appropriate alcohol with (*E*)- β -bromoacrylic acid **4.11**. However, this resulted in especially the methyl and t-butyl bromoacrylic esters being prepared in very low yields. This is most probably due to the volatility of the products, which often evaporated during concentration under reduced pressure. In procedure B, acrylate **4.17** and acrylamides **4.18** and **4.19** were prepared by coupling either benzylalcohol, benzylamine or pentylamine to (*E*)- β -bromoacrylic acid **4.11**. This was conducted by using standard *N,N*-diisopropylcarbodiimide (DIC) and 4-*N,N*-dimethylaminopyridine (DMAP)-mediated coupling procedures since initial attempts to synthesize acrylamides **4.18** and **4.19** using isobutyl chloroformate were unsuccessful. This procedure gave the benzyl acrylic ester **4.17** in a good yield (63%), while the benzyl acrylamide **4.18** and *N*-pentyl acrylamide **4.19** were obtained in moderate to very low yields (47% and 12% respectively).

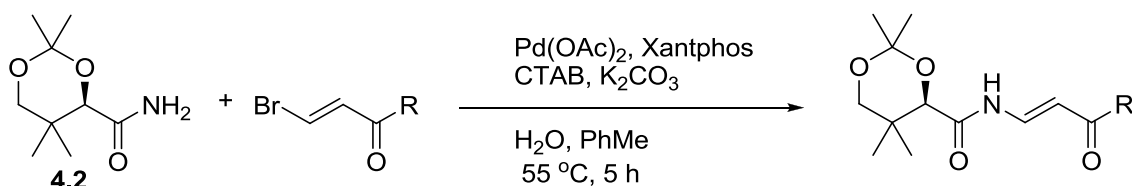
Table 4.1. Synthesis of *E*-bromoacrylic ester and bromoacrylamide substrates

Bromoacrylate or Bromoacrylamide	Procedure	% Yield
<p style="text-align: center;">4.12</p>	A	25
<p style="text-align: center;">4.15</p>	A	61
<p style="text-align: center;">4.16</p>	A	19
<p style="text-align: center;">4.17</p>	B	63
<p style="text-align: center;">4.18</p>	B	47
<p style="text-align: center;">4.19</p>	B	12

4.8.2 Coupling of amide 4.2 and β -bromoacrylates and β -bromoacrylamides

In the original studies on the preparation of *N*-acyl vinylogous carbamates of Han⁴ and Tanoury⁸ discussed earlier (Sections 4.1.1 and 4.2) the authors investigated a diverse range of amide and carbamate substrates in the respective coupling reactions. However, in both cases only a limited

number of acrylate and acrylamide substrates were tested as partners in these couplings. We therefore investigated the Pd-catalyzed coupling of the range of bromoacrylates and bromoacrylamides prepared above to a single amide substrate, the protected pantoic amide **4.2** (Table 4.2).

Table 4.2. Pd-catalyzed coupling of β -bromoacrylate and β -bromoacrylamide substrates to amide **4.2**.

Entry	Substrate	Product	^a <i>E/Z</i>	% Yield (% <i>E</i> and % <i>Z</i>)
1	 4.12	 4.14	18:1	75 (71 and 4)
2	 4.15	 4.3	5:1	66 (55 and 11)
3	 4.16	 4.20	<i>E</i> only	59
4	 4.17	 4.21	<i>E</i> only	74
5	 4.18	 4.4	3:1	52 (39 and 13)
6	 4.19	 4.22	3:1	49 (37 and 12)

^a*E/Z* ratios were determined from the isolated yields of each isomer separated by chromatography.

The results show that when β -bromoacrylates are used as substrates (entries 1-4) the coupling reaction is highly stereoselective and nearly exclusively forms the *E*-isomer. The only exception to

this general trend is the allyl ester **4.3** which also preferentially forms the *E*-isomer, albeit in a lower ratio (5:1) than in the other cases. The reason for this may be due to an additional interaction between the catalyst and the allyl protecting group. The yields for the syntheses of the acrylic esters are all moderate to good, ranging from 59% to 74%. In contrast, the coupling of acrylamides (entries 5-6) proceeded in much lower yields of ~50%. Moreover, although the *E*-enamide is also still favoured in these cases, the stereoselectivity is much lower and as a result there is a significant increase in the amount of *Z*-enamide that is formed in these reactions. Taken together, these results suggest that a wide range of acrylate and acrylamide substrates can be coupled to amide **4.2** to yield valuable ester and amide precursors of the antibiotic CJ-15,801.

Although the Pd-catalyzed coupling reaction clearly has a high stereoselectivity which favours the *E*-isomer at room temperature, the mechanistic basis for this is less clear. The following factors could play a role in determining the stereochemistry of the product: the stereochemistry of the starting acrylate or acrylamide, stabilization of the reaction intermediate by oxygen chelation (Figure 4.1A) and stabilization of the *Z*-isomer by an intermolecular hydrogen bond (Figure 4.1B). With the limited number of substrates used it would seem that the size of the R-group does not have an effect on the stereochemistry of the product (for example, the R-groups in entries 4 and 5 have the same size but the reactions differ significantly in terms of stereoselectivity). Instead, the electronic differences between acrylic esters and the acrylamides may play a determining role in both the yield and stereochemical outcome of the reactions. The potential of the acrylamides forming an additional hydrogen bond in the catalyst complex also cannot be excluded. Interestingly, there is a reversal in the selectivity when acrylates are coupled to benzamide to yield **4.13** (*E/Z* 1:2), compared to its coupling to amide **4.2** to give **4.14** (*E/Z* 18:1). A possible reason for the reversed selectivity could be that due to the increased acidity of the conjugated amide NH of benzamide, it more readily forms a hydrogen bond that stabilizes the *Z*-isomer (Figure 4.1B). This stereo-preference for the *Z*-isomer is consistent with the results of Han *et al.* (*Methodology* 1) who found only the *Z*-isomer when coupling conjugated and aromatic amides to β -iodo-acrylamides.⁴

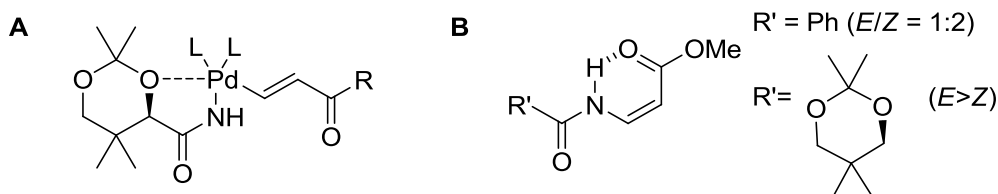
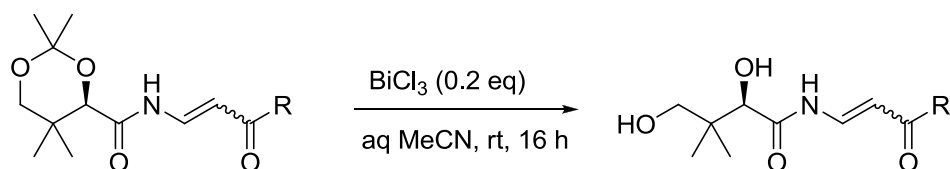


Figure 4.1. (A) Oxygen chelation could stabilize the formed reaction intermediate. (B) Intramolecular hydrogen bond stabilizes the *Z*-isomer leading to reversal of *E/Z* selectivity. L = Xantphos

4.8.3 Acetonide deprotection of prepared *N*-acyl vinylogous carbamates and ureas

With the di-protected *E*- and *Z*-CJ-15,801 analogues in hand, we set out to remove their acetonide protecting groups. The acetonide deprotection was accomplished by using the literature procedure of Han.⁴ This procedure utilized the Lewis acid BiCl₃ in catalytic amounts for the deprotection of acetonide groups under mild conditions. In most cases the yield was moderate to very good (Table 4.3). The low yield obtained with CJ amide analogue **4.26** was presumably due to some of the product dissolving in the water layer during aqueous work-up. Overall, the acetonide deprotection using BiCl₃ proved to be a versatile method which is amenable to the deprotection of a variety of acrylate and acrylamide CJ analogues.

Table 4.3. Acetonide deprotection of *N*-acyl vinylogous carbamates and ureas.



R	<i>E</i> -Product	% Yield	<i>Z</i> -Product	% Yield
OMe	3.2	79	Z-3.2	19
OAllyl	4.5	71	Z-4.5	80
OtBu	4.23	62	a	a
OCH ₂ Ph	4.24	90	a	a
NHCH ₂ Ph	4.25	34	Z-4.25	58
NH(CH ₂) ₄ CH ₃	4.26	6	Z-4.26	83

^aNo *Z*-enamide was isolated during coupling.

4.9 *S. aureus* growth inhibition by synthesized enamides

To determine if the prepared compounds are biologically active the acetonide-protected and deprotected CJ analogues were all subjected to *S. aureus* growth assays. We envisaged that upon entry of the cell, the di-protected CJ-15,801 analogues would presumably be metabolized, and that these reactions could remove the acetonide and ester or amide protecting groups to give CJ-15,801. In this manner the antibiotic activity of CJ-15,801 could potentially be improved, as these analogues are presumably more cell permeable than the parent compound.

We performed an initial screen in triplicate at a compound concentration of 200 μM. Pantothenamide **8a** (Chapter 2) was used as a positive control, and showed 0 % growth at 200

μM . Curiously, the results indicated that none of the compounds had an MIC of lower 200 μM , i.e. none completely inhibited growth (Figure 4.2). The only compound that significantly inhibited *S. aureus* growth was **4.26**, although much less potently than the pantothenamide **8a**. This suggests that the CJ analogues are not converted to free CJ-15,801 *in vivo*, and that introduction of the *E*-enamide functionality into the β -alanine moiety of pantothenamides decreases their ability to exert their antibacterial effect.

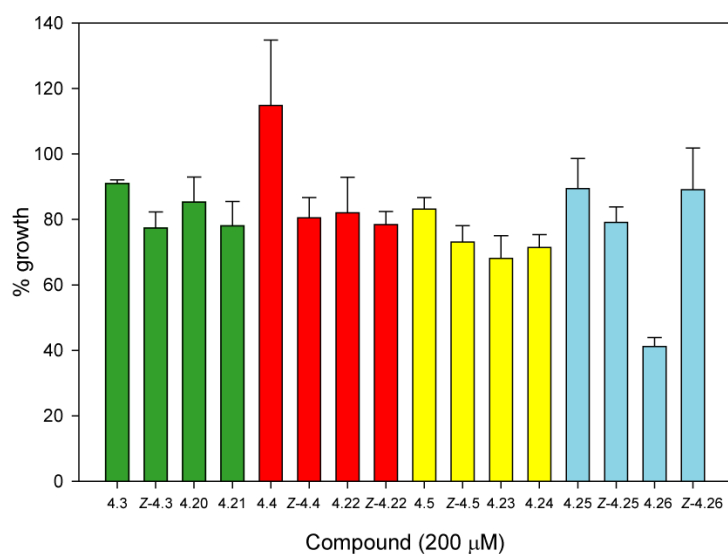


Figure 4.2. The % growth of *S. aureus* in the presence of 200 μM protected and unprotected CJ-ester and amide analogues. Green bars = acetonide esters, red = acetonide amides, yellow = CJ-esters and blue = CJ-amides. Bars donate the average growth of an experiment performed in triplicate and error bars donate the standard error.

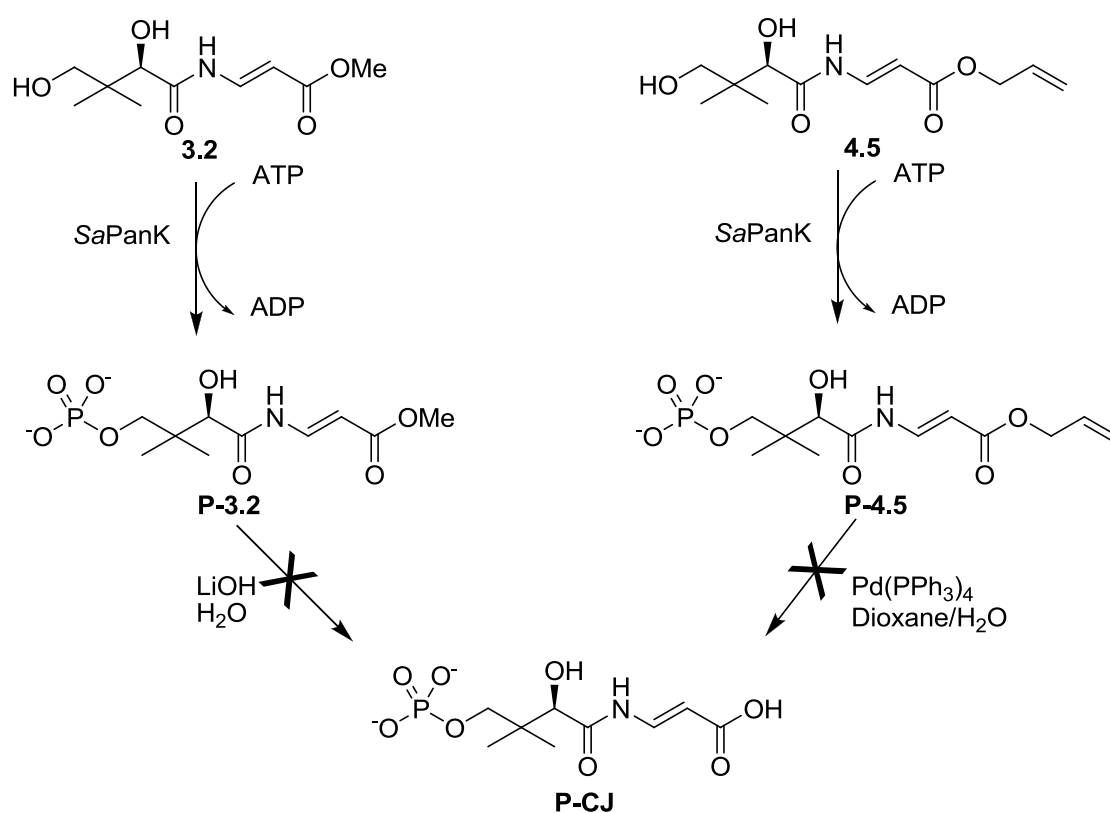
4.10 Preliminary *M. smegmatis* growth inhibition studies by enamides

The synthesized CJ-15,801 ester and amide analogues was subsequently similarly tested for the growth inhibition of *Mycobacterium smegmatis*, a fast growing member of the family of mycobacteria to which *M. tuberculosis* also belongs. The analogues were tested alongside CJ-15,801 and Z-CJ-15,801 (synthesized by our collaborators), all at a concentration of 200 μM , and in duplicate. The results showed that neither CJ-15,801 nor Z-CJ-15,801 inhibits *M. smegmatis* growth, and that none of the CJ ester and amide analogues (with acetonide deprotected) showed inhibition. However, 200 μM of di-protected allyl ester **4.3** completely abolished bacterial growth, suggesting that this compound has an MIC of lower than 200 μM . Moreover, all of the acetonide protected amides showed modest growth inhibition with the *Z*-isomer more potent than the *E*-isomer and the benzyl amide more potent than the pentyl amide. This finding suggests that the mechanism of action of the latter group of compounds is unrelated to CoA biosynthesis, as the

results of chapter 3 clearly showed that the *E*-stereochemistry of CJ is essential for inhibition of PPCS.

4.11 Chemo-enzymatic synthesis of P-CJ

In chapter 3 it was shown that P-CJ is an inhibitor of PPCS based on studies in which this compound was generated *in situ* by action of SaPanK during enzymatic assays. Although the synthesis of P-CJ is currently underway in the laboratories of our collaborators, we envisaged that SaPanK and **3.2** or **4.5** could be used to synthesize P-CJ using a chemo-enzymatic approach. In such a method, a 4'-phosphate group is first introduced onto **3.2** and **4.5** by using SaPanK, followed by purification of the phosphorylated ester to remove residual ATP, ADP and the enzyme (Scheme 4.10). In the second step the deprotection of the ester is required. For the deprotection of the methyl ester of **P-3.2** we decided to employ LiOH, while Pd(PPh₃)₄ was used for the deprotection of the allyl ester of **P-4.5**. It is not expected that the phosphate group would significantly affect the ability of Pd(PPh₃)₄ to perform the deprotection, since it is often used to deprotect phosphates protected by allyl protecting groups. The formation of the deprotected P-CJ could easily be tracked by HPLC since its retention time differs significantly from that of the ester.



Scheme 4.10. Attempted synthesis of P-CJ using a chemo-enzymatic approach.

The first step (the phosphorylation reaction) was conducted on a 15 ml scale (~10 mg) and the products subsequently purified by using 5 g SPE cartridges. According to HPLC analysis of the purified phosphorylated esters all of the starting material was converted into product, which was isolated in good yield with only a very small amount of ATP and ADP contamination (Figure 4.3). Unfortunately, in the second step neither of the deprotection reactions gave the desired products due to decomposition during the course of the reaction as indicated by HPLC analysis.

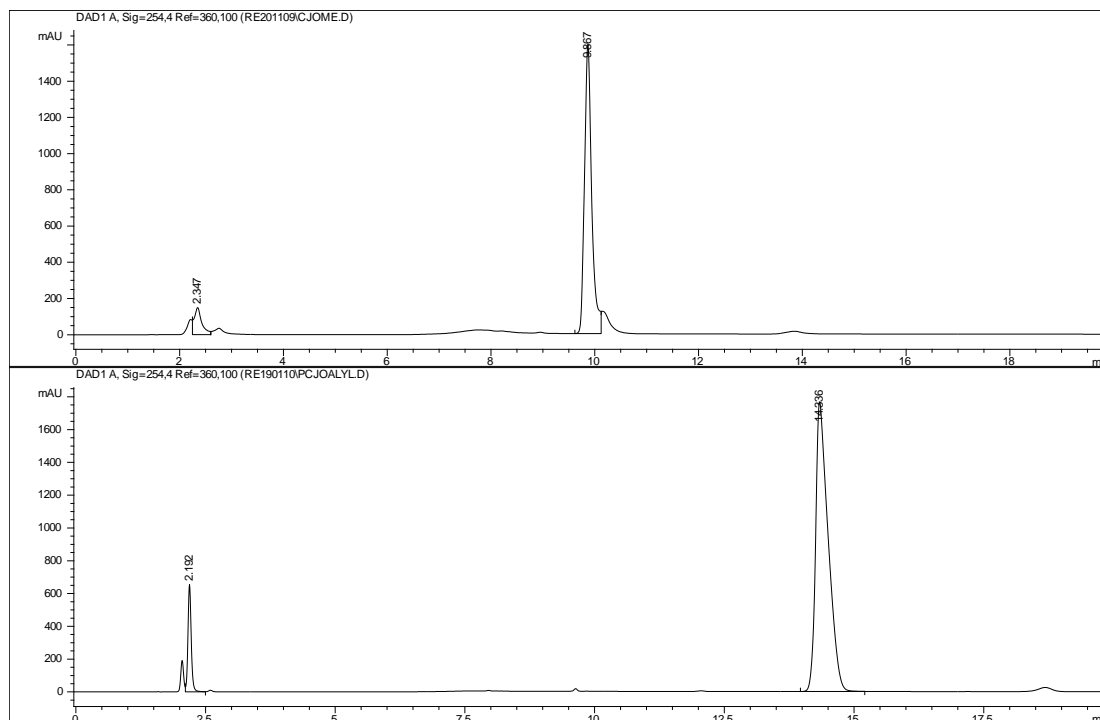


Figure 4.3. HPLC chromatograms of **P-3.2** (top) and **P-4.5** (bottom) biosynthesis after purification. Peaks below 3 min represent residual ATP and ADP.

4.12 Conclusion

In this chapter we presented a Pd-catalyzed formation of the unusual enamide moiety of antibiotic CJ-15,801. This stereoselective methodology favored the *E*-isomer in all cases when the reaction was carried out at 55 °C. It was found that the *Z*-isomer was formed when the reaction was carried out at higher temperatures, presumably due to *E* to *Z* isomerization.

In total six acrylate and acrylamide substrates were coupled to the amide, and deprotected to give CJ-15,801 ester and amide analogues. *S. aureus* growth inhibition studies with di-protected CJ analogues and CJ esters and amides were preformed, which revealed that apart from pentyl amide **4.26** none of these compounds effected growth at 200 µM concentrations. However, similar studies on *M. smegmatis* showed that di-protected allyl ester **4.3** completely abolished its growth at this concentration.

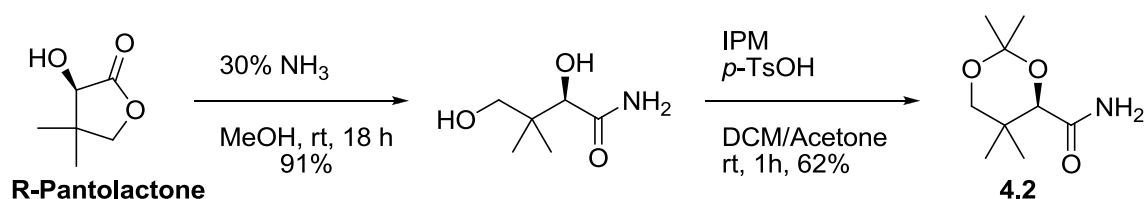
We believe that this methodology is very well suited for the synthesis of enamides on a large scale and could therefore in particular facilitate the synthesis of P-CJ, and other analogues of CJ as potential enhanced antistaphylococcal agents.

4.13 Experimental

4.13.1 Materials and methods

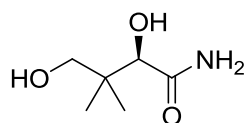
The materials and methods used in this chapter are the same as in Chapter 2. The only differences are as follows. All reagents and anhydrous toluene were from Sigma-Aldrich and used without further purification. Anhydrous acetone was distilled and pre-dried overnight over 3 Å molecular sieves before use. Strata C18-E (55µm, 70Å) solid phase extraction (SPE) cartridges (5 g/30 mL) were from Phenomenex. HPLC method B was used for all HPLC analysis in this chapter (see chapter 2).

The amide **4.2** was synthesized from Pantolactone as set out in scheme 4.11. This was conducted according to literature procedures with minor modification.^{10, 12}



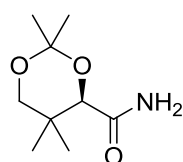
Scheme 4.11. Synthesis of amide **4.2** from pantolactone.

4.13.2 Synthesis of 2,4-Dihydroxy-3,3-dimethyl-butamide



To an oven dried round bottom flask containing pantolactone **4.1** (2.00 g, 15.4 mmol) was added anhydrous 30% ammonia in methanol (23 mL). This solution was stirred overnight at rt where after it was concentrated *in vacuo* to yield the amide as a white solid (2.44 g, 91%), which was used in the next step without any further purification. The ¹H NMR spectrum agrees with the published spectra.¹⁰ ¹H NMR (DMSO-D₆, 400MHz): δ = 7.10 (br s, 2H), 5.21 (d, J = 6.0 Hz, 1H), 4.47 (t, J = 5.5 Hz, 1H), 3.66 (d, J = 6.0 Hz, 1H), 3.30 (dd, J = 10.2, 5.5 Hz, 1H), 3.18 (dd, J = 10.4, 5.4 Hz, 1H), 0.82 (s, 3H), 0.81 (s, 3H).

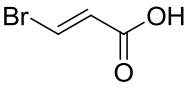
4.13.3 Synthesis of 2,2,5,5-Tetramethyl-[1,3]dioxane-4-carboxylic acid amide (**4.2**)



The synthesis of **4.2** was performed according to the literature procedure of Aquino *et al.*¹⁰ To an oven dried two-neck round bottom flask containing 2,4-dihydroxy-3,3-dimethyl-butamide (1.58 g, 10.7 mmol) was added anhydrous acetone (27 mL)

and DCM (27 mL). To this solution was added isopropylmetethyl ether (IPM) (2.10 mL, 21.4 mmol) and toluenesulfonic acid (*p*-TsOH) (0.204 g, 1.07 mmol). The resulting mixture was then stirred for 1h at rt followed by filtration and neutralized by adding triethyl amine (0.30 mL). The resulting mixture was dried over Na₂SO₄. After filtration the solution was concentrated *in vacuo* and the amide purified using flash chromatography (Hex/EtOAc 2:1) to afford **4.2** as a yellow oil (1.24 g, 62%) which solidified on standing. The ¹H NMR spectrum agreed with the published spectra.¹⁰ ¹H NMR (DMSO–D₆, 400MHz): δ = 7.10 (br s, 2H), 5.21 (d, J = 6.0 Hz, 1H), 4.47 (t, J = 5.5 Hz, 1H), 3.66 (d, J = 6.0 Hz, 1H), 3.30 (dd, J = 10.2, 5.5 Hz, 1H), 3.18 (dd, J = 10.4, 5.4 Hz, 1H), 0.82 (s, 3H), 0.81 (s, 3H).

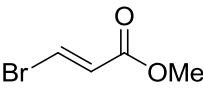
4.13.4 Synthesis of (*E*)-β-bromoacrylic acid (**4.11**)

 (*E*)-β-bromoacrylic acid was synthesized according to the literature procedure of Weir.⁹ Propiolic acid (4.65 g, 66.4 mmol) was added drop-wise to a solution of 48% aqueous hydrobromic acid (25 mL) at rt. The resulting solution was stirred at reflux for 1.5 h, where after it was cooled on an ice bath. Pure bromo acid **4.11** (6.27 g, 63%) was isolated as a grey solid by filtration of the resulting precipitate. ¹H NMR (DMSO–D₆, 400MHz): δ = 7.73 (d, J = 13.6 Hz, 1H), 6.56 (d, J = 13.6 Hz, 1H).

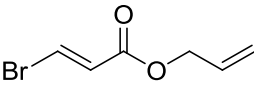
4.13.5 General procedure for the synthesis of β-bromoacrylates:

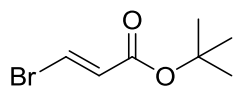
Bromoacrylic acid **4.11** was dissolved in a 0.8 M solution of the appropriate alcohol. To this solution was added 0.1 eq of conc. H₂SO₄ and the mixture heated to reflux overnight. After cooling to rt and concentration *in vacuo* the desired ester was purified using flash chromatography.

(*E*)-Methyl 3-bromoacrylate (**4.12**)

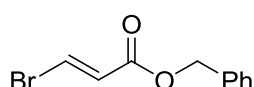
 Methyl ester **4.12** was prepared according to the general procedure using methanol and yielded a yellow liquid (1.63 g, 25%) after flash chromatography (Hexane:EtOAc 3:1). ¹H NMR (CDCl₃, 400MHz): δ = 7.60 (d, J = 13.9 Hz, 1H), 6.53 (d, J = 14.1 Hz, 1H), 3.75 (s, 3H); ¹³C NMR (CDCl₃, 150MHz): δ = 164.5, 128.4, 126.8, 52.0.

(*E*)-Allyl 3-bromoacrylate (**4.15**)

 Allyl ester **4.15** was prepared according to the general procedure using allyl alcohol and yielded a colorless liquid (1.54 g, 61%) after flash chromatography (Hexane:EtOAc 19:1). ¹H NMR (CDCl₃, 300MHz): δ = 7.64 (d, J = 13.8 Hz, 1H), 6.56 (d, J = 14.0 Hz, 1H), 6.00-5.87 (m, 1H), 5.35 (d, J = 17.0 Hz, 1H), 5.28 (d, J = 10.3 Hz, 1H), 4.65 (d, J = 5.5 Hz, 2H); ¹³C NMR (CDCl₃, 75.5MHz): δ = 163.7, 131.6, 128.5, 127.0, 118.7, 65.6.

(E)-tert-Butyl 3-bromoacrylate (4.16)

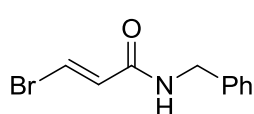
Tertiary-butyl ester **4.16** was prepared according to the general procedure using *tert*-butyl alcohol and yielded a colorless liquid (0.51 g, 19%) after flash chromatography (Hexane:EtOAc 4:1). ^1H NMR (CDCl_3 , 300MHz): δ = 7.47 (d, J = 14.1 Hz, 1H), 6.45 (d, J = 13.7 Hz, 1H), 1.49 (s, 9H); ^{13}C NMR (CDCl_3 , 150MHz): δ = 28.0, 81.6, 125.3, 130.6, 163.3.

4.13.6 (E)-Benzyl 3-bromoacrylate (4.17)

To (*E*)- β -Bromoacrylic acid (1.00 g, 6.62 mmol) and DMAP (0.162 g, 1.32 mmol) in a oven-dried two-neck flask were added DCM (8 ml) and benzylalcohol (3.44 mL, 33.1 mmol) using oven-dried syringes. The solution was cooled to 0 °C and DIC (1.13 mL, 7.29 mmol) was added dropwise using an oven dried syringe. The reaction was allowed to warm to rt and stirred for 1h. The reaction mixture was then filtered through Celite and concentrated *in vacuo*. The resulting syrup was taken up in EtOAc (50 mL) and washed with saturated NaHCO_3 (2 x 10 mL) and brine (1 x 10 mL). The organic layer was dried over Na_2SO_4 and concentrated *in vacuo*. The desired product was purified using flash chromatography (Hexane/EtOAc 19:1) to give **4.17** (1.0 g, 63%) as a pail yellow liquid. ^1H NMR (CDCl_3 , 400MHz): δ = 7.65 (d, J = 13.9 Hz, 1H), 7.39-7.33 (m, 5H), 6.58 (d, J = 13.6 Hz, 1H), 5.19 (s, 2H); ^{13}C NMR (CDCl_3 , 150MHz): δ = 163.8, 135.4, 128.6, 128.5, 128.4, 128.3, 127.2, 66.7.

4.13.7 General procedure for the synthesis of β -bromoacrylamides

To an oven-dried two neck flask were added (*E*)- β -bromoacrylic acid (1.00 g 6.62 mmol) and DMAP (0.162 g, 1.32 mmol). The amine (9.94 mmol) and DCM (13 mL) were then added to the flask using oven-dried syringes. The solution was cooled to 0 °C and DIC (1.13 mL, 7.29 mmol) was added drop-wise with a syringe. The reaction was warmed to rt and stirred for 6 h, after which it was filtered through Celite and concentrated under reduced pressure. After dilution with ethyl acetate, the organic layer was washed with saturated NaHCO_3 (2 x 10 mL), brine (1 x 10 mL) and the organic layer dried over Na_2SO_4 . After filtration and concentration *in vacuo* the amide was purified using flash chromatography.

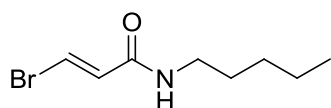
(E)-N-Benzyl-3-bromoacrylamide (4.18)

The acrylamide **4.18** was prepared according to the general procedure using benzylamine (0.982 mL, 9.94 mmol). A white solid (0.774 g, 47%) was obtained after purification with flash chromatography (Hexane:EtOAc 3:1).

The ^1H NMR spectrum agreed with the published spectra.⁸ ^1H NMR (CDCl_3 , 300MHz): δ = 7.50 (d,

$J = 13.4$ Hz, 1H), 7.37-7.26 (m, 5H), 6.49 (d, $J = 13.6$ Hz, 1H), 5.85 (br s, 1H), 4.48 (d, $J = 5.9$ Hz, 2H).

(*E*)-3-Bromo-*N*-pentylacrylamide (**4.19**)

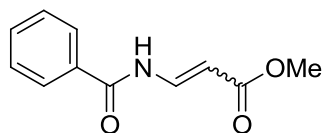


The acrylamide **4.19** was prepared according to the general procedure using pentylamine (1.15 mL, 9.94 mmol). A pale yellow solid (0.34 g, 12%) was obtained after purification with flash chromatography (Hexane:EtOAc 8:2). ^1H NMR (CDCl_3 , 300MHz): $\delta = 7.43$ (d, $J = 13.5$ Hz, 1H), 6.46 (d, $J = 13.1$ Hz, 1H), 5.68 (br s, 1H), 3.34-3.26 (m, 2H), 1.53 (p, $J = 14.1$, 7.5 Hz, 2H), 1.38-1.28 (m, 4H), 0.90 (t, $J = 7.0$ Hz, 3H); ^{13}C NMR (CDCl_3 , 75.5MHz): $\delta = 163.4$, 130.9, 122.4, 39.7, 29.1, 29.0, 22.3, 13.9; HRMS-ESI: m/z $[\text{M}+1]^+$ calcd for $\text{C}_8\text{H}_{15}\text{BrNO}$: 220.0337; found: 220.0333;

4.13.8 General procedure for Pd-catalyzed couplings

These reactions were conducted according to an adapted procedure of Tanoury *et al.*⁸ To a oven dried Schlenk tube under a nitrogen atmosphere were added $\text{Pd}(\text{OAc})_2$ (0.1 eq), xantphos (0.15 eq), K_2CO_3 (2 eq), CTAB (0.2 eq), the bromide (1.1 eq), the amide (Benzamide or **4.2**) (1 eq) and toluene (0.4 M with respect to amide). The suspension was then degassed under high vacuum until no further gas evolution was observed, after which it was warmed to 55 °C. After stirring for 1h, 3 eq of water was added and the reaction stirred for a further 4h at 55 °C. After cooling to rt the reaction was diluted with EtOAc, washed with water and the organic layer dried over Na_2SO_4 . After filtration and concentration *in vacuo* the *E* and *Z*-enamides were separated and purified using flash chromatography. The stereochemistry of the products was assigned by comparing the coupling constants of the alkene protons.

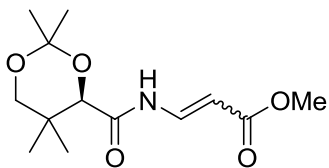
N-[Methoxy-propenoyl]benzamide (**4.13**)



The synthesis of **4.13** was performed according to the general procedure using bromoacrylate **4.12** (0.150 g, 0.908 mmol). Both *E* and *Z* products were obtained after purification by flash chromatography (Hexane/EtOAc 2:1 to 1:1) in a combined yield of 71% (*E/Z* ratio of 1:2).

(**4.13**, *E*-isomer) ^1H NMR (CDCl_3 , 400MHz): $\delta = 8.76$ (br d, $J = 11.2$ Hz, 1H), 8.24 (dd, $J = 14.0$, 11.3 Hz, 1H), 7.87-7.84 (m, 2H), 7.58-7.54 (m, 1H), 7.47-7.44 (m, 2H), 5.66 (d, $J = 14.0$ Hz, 1H), 3.72 (s, 3H).

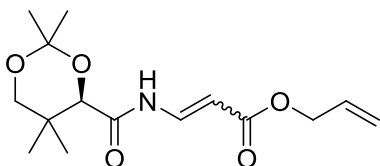
(**Z-4.13**) ^1H NMR (CDCl_3 , 400MHz): $\delta = 11.49$ (br d, $J = 12.0$ Hz, 1H), 7.98-7.95 (m, 2H), 7.76 (dd, $J = 10.8$, 8.9 Hz, 1H), 7.62-7.57 (m, 1H), 7.53-7.49 (m, 2H), 5.28 (d, $J = 8.6$ Hz, 1H), 3.78 (s, 3H).

(R)-Methyl 3-(2,2,5,5-tetramethyl-1,3-dioxane-4-carboxamido)acrylate (4.14)

The synthesis of **4.14** was performed according to the general procedure using bromoacrylate **4.12** (0.194 g, 1.18 mmol). Both *E* and *Z* products were obtained after purification by flash chromatography (Hexane/EtOAc 3:1 to 2:1) in a combined yield of 75% (*E/Z* ratio of 18:1).

(4.14, E-isomer) ^1H NMR (CDCl_3 , 400MHz): δ = 8.39 (br d, J = 11.2 Hz, 1H), 7.98 (dd, J = 14.1, 12.2 Hz, 1H), 5.60 (d, J = 13.9 Hz, 1H), 4.19 (s, 1H), 3.73 (s, 3H), 3.71 (d, J = 12.2 Hz, 1H), 3.31 (d, J = 11.7 Hz, 1H), 1.51 (s, 3H), 1.45 (s, 3H), 1.05 (s, 3H), 1.00 (s, 3H); ^{13}C NMR (CDCl_3 , 100MHz): δ = 168.2, 167.8, 136.4, 102.8, 99.8, 77.4, 71.5, 51.6, 33.6, 29.7, 22.1, 19.0, 18.9; HRMS–ESI: m/z $[\text{M}+1]^+$ calcd for $\text{C}_{13}\text{H}_{22}\text{NO}_5$: 272.1498; found: 272.1494.

(Z-4.14) ^1H NMR (CDCl_3 , 400MHz): δ = 11.07 (br d, J = 10.5 Hz, 1H), 7.43 (dd, J = 11.7, 9.0 Hz, 1H), 5.17 (dd, J = 9.0 Hz, 1H), 4.21 (s, 1H), 3.74 (s, 3H), 3.73 (d, J = 13.7 Hz, 1H), 3.32 (d, J = 11.7 Hz, 1H), 1.59 (s, 3H), 1.47 (s, 3H), 1.05 (s, 3H), 1.03 (s, 3H); ^{13}C NMR (CDCl_3 , 100MHz): δ = 169.0, 168.8, 136.3, 99.5, 97.8, 77.5, 71.5, 33.5, 31.1, 29.6, 22.1, 19.2, 18.9.

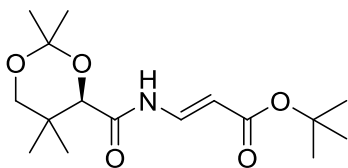
(R)-Allyl 3-(2,2,5,5-tetramethyl-1,3-dioxane-4-carboxamido)acrylate (4.3)

The synthesis of **4.3** was performed according to the general procedure using bromoacrylate **4.15** (0.393 g, 2.06 mmol). Both *E* and *Z* products were obtained after purification by flash chromatography (Hexane/EtOAc 4:1) in a combined yield of 66%

yield (*E/Z* ratio of 5:1).

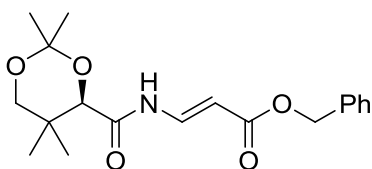
(4.3, E-isomer) The ^1H NMR of matches the literature spectra.⁴ ^1H NMR (CDCl_3 , 400MHz): δ = 8.39 (br d, J = 11.1 Hz, 1H), 8.00 (dd, J = 14.1, 12.1 Hz, 1H), 5.99-5.89 (m, 1H), 5.63 (d, J = 14.0 Hz, 1H), 5.33 (d, J = 17.0 Hz, 1H), 5.23 (d, J = 10.3 Hz, 1H), 4.64 (d, J = 5.5 Hz, 2H), 4.20 (s, 1H), 3.71 (d, J = 11.8 Hz, 1H), 3.31 (d, J = 11.7 Hz, 1H), 1.51 (s, 3H), 1.45 (s, 3H), 1.05 (s, 3H), 1.00 (s, 3H).

(Z-4.3) ^1H NMR (CDCl_3 , 400MHz): δ = 11.07 (br d, J = 10.9 Hz, 1H), 7.45 (dd, J = 11.7, 9.0 Hz, 1H), 6.00-5.87 (m, 1H), 5.33 (d, J = 17.2 Hz, 1H), 5.25 (d, J = 11.7 Hz, 1H), 5.20 (d, J = 9.0 Hz, 1H), 4.65 (d, J = 5.2 Hz, 2H), 4.21 (s, 1H), 3.73 (d, J = 11.7 Hz, 1H), 3.33 (d, J = 11.7 Hz, 1H), 1.58 (s, 3H), 1.46 (s, 3H), 1.04 (s, 3H), 1.03 (s, 3H); ^{13}C NMR (CDCl_3 , 75.5MHz): δ = 168.8, 167.3, 136.3, 132.2, 118.2, 99.3, 97.6, 77.2, 71.3, 66.7, 33.3, 29.3, 21.8, 19.0, 18.6.

(*R,E*)-tert-Butyl 3-(2,2,5,5-tetramethyl-1,3-dioxane-4-carboxamido)acrylate (4.20)

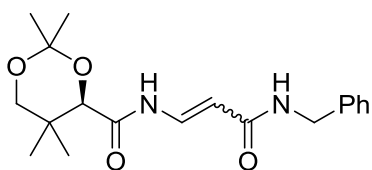
The synthesis of **4.20** was performed according to the general procedure using bromoacrylate **4.16** (0.304 g, 1.47 mmol). The product was obtained after purification by flash chromatography (Hexane/EtOAc 4:1) and gave only the *E*-isomer in 59% yield. ^1H

NMR (CDCl_3 , 400MHz): δ = 8.31 (br d, J = 11.6 Hz, 1H), 7.85 (dd, J = 14.4, 12.0 Hz, 1H), 5.52 (d, J = 14.5 Hz, 1H), 4.18 (s, 1H), 3.71 (d, J = 11.8 Hz, 1H), 3.31 (d, J = 12.1 Hz, 1H), 1.50 (s, 3H), 1.48 (s, 9H), 1.45 (s, 3H), 1.05 (s, 3H), 1.00 (s, 3H); ^{13}C NMR (CDCl_3 , 100MHz): δ = 167.9, 166.4, 135.0, 105.1, 99.5, 80.2, 77.2, 71.3, 33.4, 29.4, 28.2, 21.9, 18.8, 18.7.

(*R,E*)-Benzyl 3-(2,2,5,5-tetramethyl-1,3-dioxane-4-carboxamido)acrylate (4.21)

The synthesis of **4.21** was performed according to the general procedure using bromoacrylate **4.17** (0.283 g, 1.17 mmol). The product was obtained after purification by flash chromatography (Hexane/EtOAc 4:1) and gave only the *E*-isomer in 74% yield. ^1H

NMR (CDCl_3 , 400MHz): δ = 8.40 (br d, J = 11.7 Hz, 1H), 8.01 (dd, J = 14.0, 11.7 Hz, 1H), 7.38–7.35 (m, 4H), 7.34–7.29 (m, 1H), 5.60 (d, J = 14.5 Hz, 1H), 5.19 (s, 2H), 4.19 (s, 1H), 3.71 (d, J = 12.1 Hz, 1H), 3.32 (d, J = 11.7 Hz, 1H), 1.51 (s, 3H), 1.45 (s, 3H), 1.05 (s, 3H), 1.00 (s, 3H); ^{13}C NMR (CDCl_3 , 75.5MHz): δ = 167.9, 166.9, 136.4, 136.2, 128.5, 128.1, 102.7, 99.5, 77.2, 71.2, 66.0, 33.4, 29.4, 21.8, 18.8, 18.7.

(*R*)-*N*-(3-(Benzylamino)-3-oxoprop-1-enyl)-2,2,5,5-tetramethyl-1,3-dioxane-4-carboxamide (4.4)

The synthesis of **4.4** was performed according to the general procedure using bromoacrylamide **4.18** (0.353 g, 1.47 mmol). Both *E* and *Z* products were obtained after purification by flash chromatography (Hexane/EtOAc 1:1 to 1:2) in a combined yield of

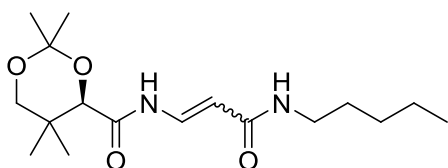
52% yield (*E/Z* ratio of 3:1).

(4.4, *E*-isomer) The ^1H NMR of matches the literature spectra.⁴ ^1H NMR (acetone- D_6 , 300MHz): δ = 9.46 (br d, J = 10.8 Hz, 1H), 7.89 (dd, J = 14.2, 11.2 Hz, 1H), 7.59 (br t, J = 4.6 Hz, 1H), 7.30–7.20 (m, 5H), 6.03 (d, J = 14.1 Hz, 1H), 4.45 (d, J = 5.9 Hz, 2H), 4.27 (s, 1H), 3.76 (d, J = 11.7 Hz, 1H), 3.27 (d, J = 11.7 Hz, 1H), 1.44 (s, 3H), 1.38 (s, 3H), 1.01 (s, 3H), 0.99 (s, 3H).

(*Z*-4.4) ^1H NMR (CDCl_3 , 300MHz): δ = 11.72 (br d, J = 10.5 Hz, 1H), 7.28–7.37 (m, 6H), 5.63 (br t, J = 5.7 Hz, 1H), 5.01 (d, J = 9.1 Hz, 1H), 4.50 (dd, J = 5.4 Hz, 2H), 4.02 (s, 1H), 3.72 (d, J = 11.7

Hz, 1H), 3.32 (d, $J = 11.7$ Hz, 1H), 1.62 (s, 3H), 1.47 (s, 3H), 1.06 (s, 3H), 1.05 (s, 3H); ^{13}C NMR (CDCl_3 , 150MHz): $\delta = 168.9, 167.5, 138.0, 133.7, 128.7, 127.9, 127.6, 100.1, 99.3, 77.3, 71.4, 43.3, 33.3, 29.3, 22.0, 19.1, 18.6$; HRMS–ESI: m/z $[\text{M}+1]^+$ calcd for $\text{C}_{19}\text{H}_{27}\text{N}_2\text{O}_4$: 347.1971; found: 347.1967.

(*R*)-2,2,5,5-Tetramethyl-*N*-(3-oxo-3-(pentylamino)prop-1-enyl)-1,3-dioxane-4-carboxamide (4.22)



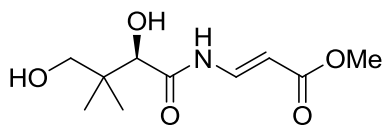
The synthesis of **4.22** was performed according to the general procedure using bromoacrylamide **4.19** (0.194 g, 0.885 mmol). Both *E* and *Z* products were obtained after purification by flash chromatography (Hexane/EtOAc 1:1 to 1:2) in a combined yield of 49% yield (*E/Z* ratio of 3:1).

(4.22, *E*-isomer) ^1H NMR (acetone- D_6 , 400MHz): $\delta = 9.38$ (br d, $J = 10.6$ Hz, 1H), 7.80 (dd, $J = 13.5, 10.9$ Hz, 1H), 7.17 (br s, 1H), 5.95 (d, $J = 14.1$ Hz, 1H), 4.26 (s, 1H), 3.76 (d, $J = 11.7$ Hz, 1H), 3.28–3.21 (m, 3H), 1.52–1.46 (m, 2H), 1.44 (s, 3H), 1.38 (s, 3H), 1.33–1.26 (m, 4H), 1.00 (s, 3H), 0.98 (s, 3H), 0.87 (t, $J = 7.1$ Hz, 3H); ^{13}C NMR (acetone- D_6 , 100MHz): $\delta = 170.3, 168.0, 134.8, 107.9, 101.0, 78.8, 72.8, 72.6, 40.9, 34.8, 34.3, 31.1, 24.0, 23.1, 20.2, 20.0, 15.3$; HRMS–ESI: m/z $[\text{M}+1]^+$ calcd for $\text{C}_{17}\text{H}_{31}\text{N}_2\text{O}_4$: 327.2284; found: 327.2269.

(*Z*-4.22) ^1H NMR (CDCl_3 , 400MHz): $\delta = 11.69$ (br d, $J = 11.0$ Hz, 1H), 7.27 (dd, $J = 11.2, 8.9$ Hz, 1H), 5.55 (br t, $J = 5.1$ Hz, 1H), 5.00 (d, $J = 8.9$ Hz, 1H), 4.19 (s, 1H), 3.72 (d, $J = 11.7$ Hz, 1H), 3.33–3.26 (m, 3H), 1.60 (s, 3H), 1.55–1.48 (m, 2H), 1.47 (s, 3H), 1.36–1.30 (m, 4H), 1.05 (s, 6H), 0.90 (t, $J = 7.1$ Hz, 3H); ^{13}C NMR (CDCl_3 , 100MHz): $\delta = 168.8, 167.7, 133.0, 131.0, 122.2, 100.7, 99.2, 77.2, 71.3, 39.1, 33.3, 29.3, 29.2, 29.0, 22.3, 19.0, 13.9$; HRMS–ESI: m/z $[\text{M}+1]^+$ calcd for $\text{C}_{17}\text{H}_{31}\text{N}_2\text{O}_4$: 327.2284; found: 327.2283.

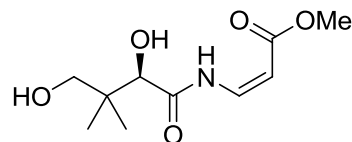
4.13.9 General procedure for the deprotection of the acetonide group

The acetonide group of each isomer was deprotected according to the procedure of Han *et al.*⁴ To a round-bottom flask containing the acetonide protected *N*-acyl vinylogous carbamate or urea (1 eq), was added BiCl_3 (0.2 eq), water (20 eq) and MeCN (0.24 M). The reaction was then stirred at rt overnight, filtered and concentrated. The residue was taken up in EtOAc and washed with sat. NaHCO_3 (2 x 10 mL) and the aqueous layer was extracted with EtOAc (1 x 10 mL). The organic layers were combined, dried over Na_2SO_4 , filtered and concentrated *in vacuo*. The crude product was then purified using flash chromatography.

(*R,E*)-Methyl 3-(2,4-dihydroxy-3,3-dimethylbutanamido)acrylate (3.2)

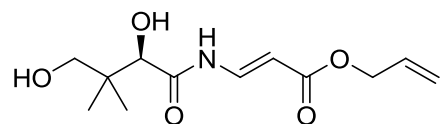
The reaction was performed according to the general procedure using **4.14** (0.300 g, 1.11 mmol), BiCl₃ (70 mg, 0.22 mmol), and water (400 μ L, 22.3 mmol) to afford the diol **3.2** (0.206 g, 79%) as a

colorless oil after purification by flash chromatography (EtOAc/Hexane 1:1 to 3:1). ¹H NMR (CD₃OD, 600MHz): δ = 7.96 (d, *J* = 14.3 Hz, 1H), 5.75 (d, *J* = 14.4 Hz, 1H), 4.02 (s, 1H), 3.71 (s, 3H), 3.49 (d, *J* = 10.8 Hz, 1H), 3.39 (d, *J* = 11.2 Hz, 1H), 0.94 (s, 3H), 0.93 (s, 3H); ¹³C NMR (CD₃OD, 150MHz): δ = 174.9, 170.1, 138.7, 102.4, 77.0, 69.7, 51.7, 40.7, 21.4, 20.4; HRMS–ESI: *m/z* [M+1]⁺ calcd for C₁₀H₁₈NO₅: 232.1185; found: 232.1174.

(*R,Z*)-Methyl 3-(2,4-dihydroxy-3,3-dimethylbutanamido)acrylate (Z-3.2)

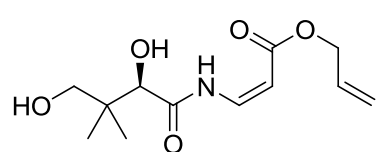
The reaction was performed according to the general procedure using **Z-4.14** (50 mg, 0.18 mmol), BiCl₃ (13 mg, 0.041 mmol), and water (73.1 μ L, 4.1 mmol) to afford the diol **Z-3.2** (8 mg, 19%) as a colorless oil after purification by flash chromatography (EtOAc/Hexane 1:1). ¹H

NMR (acetone–D₆, 400MHz): δ = 11.33 (br d, *J* = 11.0 Hz, 1H), 7.48 (dd, *J* = 11.6, 9.0 Hz, 1H), 5.37 (d, *J* = 4.7 Hz, 1H), 5.18 (d, *J* = 9.0 Hz, 1H), 4.19 (d, *J* = 4.7 Hz, 1H), 4.02 (t, *J* = 5.4 Hz, 1H), 3.69 (s, 3H), 3.45–3.55 (m, 2H), 0.96 (s, 6H); HRMS–ESI: *m/z* [M+1]⁺ calcd for C₁₀H₁₈NO₅: 232.1185; found: 232.1181.

(*R,E*)-Allyl 3-(2,4-dihydroxy-3,3-dimethylbutanamido)acrylate (4.5)

The reaction was performed according to the general procedure using **4.3** (0.133 g, 0.517 mmol), BiCl₃ (28 mg, 0.089 mmol), and water (161 μ L, 8.95 mmol) to afford the diol **4.5** (85

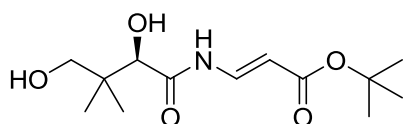
mg, 71%) as a colorless oil after purification by flash chromatography (EtOAc/Hexane 1:1). The ¹H NMR matches the literature spectra.⁴ ¹H NMR (CD₃OD, 400MHz): δ = 7.97 (d, *J* = 14.2 Hz, 1H), 6.00–5.92 (m, 1H), 5.76 (d, *J* = 14.2 Hz, 1H), 5.31 (d, *J* = 17.1 Hz, 1H), 5.21 (d, *J* = 10.6 Hz, 1H), 4.62 (d, *J* = 5.5 Hz, 1H), 4.01 (s, 1H), 3.48 (d, *J* = 10.5 Hz, 1H), 3.38 (d, *J* = 10.8 Hz, 1H), 0.93 (s, 3H), 0.92 (s, 3H).

(*R,Z*)-Allyl 3-(2,4-dihydroxy-3,3-dimethylbutanamido)acrylate (Z-4.5)

The reaction was performed according to the general procedure using **Z-4.3** (0.100 g, 0.389 mmol), BiCl₃ (21 mg, 0.067 mmol), and water (121 μ L, 6.72 mmol) to afford the diol **Z-4.5** (72 mg, 80%) as

a colorless oil after purification by flash chromatography (EtOAc/Hexane). The ^1H NMR matches the literature spectra.⁶ ^1H NMR (CDCl_3 , 400MHz): δ = 11.25 (br d, J = 11.4 Hz, 1H), 7.48 (dd, J = 11.6, 8.9 Hz, 1H), 5.99-5.89 (m, 1H), 5.33 (d, J = 17.2 Hz, 1H), 5.25 (d, J = 10.5 Hz, 1H), 5.23 (d, J = 8.6 Hz, 1H), 4.64 (d, J = 5.9 Hz, 2H), 4.21 (s, 1H), 3.59 (d, J = 10.9 Hz, 1H), 3.54 (d, J = 10.9 Hz, 1H), 1.04 (s, 3H), 0.99 (s, 3H).

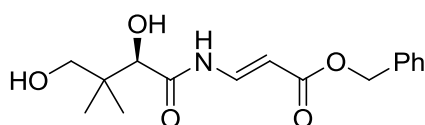
(*R,E*)-*tert*-Butyl 3-(2,4-dihydroxy-3,3-dimethylbutanamido)acrylate (4.23)



The reaction was performed according to the general procedure using **4.20** (0.078 g, 0.25 mmol), BiCl_3 (16 mg, 0.050 mmol), and water (89.7 μL , 4.98 mmol) to afford the diol **4.23** (42 mg, 62%)

as a colorless oil after purification by flash chromatography (EtOAc/Hexane 1:1). ^1H NMR (CD_3OD , 400MHz): δ = 7.85 (d, J = 14.3 Hz, 1H), 5.59 (d, J = 14.3 Hz, 1H), 4.02 (s, 1H), 3.47 (d, J = 10.9 Hz, 1H), 3.39 (d, J = 11.3 Hz, 1H), 1.46 (s, 9H), 0.93 (s, 3H), 0.92 (s, 3H); ^{13}C NMR (CD_3OD , 100MHz, 25°C): δ = 173.8, 168.4, 136.9, 104.5, 80.8, 76.8, 69.7, 40.0, 28.2, 21.1, 20.1; HRMS–ESI: m/z $[\text{M}+1]^+$ calcd for $\text{C}_{13}\text{H}_{24}\text{NO}_5$: 274.1654; found: 274.1660.

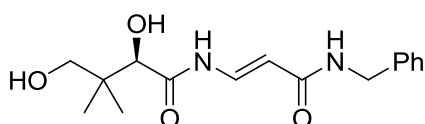
(*R,E*)-Benzyl 3-(2,4-dihydroxy-3,3-dimethylbutanamido)acrylate (4.24)



The reaction was performed according to the general procedure using **4.21** (0.118 g, 0.384 mmol), BiCl_3 (21 mg, 0.068 mmol), and water (122 μL , 6.79 mmol) to afford the diol **4.24** (90 mg, 90%)

as a colorless oil after purification by flash chromatography (EtOAc/Hexane 1:1). ^1H NMR (CD_3OD , 300MHz): δ = 7.8 (d, J = 14.2 Hz, 1H), 7.35-7.31 (m, 4H), 7.28 (m, 1H), 5.78 (d, J = 14.2 Hz, 1H), 5.14 (s, 2H), 4.02 (s, 1H), 3.47 (d, J = 11.1 Hz, 1H), 3.37 (d, J = 10.9 Hz, 1H), 0.92 (s, 3H), 0.91 (s, 3H); ^{13}C NMR (CD_3OD , 100MHz): δ = 175.0, 169.4, 139.1, 137.8, 129.5, 129.1, 129.1, 102.6, 77.1, 69.8, 67.0, 40.8, 21.5, 20.5; HRMS–ESI: m/z $[\text{M}+1]^+$ calcd for $\text{C}_{16}\text{H}_{22}\text{NO}_5$: 308.1498; found: 308.1500.

(*R,E*)-*N*-(3-(Benzylamino)-3-oxoprop-1-enyl)-2,4-dihydroxy-3,3-dimethylbutanamide (4.25)

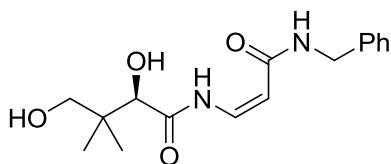


The reaction was performed according to the general procedure using **4.4** (0.100 g, 0.289 mmol), BiCl_3 (18 mg, 0.058 mmol), and water (105 μL , 5.78 mmol) to afford the diol **4.25** (30 mg, 34%)

as a yellow oil after purification by flash chromatography (EtOAc 100%). The ^1H NMR matches the literature spectra.⁴ ^1H NMR (acetone- D_6 , 300MHz): δ = 9.90 (br d, J = 11.1 Hz, 1H), 8.00 (dd, J = 13.8, 11.1 Hz, 1H), 7.92 (br t, J = 5.9 Hz, 1H), 7.34-7.29 (m, 4H), 7.27-7.19 (m, 1H),

6.11 (d, $J = 14.2$ Hz, 1H), 4.50 (d, $J = 5.9$ Hz, 2H), 4.23 (d, $J = 5.03$ Hz, 1H), 3.51 (d, $J = 12.1$ Hz, 1H), 3.46 (d, $J = 12.4$ Hz, 1H), 0.96 (s, 3H), 0.93 (s, 3H).

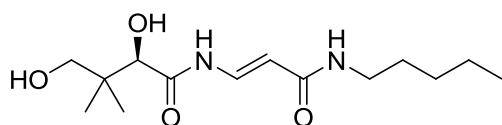
(*R,Z*)-N-(3-(Benzylamino)-3-oxoprop-1-enyl)-2,4-dihydroxy-3,3-dimethylbutanamide (Z-4.25**)**



The reaction was performed according to the general procedure using **Z-4.4** (0.056 g, 0.16 mmol), BiCl₃ (10 mg, 0.032 mmol), and water (58 μ L, 3.2 mmol) to afford the diol **Z-4.25** (29 mg, 58%) as a colorless oil after purification by flash chromatography

(EtOAc/Hexane 1:1 to 3:1). ¹H NMR (acetone- D_6 , 300MHz): δ = 12.08 (br d, $J = 10.6$ Hz, 1H), 7.74 (br t, $J = 5.6$ Hz, 1H), 7.20–7.33 (m, 6H), 5.32–5.36 (m, 2H), 4.48–4.41 (m, 3H), 4.22 (d, $J = 4.92$ Hz, 1H), 3.53–3.50 (m, 2H), 0.99 (s, 3H), 0.94 (s, 3H); ¹³C NMR (acetone- D_6 , 75.5MHz): δ = 174.4, 169.6, 141.2, 134.7, 130.2, 129.4, 128.8, 102.6, 78.3, 71.3, 44.1, 41.3, 22.3, 21.9; HRMS–ESI: m/z [M+1]⁺ calcd for C₁₆H₂₃N₂O₄: 307.1658; found: 307.1652.

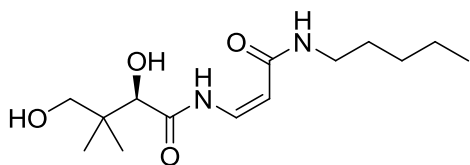
(*R,E*)-2,4-Dihydroxy-3,3-dimethyl-N-(3-oxo-3-(pentylamino)prop-1-enyl)butanamide (4.26**)**



The reaction was performed according to the general procedure using **4.22** (0.088 g, 0.27 mmol), BiCl₃ (17 mg, 0.54 mmol), and water (97.1 μ L, 5.39 mmol) to afford the

diol **4.26** (5 mg, 6%) as a yellow oil after purification by flash chromatography (EtOAc 100%). ¹H NMR (CD₃OD, 400MHz): δ = 7.81 (d, $J = 14.1$ Hz, 1H), 5.89 (d, $J = 14.1$ Hz, 1H), 4.00 (s, 1H), 3.48 (d, $J = 10.9$ Hz, 1H), 3.38 (d, $J = 10.9$ Hz, 1H), 3.21 (t, $J = 7.1$ Hz, 2H), 1.55–1.50 (m, 2H), 1.36–1.31 (m, 4H), 0.93–0.89 (m, 9H); HRMS–ESI: m/z [M+1]⁺ calcd for C₁₄H₂₇N₂O₄: 287.1971; found: 287.1973.

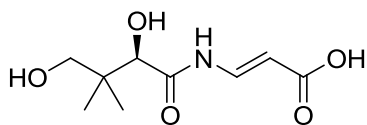
(*R,Z*)-2,4-Dihydroxy-3,3-dimethyl-N-(3-oxo-3-(pentylamino)prop-1-enyl)butanamide (Z-4.26**)**



The reaction was performed according to the general procedure using **Z-4.22** (0.035 g, 0.11 mmol), BiCl₃ (7 mg, 0.021 mmol), and water (39 μ L, 2.1 mmol) to afford the diol **Z-4.26** (25 mg, 83%) as a pale solid after purification by

flash chromatography (EtOAc/Hexane 3:1). ¹H NMR (CD₃OD, 400MHz): δ = 7.20 (d, $J = 9.4$ Hz, 1H), 5.19 (d, $J = 8.8$ Hz, 1H), 4.03 (s, 1H), 3.49 (d, $J = 11.1$ Hz, 1H), 3.40 (d, $J = 11.0$ Hz, 1H), 3.17 (t, $J = 7.5$ Hz, 2H), 1.55–1.47 (m, 2H), 1.36–1.30 (m, 4H), 0.93–0.89 (m, 9H); ¹³C NMR (CD₃OD, 100MHz): δ = 174.6, 170.0, 133.3, 102.0, 77.0, 70.0, 40.8, 40.1, 30.3, 30.2, 23.5, 21.3, 20.7, 14.4; HRMS–ESI: m/z [M+1]⁺ calcd for C₁₄H₂₇N₂O₄: 287.1971; found: 287.1981.

4.13.10 Synthesis of CJ-15,801



To a 0.1 M solution of allyl ester **4.5** (85 mg, 0.33 mmol) in dioxane/H₂O (4:1) was added Pd(PPh₃)₄ (76 mg, 0.066 mmol) and stirred over night at rt. To the reaction was added H₂O (5 mL), then the pH was adjusted to 8 using a diluted solution of NaOH and transferred to a separatory funnel. The aqueous layer was washed with DCM (3 x 3 mL) and freeze dried. The crude product was purified using flash chromatography (EtOAc/MeOH/MeCN/H₂O 5:1:1:1) followed by C18 SPE purification (H₂O to MeCN/H₂O 2:8) which yielded **3.1** (22 mg, 32%) as a pale yellow oil. The ¹H NMR agreed with the published spectra.⁴ ¹H NMR (D₂O, 400MHz): δ = 7.76 (d, *J* = 14.0 Hz, 1H), 5.59 (d, *J* = 14.3 Hz, 1H), 3.98 (s, 1H), 3.38 (d, *J* = 11.7 Hz, 1H), 3.27 (d, *J* = 10.8 Hz, 1H), 0.80 (s, 3H), 0.77 (s, 3H).

4.13.11 Growth inhibition of *S. aureus* by CJ ester and amide analogues

To determine whether the mono- and di-protected CJ ester and amide analogues showed any inhibition of *S. aureus* growth, growth inhibition assays were performed. A starter culture of *S. aureus* RN4220 was prepared by inoculating 1% tryptone broth with four colonies from cultures grown on LB agar plates. The starter culture was subsequently diluted 30-fold in the same medium and grown at 37 °C until the OD₆₀₀ reached 1.0. It was then diluted 10 000-fold, and 10 µL of the diluted cell suspension was used to inoculate each well of a 96-well flat-bottomed plate containing 110 µL 1% tryptone broth and one of the CJ analogues in final concentration of 200 µM. The plates were subsequently incubated without shaking at 37 °C for 20 h, and the amount of growth inhibition was subsequently assessed by determination of the OD₆₀₀.

4.13.12 Growth inhibition of *M. smegmatis* by CJ ester and amide analogues

To determine whether the prepared CJ analogues showed any inhibition of *M. smegmatis* growth, growth inhibition assays were performed. A starter culture of *M. smegmatis* ATCC 19420 was prepared by inoculating a 5 ml solution of Middlebrook broth (prepared according to the manufacturer's procedure) with a 100 µL of a freezer stock and grown overnight at 37 °C. The starter culture was subsequently diluted 1000-fold in the same medium and grown at 37 °C for another hour. Then, 2 µL of this cell suspension was used to inoculate each well of a 24-well flat-bottomed plate containing 2 ml Middlebrook broth and one of the CJ analogues in final concentration of 200 µM. The plates were subsequently incubated with shaking at 37 °C for 48 h, and the amount of growth inhibition was subsequently assessed by determination of the OD₆₀₀.

4.13.13 Biosynthesis of P-3.2 and P-4.5

A 9 mL reaction mixture contained either **3.2** or **4.5** (5 mM) and 8 mM ATP, 5 mM MgCl₂ and 50 mM Tris-HCl buffer (pH 7.6). The biosynthetic reaction was initiated by addition of 1.53 mg SaPanK. The reaction mixture was subsequently incubated for 18 hours at 37 °C. The reaction was stopped by removing the enzymes by syringe filtration (GHP Acrodisc 13mm from PALL Life Sciences). The desired P-CJ ester was subsequently purified using SPE cartridges (5 g). Prior to loading the reaction mixture, the cartridge was pre-conditioned with methanol (~20 mL) followed by equilibration with 10 mM NH₄OAc (~20 mL), pH 6.0. The crude reaction mixture was then loaded onto the column followed by washing with 10 mM NH₄OAc (30 mL) (pH 6.0). The products were eluted with 20% acetonitrile in H₂O (20 mL) and concentrated using a Labconco Centrivap concentrator. The compounds were then re-dissolved in H₂O (5 mM stocks) and analyzed using HPLC. To further confirm that the desired product **P-3.2** was obtained it was subjected to analysis with ¹H, ¹³C and ³¹P NMR.

P-3.2:

¹H NMR (CDCl₃, 400MHz): δ = 7.95 (d, *J* = 14.2 Hz, 1H), 5.78 (d, *J* = 14.4 Hz, 1H), 4.26 (s, 1H), 3.76 (s, 3H), 3.65 (dd, *J* = 11.7, 4.3 Hz, 1H), 3.56 (dd, *J* = 11.7, 6.8 Hz, 1H), 1.01 (s, 3H), 0.89 (s, 3H); ¹³C NMR (D₂O, 100MHz): δ = 175.0, 171.3, 138.3, 103.1, 75.4, 60.2, 52.6, 39.6, 21.6, 18.9; ³¹P NMR (D₂O, 100MHz): δ = 4.21.

4.14 References

1. Suh, E. M.; Kishi, Y., Synthesis of Palytoxin from Palytoxin Carboxylic Acid. *J. Am. Chem. Soc.* **1994**, *116* (24), 11205-11206.
2. Koshino, S.; Koshino, H.; Matsuura, N.; Kobinata, K.; Onose, R.; Isono, K.; Osada, H., A new cyclic lipopeptide antibiotic, enamidonin. *J. Antibiot.* **1995**, *48* (2), 185-187.
3. Tracey, M. R.; Hsung, R. P.; Antoline, J.; Kurtz, K. C. M.; Shen, L.; Slafer, B. W.; Zhang, Y., Product class 4: *N*-Arylalkanamides, ynamides, enamides, dienamides, and allenamides. *Sci. Synth.* **2005**, *21*, 387-475.
4. Han, C.; Shen, R.; Su, S.; Porco, J. A., Jr., Copper-Mediated Synthesis of *N*-Acyl Vinylogous Carbamic Acids and Derivatives: Synthesis of the Antibiotic CJ-15,801. *Org. Lett.* **2004**, *6* (1), 27-30.
5. Nicolaou, K. C.; Mathison, C. J. N., Synthesis of imides, *N*-acyl vinylogous carbamates and ureas, and nitriles by oxidation of amides and amines with Dess-Martin periodinane. *Angew. Chem., Int. Ed.* **2005**, *44* (37), 5992-5997.
6. Lee, J. M.; Ahn, D.-S.; Jung, D. Y.; Lee, J.; Do, Y.; Kim, S. K.; Chang, S., Hydrogen-Bond-Directed Highly Stereoselective Synthesis of *Z*-Enamides via Pd-Catalyzed Oxidative Amidation of Conjugated Olefins. *J. Am. Chem. Soc.* **2006**, *128* (39), 12954-12962.
7. Villa, M. V. J.; Targett, S. M.; Barnes, J. C.; Whittingham, W. G.; Marquez, R., An efficient approach to the stereocontrolled synthesis of enamides. *Org. Lett.* **2007**, *9* (9), 1631-3.
8. Tanoury, G. J.; Chen, M.; Dong, Y.; Forslund, R. E.; Magdziak, D., Development of a Novel Pd-Catalyzed *N*-Acyl Vinylogous Carbamate Synthesis for the Key Intermediate of ICE Inhibitor VX-765. *Org. Lett.* **2008**, *10* (2), 185-188.
9. Weir, J. R.; Patel, B. A.; Heck, R. F., Palladium-catalyzed triethylammonium formate reductions. 4. Reduction of acetylenes to *cis*-monoenes and hydrogenolysis of tertiary allylic amines. *J. Org. Chem.* **1980**, *45* (24), 4926-4931.
10. Aquino, F.; Pauling, H.; Walther, W.; Plattner, D. A.; Bonrath, W., A convenient dehydration procedure for the synthesis of enantiomerically pure cyanohydrins. *Synthesis* **2000**, (5), 731-737.
11. Green, T. W.; Wuts, P. G. M., *Protective Groups in Organic Synthesis*. Third ed.; John Wiley & Sons, Inc: New York, 1999.
12. Barrios, I.; Camps, P.; Comes-Franchini, M.; Munoz-Torrero, D.; Ricci, A.; Sanchez, L., One-pot synthesis of *N*-substituted pantolactams from pantolactone. *Tetrahedron* **2003**, *59* (11), 1971-1979.

Chapter 5

Conclusion and future work

5.1 Summary of results achieved

In this study we set out to identify and evaluate new targets involved in CoA biosynthesis and its metabolism for the development of new anti-staphylococcal agents. We were successful in the discovery of inhibitors for CoADR and PPCS enzymes. Moreover, the precursors of these inhibitors were found to inhibit *S. aureus* growth. These compounds serve as valuable lead compounds for the development of inhibitors with improved activity. The accompanying biological evaluations not only showed that these compounds are potent inhibitors but also established procedures for future studies.

This study also presented advances in synthetic organic chemistry. A Pd-catalyzed methodology was adapted to synthesize the reported antibiotic CJ-15,801, which is only the third reported total synthesis of this compound. This methodology also enabled us to prepare various *N*-acyl vinyllogous carbamate and urea analogues which were evaluated as *S. aureus* growth inhibitors. The objectives as outlined in Chapter 1 have been achieved as follows:

5.1.1 Objective 1: Michael acceptor-containing CoA analogues as inhibitors of CoADR

In chapter 2 a rational drug design strategy was employed to synthesize the first inhibitors of the essential *S. aureus* enzyme CoADR. We successfully adopted the approach of coupling warheads to substrate analogues which is often used in the irreversible inhibition of cysteine proteases. Using this approach we designed CoA-based substrate analogues containing α,β -unsaturated ester, ketone and vinyl sulfone moieties. Our inhibition studies showed that these compounds were time-dependent inhibitors of CoADR and that a phenyl vinyl sulfone inhibitor was the most potent with a k_{inact}/K_i value of nearly 40000. The inhibition of *S. aureus* growth by the pantothenamide precursors of the prepared CoA analogues showed that only the α,β -unsaturated ester analogues had inhibitory effects. Although this could suggest off-target effects, the lack of inhibition by vinyl sulfones could be due to cell permeability issues and a future study to clarify this should be undertaken.

The successful adoption of the inhibition strategy used for irreversible inhibition of cysteine protease not only opens a wide diversity of warheads that can be used to target CoADR, it

also could be useful for the design of compounds that could inhibit other disulfide reductase enzymes. As motioned in Chapter 1, most disulfide reductase has two active site cysteines and could therefore have different reactivities to the single active site Cys of CoADR. However, dithiol disulfide reductase enzymes could potentially also be targeted by the warheads that were employed in this study. The success of such a strategy is further supported by the reported time-dependent inhibitor of trypanothione reductase lunarine which is an α,β -unsaturated amide containing-substrate analogue of trypanothione.¹ These observations suggest that future investigations on this topic are warranted.

5.1.2 Objective 2: Determination of the mechanism of action of CJ-15,801

Our initial investigation on the target of the reported antibacterial activity of CJ-15,801 showed that PPCS is the target of this novel vinylogous carbamic acid. The studies undertaken in chapter three suggests that after entering the cell CJ-15,801 is converted to P-CJ by SaPanK, which in turn is converted to an unreactive analogue of the PPCS reaction intermediate. Our determination of the kinetic parameters for the inhibition was hampered by the use of *in situ* generated P-CJ, but indicated potent PPCS inhibition (nM range). The preliminary kinetic results using this system indicate tight binding inhibition similar to the compounds reported in the only other study of PPCS inhibitors. However, CJ-15,801 shows *S. aureus* growth inhibition where the reported compounds were inactive.

5.1.3 Objective 3: Synthesis of CJ-15,801 and its analogues

Due to the unusual nature of the *N*-acyl vinylogous carbamic acid CJ-15,801 only a few methodologies for its synthesis exists. Since these procedures are all considered to be inefficient in one way or another for the synthesis of CJ-15,801 and its analogues we adapted a Pd-catalyzed methodology in order to synthesize these compounds. Using this methodology various *N*-acyl vinylogous carbamates and ureas were prepared in a stereocontrolled fashion. Furthermore, the acetonide protecting group of all the prepared CJ-15,801 ester and amide analogues was successfully removed. With the successful preparation of these compounds we achieved the third aim of this study. The resulting panel of mono- and di-protected CJ-15,801 analogues was then examined for their *S. aureus* growth inhibitory abilities and it was found that they did not exhibit considerable inhibition.

5.2 Follow-up work on the inhibition of CoADR

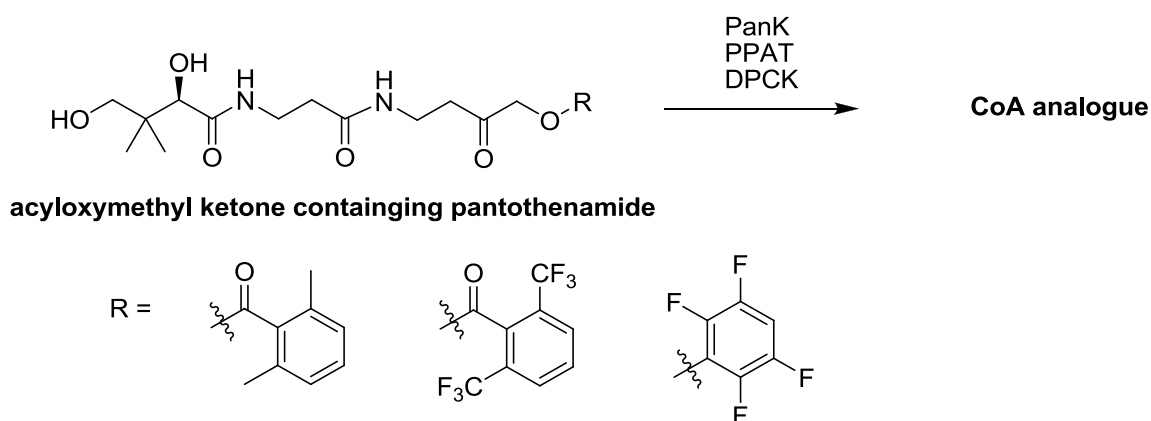
5.2.1 Inhibition by CoA analogues with electrophile removed

In order to gain further evidence that the inhibition of CoADR is due to Michael addition of the active site Cys to the activated alkene the removal of the double bond from the inhibitor

followed by determination of the inhibition of CoADR would be a useful exercise. This can be accomplished by reduction of the alkene of the pantothenamide followed by biotransformation to the CoA analogue.

5.2.2 Synthesis of compounds with improved inhibition

The discovery of the potent inhibition of CoADR by the phenyl vinylsulfone-containing CoA analogue indicates that large substituents are accepted at this position and makes it possible to replace the phenyl moiety with various other groups, such as vinyl sulfonates and sulfonamides.² Due to the tolerance of aromatic substituents another potential warhead which can be incorporated into CoA is the acyloxymethyl ketone warhead (Scheme 5.1).³ This moiety has been well studied as an irreversible inhibitor of cysteine proteases and can lead to irreversible inhibition without the need for protonation. The 2,6-dimethyl-, 2,6-bis-trifluoromethyl acyloxymethyl ketone and 2,3,5,6-tetrafluorophenol aryloxymethyl ketone warheads (Scheme 5.1) have been used often in cysteine protease inhibition.



Scheme 5.1. The acyloxymethyl ketone warhead could improve inhibition of CoADR.

5.2.3 Inhibition of *S. aureus* growth under oxidative stress conditions

CoADR is responsible for maintaining the redox homeostasis in *S. aureus* which can be disturbed by ROS generated by the host's immune system. Therefore it is expected that *S. aureus* would be more sensitive to compounds that inhibit CoADR under conditions of elevated ROS. In future studies this theory will be investigated by conducting *S. aureus* growth assays under oxidative stress conditions. These conditions can easily be mimicked by performing growth assays in the presence of 1.5% hydrogen peroxide as was used by Lui *et al.*⁴

5.3 Future studies on mechanism of action of CJ-15,801

5.3.1 Inhibition of PPCS by P-CJ

Our preliminary analysis in chapter 3 showed that PPCS is the target of the antibiotic activity of CJ-15,801. In future studies the inhibition of PPCS will be fully characterized by using synthetic P-CJ. We will therefore focus on the preparation of P-CJ which will be followed by repeating the kinetic experiments performed in chapter 3.

5.3.2 Pd-catalyzed synthesis of CJ-15,801 and its analogues

We would like to broaden the substrate scope of the Pd-catalyzed synthesis of *N*-acyl vinylogous carbamates and ureas by coupling additional substrates to amide **4.2**. These include: 3-Bromo-1-phenyl-propenone **5.1**, β -bromomethylacrylates **5.2**, and **5.3** (Figure 5.1). The synthesis of **5.1** and the methyl ester of **5.3** have already been reported in the literature.^{5, 6} Couplings with a secondary amide derivative of **4.2** such as **5.4** would also be useful to expand the scope of amide that can be used in this methodology. These compounds can again be investigated as *S. aureus* growth inhibitors.

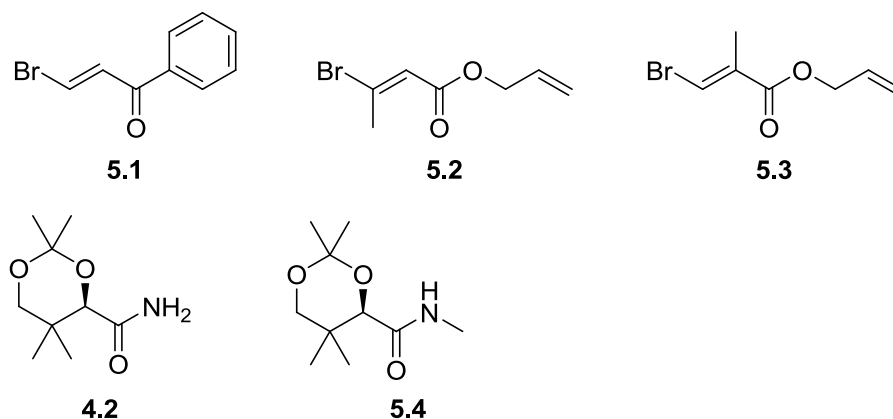


Figure 5.1. Additional substrates for Pd-catalyzed synthesis of *N*-acyl vinylogous carbamic acids, carbamates and ureas.

5.4 Final remarks

This study has revealed compounds that can be used as valuable lead compounds for the development of antistaphylococcal agents with novel mechanisms of action. These mechanisms relate to CoA biosynthesis and metabolism in the form of the PPCS and CoADR enzymes respectively. Since *S. aureus* is unique amongst nearly all bacteria (with the exception of certain other Gram-positives, of which *B. anthracis* is probably the most important) in its reliance on CoA for maintenance of its intracellular redox potential, these studies have potentially opened up a new avenue for future narrow spectrum drug discovery

explorations.⁷ It is quite possible that the desperate need for new antistaphylococcal agents could be addressed by exploiting this particular characteristic of this organism.

5.5 References

1. Hamilton, C. J.; Saravanamuthu, A.; Poupat, C.; Fairlamb, A. H.; Eggleston, I. M., Time-dependent inhibitors of trypanothione reductase: Analogues of the spermidine alkaloid lunarine and related natural products. *Bioorg. Med. Chem.* **2006**, *14* (7), 2266-2278.
2. Roush, W. R.; Gwaltney, S. L., II; Cheng, J.; Scheidt, K. A.; McKerrow, J. H.; Hansell, E., Vinyl Sulfonate Esters and Vinyl Sulfonamides: Potent, Irreversible Inhibitors of Cysteine Proteases. *J. Am. Chem. Soc.* **1998**, *120* (42), 10994-10995.
3. Brak, K.; Kerr, I. D.; Barrett, K. T.; Fuchi, N.; Debnath, M.; Ang, K.; Engel, J. C.; McKerrow, J. H.; Doyle, P. S.; Brinen, L. S.; Ellman, J. A., Nonpeptidic Tetrafluorophenoxymethyl Ketone Cruzain Inhibitors as Promising New Leads for Chagas Disease Chemotherapy. *J. Med. Chem.* **2010**, *53* (4), 1763-1773.
4. Liu, C. I.; Liu, G. Y.; Song, Y.; Yin, F.; Hensler, M. E.; Jeng, W. Y.; Nizet, V.; Wang, A. H.; Oldfield, E., A cholesterol biosynthesis inhibitor blocks *Staphylococcus aureus* virulence. *Science* **2008**, *319* (5868), 1391-1394.
5. Feray, L.; Perfetti, P.; Bertrand, M., $\text{AlCl}_3\text{-NaI}(\text{NaBr})\text{-t-BuOH}$: mild, chemo- and stereoselective reagents for hydrohalogenation of propiolic derivatives. *Tetrahedron* **2009**, *65* (42), 8733-8737.
6. Li, X.; Zeng, X., Sequential trans-halogenation and Heck reaction for efficient access to dioxo-tetra-substituted 2,4 *E,E*-dienes: synthesis of segment C1-C6 of apoptolidin. *Tetrahedron Lett.* **2006**, *47* (38), 6839-6842.
7. Fischbach, M. A.; Walsh, C. T., Antibiotics for Emerging Pathogens. *Science* **2009**, *325* (5944), 1089-1093.